POLITECNICO MILANO 1863

SCUOLA DI INGEGNERIA INDUSTRIALE E DELL'INFORMAZIONE

PRELIMINARY DESIGN OF THE LOCOMOTION SYSTEM OF A ROVER FOR AN ASTEROID EXPLORATION MISSION

Tesi di Laurea Magistrale in
Space Engineering - Ingegneria Spaziale

Author: **Chiara Giardini**

Student ID: 242297
Advisor: Prof. Fabio Ferrari
Co-advisors: Iosto Fodde, Samuele Vaghi
Academic Year: 2025-26

Huston, abbiamo un problema
- Apollo 13

Abstract

This thesis presents the preliminary design of a locomotion system for a mobile rover deployed on the asteroid (4) Vesta, combining in-situ exploration with sample-return capabilities. Small Solar System Bodies (SSSBs) like Vesta act as archives of early Solar System evolution and planet formation; however, their harsh environments, characterized by microgravity, the lack of an atmosphere, and highly uncertain surface mechanical properties, pose severe engineering challenges for stable surface mobility. Traditional locomotion systems designed for planetary exploration face significant risks of slippage, capsizing, or escaping into space due to low local gravity and irregular gravitational fields.

To determine the optimal mobility architecture, a systematic trade-off analysis using the Analytical Hierarchy Process (AHP) was conducted across four candidate locomotion technologies; the modified wheeled rover configuration was selected as the baseline solution for its robust, adaptable performance and high safety margins.

The resulting locomotion design incorporates a 6x6x6 architecture with six wheel-walking capabilities, heavily drawing upon the design heritage of JAXA's MMX rover and ESA's Rosalind Franklin (ExoMars) rover. The architecture consists of an optimized, rigid aluminum alloy wheel design featuring curved grousers to prevent soil sinkage and maximize tractive efficiency, paired with a highly adaptable triple-bogie suspension system to ensure continuous ground contact on rough and uneven terrain. The structural integrity and mass minimization of the wheel disk and suspension beams were verified using Finite Element Method (FEM) static analysis under worst-case loading configurations. Built from high-strength aluminum alloy, the complete locomotion system has a total mass of approximately 25 Kg and utilizes high-torque electromechanical actuators. It features two distinct operational states: a stowed configuration for compact transport and an active operating configuration; and supports precise driving, steering, and active wheel-walking modes. Backed by experimental test data from granular soil simulants, this design demonstrates a highly reliable, low-power solution for navigating challenging extraterrestrial surfaces, ensuring successful multi-point scientific sampling on Vesta.

Keywords: asteroid exploration, asteroid locomotion system, modified wheeled rover

Abstract in lingua italiana

Questa tesi presenta il progetto preliminare di un sistema di locomozione per un rover mobile destinato all'asteroide (4) Vesta, combinando esplorazione in-situ e capacità di ritorno di campioni. I corpi celesti di piccole dimensioni, come Vesta, rappresentano archivi dell'evoluzione del Sistema Solare e della formazione dei pianeti; tuttavia, i loro ambienti ostili, caratterizzati da microgravità, assenza di atmosfera e proprietà meccaniche incerte, pongono sfide ingegneristiche per una mobilità stabile. I sistemi di locomozione tradizionali progettati per l'esplorazione planetaria affrontano rischi di slittamento, ribaltamento o di fuga nello spazio a causa della bassa gravità locale e dei campi gravitazionali irregolari.

Per determinare l'architettura ottimale, è stata condotta un'analisi comparativa con il metodo Analytical Hierarchy Process (AHP) su quattro tecnologie candidate; la configurazione di modified wheeled rover è stata selezionata come soluzione di riferimento grazie alle sue prestazioni robuste e adattabili e agli elevati margini di sicurezza.

Il progetto integra un'architettura 6x6x6 con capacità di wheel-walking, ispirata all'eredità del rover MMX della JAXA e del rover Rosalind Franklin (ExoMars) dell'ESA. L'architettura consiste in ruote rigide in lega di alluminio, dotate di grousers curvi per prevenire l'affondamento nel terreno e massimizzare l'efficienza di trazione, abbinate a un sistema di sospensione triple-bogie adatto a garantire un contatto continuo con il suolo su terreni accidentati e irregolari. L'integrità strutturale e la minimizzazione della massa del disco ruota e dei bracci della sospensione sono state verificate mediante analisi statica degli elementi finiti nelle configurazioni di carico peggiori. Realizzato in lega di alluminio ad alta resistenza, il sistema completo di locomozione ha una massa totale di circa 25 Kg e utilizza attuatori elettromeccanici ad alta coppia. Presenta due distinti stati operativi: una configurazione ripiegata per il trasporto e una configurazione attiva operativa; inoltre supporta modalità di guida, sterzata e wheel-walking. Supportato da dati sperimentali ottenuti tramite test su simulanti granulari, questo progetto dimostra una soluzione affidabile e a basso consumo energetico per la navigazione su superfici extraterrestri complesse, garantendo il successo di campagne scientifiche di campionamento multiplo su Vesta.

Parole chiave: esplorazione asteroidale, sistema di locomozione, modified wheeled rover

Contents

Introduction

The solar system hosts a vast population of Small Solar System Bodies (SSSB), that range considerably both in size and characteristics. These objects, like asteroids and comets, are the remnants of planetesimals; hence, a considerable amount of information on the evolutionary process of the Solar System between the collapse of the protoplanetary nebula and the formation of the planets is likely archived in their population. Since the timeline for the formation of planets is still poorly understood, many of them are considered as records of the original Solar System protoplanetary disk, and the wide range of differences come from different formation regions and different histories of evolution. [1]

In addition to the scientific questions, a number of asteroids considered as potentially hazardous (PHA) exists. These asteroids have a non zero probability of impacting Earth, that could lead to serious danger for people or even to natural disasters. Therefore, in order to mitigate the possibility of cataclysmic impacts, a detailed understanding of the dynamics, the structure and the properties of such bodies is imperative. [2]

Alongside scientific significance and planetary defense, the interest in asteroids has also increased for economic reasons. The extraction and exploitation of possible resources in space is raising interest from industries, making Near-Earth asteroids the intended targets for the next exploration mission for their resource value. This also requires a well-rounded knowledge of the targeted object, where and how to mine. [2]

Accounting for their scientific relevance, importance in planetary defense and their increasing resource value, the study and exploration of SSSB is a major objective in space science. Remote observations from Earth and flyby missions are the first indispensable step into the investigation of these objects, but the valuable information provided is only partial. To obtain a complete characterization the small body, in situ exploration is needed; therefore, sample-return, roving and landing missions are required steps to take.

Current mission architectures reveal a technology gap regarding the movement on the surface of SSSB: existing locomotion systems are still mainly designed for planetary exploration endeavors, like the Moon or Mars. Landing and moving on small bodies is further complicated by the harsh environment that characterizes this type of objects:

very low gravity, no atmosphere and mostly no prior knowledge of the surface properties. The low gravity causes serious challenges in the locomotion of any kind of rover, without considering that the surface escape velocity is just a few cm/s, leading the rover to rebounds or loss of contact during the movement, even after a controlled touchdown during landing. Furthermore, the gravity field is not always perpendicular to the local surface because of the irregular shape and heterogeneous mass distribution, and this complicates more the surface interaction while roving. Evidence of surface mechanical properties is extremely limited at best before in-situ operations, therefore the scientific community is adjusting toward the development of technologies, that can provide stable and reliable locomotion on a wide variety of surfaces. All these challenges highlight the importance of a strong and stable locomotion design developed for exploration missions where the targets are asteroids, comets and in general small solar system bodies. For operations like in situ resource utilization or to answer deep questions on the origin of the solar System, the probe created for the mission must be capable of reaching multiple target points on the surface of the body, without compromising its attitude or drifting away into space.

This work wants to answer the question of what existing locomotion technology could deliver the most robust performance for an asteroid exploratory mission. Accordingly, the objective of the thesis is to deliver a preliminary design that guarantees reliable locomotion for the exploration.

Thesis outline

The outline of the thesis work is presented with a summary of the content for each chapter, that provides an overview of the logical progression followed throughout the study.

Chapter 1 reviews the exploration of small bodies within the Solar System and outlines their principal physical and mechanical characteristics. Following, Chapter 2 provides an overview of the mission concept: the targeted body, the scientific relevance within the context of small-body exploration and the primary scientific objectives. In Chapter 3, the principal locomotion technologies are presented through their working principles, advantages, and limitations. A systematic trade-off analysis, based on the Analytical Hierarchy Process, is then carried out to identify the most suitable system accounting for different criteria. The selected locomotion technology is the modified wheeled rover. The design of the locomotion system created for the mission scenario proposed is presented next in Chapter 4, with a particular focus on the wheel and suspension system design. Lastly, Chapter 5 summarizes the main outcomes of the study, discussing limitations and future developments to improve the design.

1 | Small solar system bodies and the history of their exploration

This chapter reviews the exploration of small bodies within the Solar System and outlines their principal physical and mechanical characteristics. It begins with an overview of the properties of small bodies, since they critically influence the design of the locomotion system. Subsequently, past and current missions are examined in order to highlight the evolution of the landing and rover technologies.

1.1. Small solar system bodies

During the General Assembly of the International Astronomical Union of 2006, all bodies in our Solar System have been categorized: [3]

- Satellites
- Planets: bodies that have enough mass to be in hydrostatic equilibrium and to completely clear their orbit
- Dwarf planets: bodies that have enough mass to be in hydrostatic equilibrium but cannot clear their orbit
- Small solar system bodies (SSSBs): the rest of the bodies

Since then, the official number of small bodies in our Solar System has increased, same as the knowledge that they can be found throughout the entire Solar System, as seen in Figure 1.1. The SSSB population includes different types of objects, such as asteroids, comets, meteoroids, Trans-Neptunian Objects (TNOs), and Centaurs (CEN). [4]

In the inner Solar System, the highest concentration of small bodies is found between Mars and Jupiter, in particular between 2 and 3.4 AU from the Sun, and it is called Main Asteroid Belt. Here the distribution of the bodies is not uniform, in fact the presence of planets creates gravitational resonances that model the shape of the belt and the density of objects in it. [3][4]

Resonant interactions, like mean-motion resonances with Jupiter and secular resonances, like the v6 resonance with Saturn, destabilize the orbits of asteroids; and coupled with collisions generate groups of objects that share similar orbital characteristics. For example, these interactions lead some asteroids into planet-crossing trajectories, thus creating the Mars-crossers (MC) and Near-Earth Objects (NEOs). The Mars-crossers are asteroids with orbits that cross the one of Mars and have perihelion distances between 1.30 and 1.66 AU. The NEO population is the other big group of small bodies, their orbits are located between the Earth and Mars perihelions. NEOs comprehend both asteroids and comets, and their lifespans are short compared to the age of the Solar System, therefore they are periodically replenished: a small part comes from dead comets, but the majority of NEOs come from the Main Asteroid Belt. [3][4]

The objects orbiting in the Lagrangian points of the orbits of a planet are called Trojans, there are Mars Trojans and the most numerous Jupiter Trojans (JT)[3]. Centaurs share characteristics with asteroids and also comets, and they are located between the orbit of Jupiter and Neptune. These bodies experience strong perturbations from the giant planets, that leads to a chaotic evolution and short life time. [3] [4]

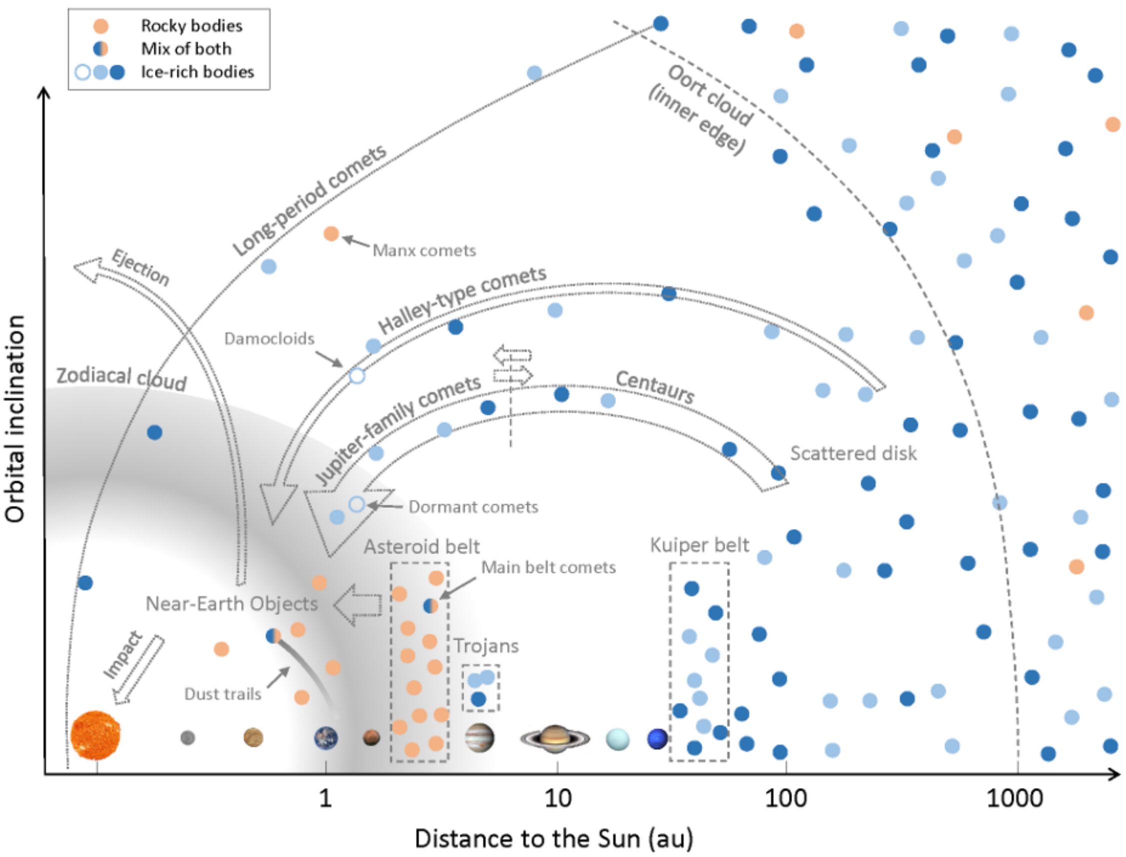

Figure 1.1: Small Solar System Bodies [5]

On the other hand, the main population of objects in the outer Solar System are the trans-Neptunian objects. TNO is any small body that orbits the Sun on average at a farther distance than Neptune; all the space is divided into the Kuiper Belt, the scattered disk and the Oort cloud. The Kuiper belt is similar to the Main Asteroid Belt but much bigger, it is a dynamically stable region that is located between 30 to 55 AU. The scattered disk is composed of objects that have extreme orbits (even above 100 AU), it is considered as the source for most periodic comets, the result of gravitational scattering by the giant planets. Lastly, the Oort cloud is only an hypothetical spherical cloud of objects at 50000 AU from the Sun, it is believed to be the region where most long-period comets come from. [3]

1.1.1. Characteristics

The small bodies of the Solar System are usually classified according to their heliocentric orbits and physical characteristics, as these properties reflect both their origin and their consequent evolutionary process. Their dynamical evolution is governed primarily by the gravitational interaction with the Sun and the planets, but non-gravitational effects and physical properties have a significant role in precisely describing their behavior. Thus, parameters such as size, shape, density, and porosity directly influence orbital determination and rotational evolution. [4] [2]

These objects display an extraordinary compositional diversity, reflecting the varying thermal and chemical conditions present across the different regions of the Solar System. In the outer Solar System, temperatures are sufficiently low to allow volatile compounds, such as water, methane, and ammonia to exist as ice. Closer to the Sun, where temperatures are significantly higher, silicate minerals become dominant, together with metallic components like iron and nickel and carbon compounds. Water remains significant even at these intermediate distances, but it is generally preserved in hydrated minerals produced through aqueous alteration processes. [3]

Beyond gravitational perturbations from the Sun and planets, the long term dynamical evolution of minor bodies is also influenced by non-gravitational forces, like thermal forces, most notably the Yarkovsky and YORP effects. These arise from the anisotropic thermal re-radiation of absorbed solar energy. The Yarkovsky effect causes gradual drift in an asteroid's semimajor axis, while the YORP (Yarkovsky–O'Keefe–Radzievskii–Paddack) effect modifies its rotation rate and obliquity. These small but cumulative forces influence the migration of asteroids and contribute to the dispersion of asteroid families over long timescales; they also play a role in shape evolution among smaller bodies. Nonetheless, their relative importance depends strongly on size: for objects larger than roughly 1 km, gravitational interactions during planetary encounters dominate, while the influence of the Yarkovsky and YORP effects are often rendered minor. So, while these non-gravitational effects are always in operation, they are often secondary in regions where planetary perturbations prevail. [4]

Asteroids

The inner Solar System is populated mainly by asteroids, which include main-belt asteroids, NEAs and Mars-crossing objects. Asteroids are generally divided in two major taxonomical groups based on spectral and mineralogical composition: silicate-rich or "stony" asteroids (S-type) and carbonaceous asteroids (C-type). S-type asteroids are rich in silicates and metallic components, on the other hand C-type asteroids contain larger fractions of carbonaceous and opaque materials. Within these wide categories, additional subclasses can be identified according to the relative abundance of specific minerals. For example, among S-type asteroids, A-type objects are dominated by olivine-rich compositions, while V-type asteroids show a composition rich in pyroxene and feldspar. This compositional distribution also has a spatial signature, in fact the distribution of these classes within the main asteroid belt is not uniform. S-type asteroids are concentrated predominantly in the inner regions of the belt, while C-type asteroids are more abundant in the outer regions. Therefore, since the main sources of NEAs are resonant regions located in the inner main belt, most NEAs belong to the S-class. [3]

Figure 1.2: Itokawa asteroid [6] and a close up of Bennu [7], both rubble pile asteroids

Asteroids have shown to exhibit a wide range of densities and internal strengths. The discovery of binary systems and in situ space missions to bodies, has allowed the determination of masses and porosities. Many asteroids are now believed to be "rubble-pile" or gravitational aggregates rather than monolithic rocks: gravitationally bound accumulations of fragments produced by collisional disruption and subsequent re-accumulation. The most known rubble pile asteroids are Itokawa and Bennu, shown in Figure 1.2. These bodies are held together mainly by self-gravity, not material strength, and often exhibit low bulk densities, high porosities, with surfaces covered by regolith, boulders, grooves, craters, and steep topographic features. Such observations demonstrate that asteroid surfaces and interiors behave similarly to granular media, composed of particles ranging from micron-sized dust to metre-scale boulders. [2]

The Main Asteroid Belt also known as just Asteroid Belt (AB) currently contains 1280724 known asteroids. These bodies are commonly classified according to their semi-major axis (a) into three principal groups:

- Inner Main-Belt Asteroids (IMB), with $2 < a < 2.5$ AU;
- Middle Main-Belt Asteroids (MMB), with $2.5 < a < 2.82$ AU;
- Outer Main-Belt Asteroids (OMB), with $2.82 < a < 3.27$ AU.

Certain asteroids within the Main Belt undergo dynamical processes that increase their orbital eccentricity, as a consequence, these objects may evolve into Mars-crossing asteroids, eventually leading to their removal from the Main Belt population. [4]

A minor body is classified as a NEO when its perihelion distance (q) satisfies $q < 1.3$ AU. NEOs are commonly divided into four dynamical classes:

- Amor asteroids, characterized by $1.017 < q < 1.3$ AU and $a > 1$ AU;
- Apollo asteroids, with $a > 1.0$ AU and $q > 1.017$ AU;
- Aten asteroids, defined by $a < 1$ AU and $q < 1$ AU;
- Inner Earth Objects (IEOs), for which $q < 0.983$ AU.

Apollo and Aten asteroids are Earth-crossing objects, whereas Amor and IEO asteroids do not intersect Earth's orbit; in particular, Amor asteroids remain entirely exterior to Earth's orbit, while IEOs orbit completely within it. The currently known population of Near-Earth Asteroids consists of 38171 objects, including 13429 Amors, 21657 Apollos, and 3050 Atens. Population estimates suggest the existence of approximately 830 ± 60 NEOs with diameters $D > 1$ Km, and about 20000 ± 2000 objects with $D > 140$ m. The dominant source region of NEOs is the Inner Main Belt. However, additional contributions arise from the Outer Main Belt, the Jupiter-family comet region, and other small-body reservoirs, including Jupiter Trojan asteroids, Centaur objects, and TNOs. [4]

The currently known population of JT asteroids consists of 15140 objects. Dynamical and compositional evidence suggests that these bodies did not originate in the vicinity of Jupiter, but they were most likely captured from the primordial Kuiper belt or broader trans-Neptunian region during an epoch of giant-planet migration and dynamical instability in the early Solar System. The relatively low bulk densities and the observed bimodal color distribution of the Trojan population further support their origin from a reservoir of icy and primitive planetesimals. Their present-day surface properties are believed to reflect both their primordial composition and the physical conditions that characterized the early stages of Solar System evolution. [4]

Centaurs are minor bodies orbiting the Sun, and are generally defined by a perihelion distances exterior to Jupiter's orbit and semimajor axes interior to Neptune's orbit. The currently known Centaur population comprises 919 objects. The diameters of most known Centaurs remain unknown; however, approximately 7% of the observed population is estimated to have diameters exceeding 1 Km. The dynamical evolution of Centaurs is highly chaotic, and it depends on close gravitational encounters with the giant planets but also to the influence of mean-motion resonances operating in this region.[4]

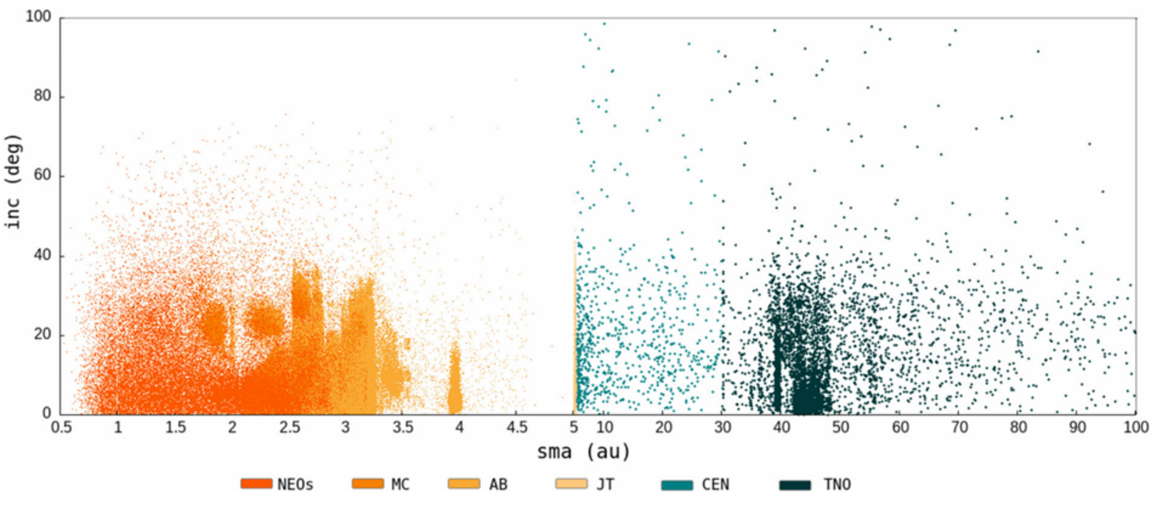

Figure 1.3: Distribution of minor bodies in the Solar System according to their dynamical classification [4]

The currently known population of Trans-Neptunian objects consists of 5335 objects. Minor bodies residing in the trans-Neptunian region are subject to a variety of dynamical perturbations, including planetary scattering processes, mean-motion resonances, and secular resonances associated with the giant planets. Objects located at greater heliocentric distances may additionally be influenced by external perturbations, such as galactic tides and gravitational interactions with passing stars. These effects play a significant role in shaping the long-term dynamical evolution of the distant Solar System population. [4]

Figure 1.3 depicts the distribution of all type of SSSBs in the Solar System, considering the currently known populations described.

Meteorites

Meteorites are defined as natural objects that survive their passage through Earth's atmosphere and reach the surface, they provide a direct means of analyzing their composition, and therefore a direct link to their parent asteroid study. Meteorites are traditionally classified into three major groups according to their metal and silicate content: stony meteorites, stony-irons, and iron meteorites. Stony meteorites are composed primarily of silicates, and are further divided into chondrites and achondrites, depending on the presence or absence of chondrules, that are millimeter-sized, spherical silicate aggregates formed in the early Solar System. Chondrites are considered chemically primitive because their composition closely resembles that of the volatile-free Sun, making them invaluable records of the primordial Solar System matter. Achondrites, on the other hand, originate from differentiated parent bodies that experienced varying degrees of melting and igneous processing. These meteorites show wide compositional diversity, from partially melted primitive achondrites to fully differentiated igneous rocks. [3]

Comets

Comets are believed to be some of the most pristine remnants of the early Solar System, preserving material that formed in the cold outer regions of the protoplanetary disk beyond the so-called “snowline”, where temperatures were sufficiently low for volatile compounds to condense, and as a result, the planetesimals formed in these distant regions were particularly rich in ices. They are composed of approximately equal proportions of dust and ice. As the comet approaches the Sun, the heat causes the volatile ices to sublimate, releasing gas that expands into space. The solid dust particles are carried by the gas, this material forms the coma and, in some cases, the characteristic cometary tails observed: Figure 1.4 shows the tail of comet 3I/ATLAS. Close to the nucleus, within the so-called collisional zone, gas densities remain sufficiently high for collisions and chemical reactions to occur before photochemical processes progressively alter the composition of the expanding gas. [8] [9]

These icy bodies originated from the solar nebula during the formation of the Solar System, and while many were incorporated into the giant planets, others were either ejected into the Oort Cloud or remained in reservoirs beyond Neptune. Comets have undergone very little alteration since their formation in the early solar nebula. [8]

The classification of comets is primarily based on orbital period, comets are traditionally divided into long-period comets, with orbital periods greater than 200 years, and short-period comets, with orbital periods below 200 years. Short period comets are thought to originate from the Kuiper Belt, while long period comets are associated with the Oort Cloud. Short-period comets are further subdivided into Halley-type comets, with orbital periods between 20 and 200 years, and Jupiter-family comets. Jupiter family comets have periods shorter than 20 years, pericenter distance $q < 5.3$ AU, and their current number is 823 bodies. Their dynamics are mainly influenced by close encounters with Jupiter, therefore, they are displaced from their region, that leads to a shorter lifespan. [10] [4]

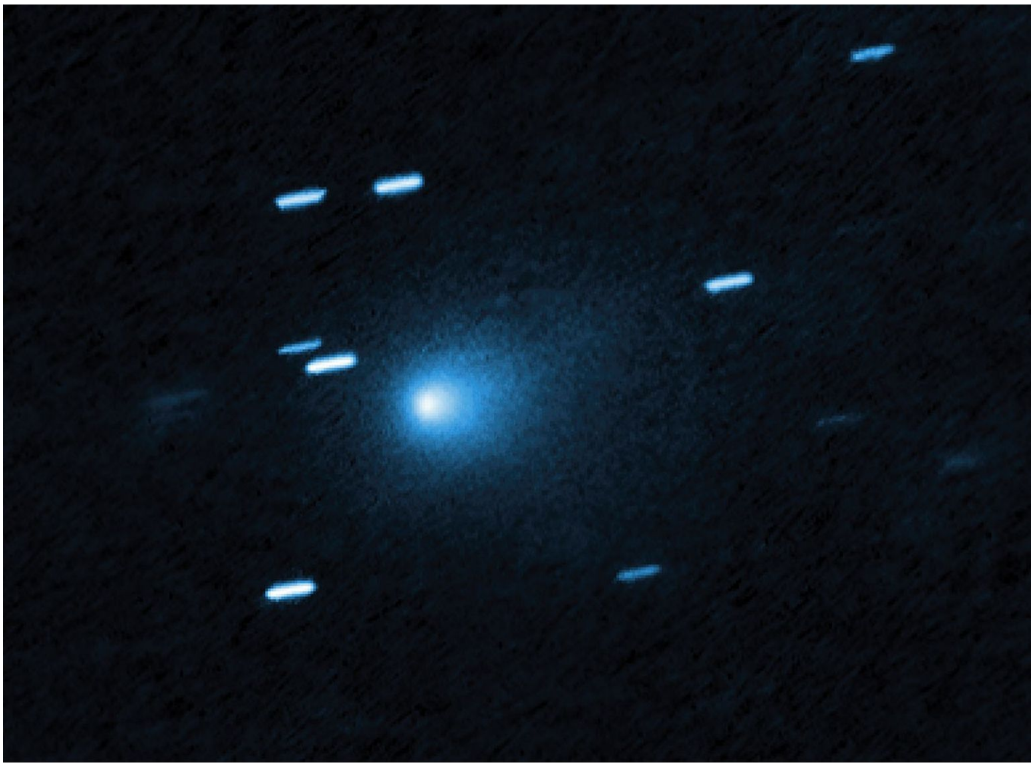

Figure 1.4: Comet 3I/ATLAS captured by Hubble telescope [7]

1.2. Small solar system bodies' hystory of exploration

Interest in asteroids and other small solar system bodies has increased significantly due to their scientific value, potential impact hazard, and opportunities for in situ resource utilization.

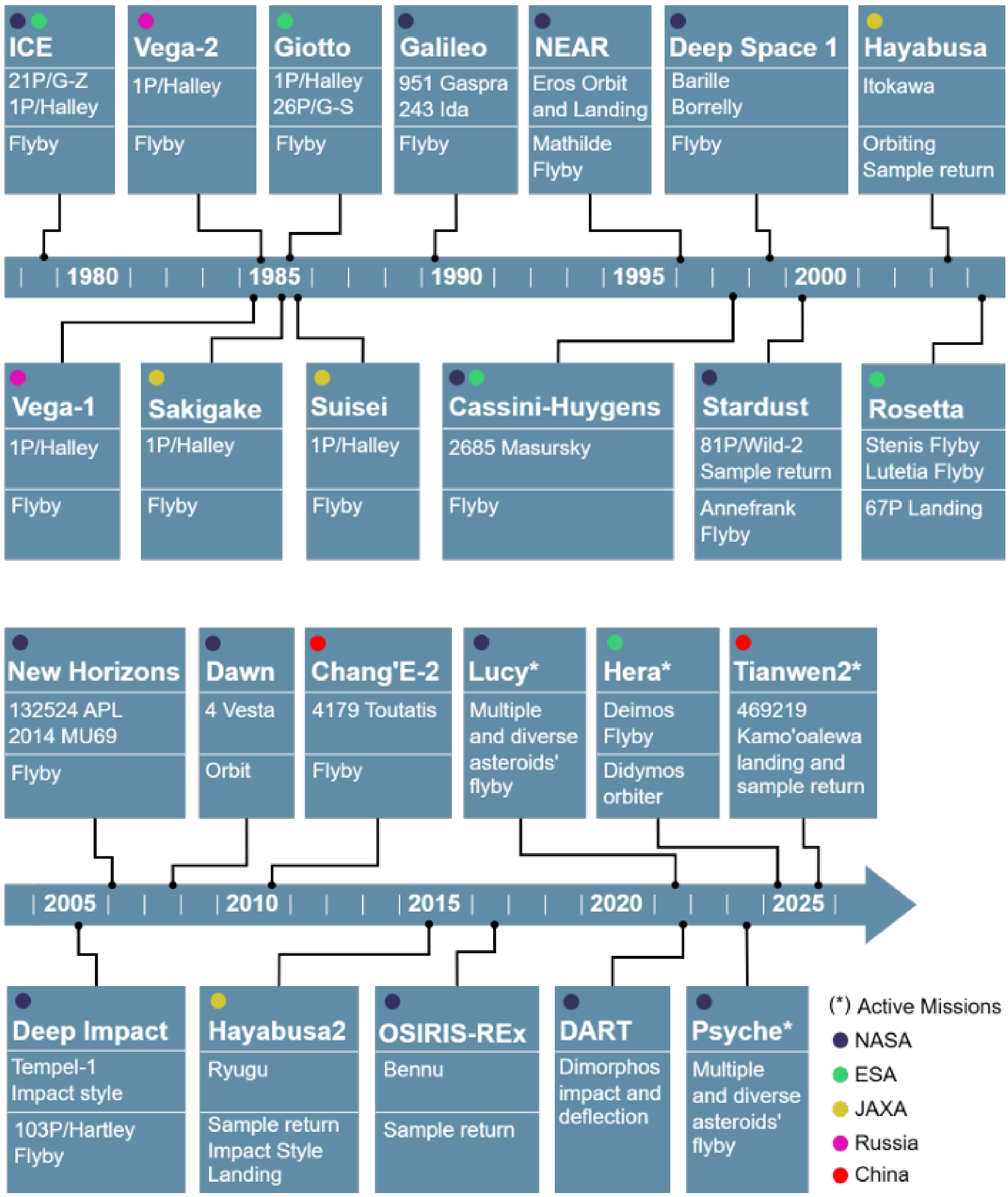

Figure 1.5: Timeline of exploration missions to SSSBs [11]

Small bodies preserve material from different stages of Solar System dynamical evolutionary history, since they retain evidence of the compositional gradients that existed within the protoplanetary disk in the solar nebula, and can represent the stages that the Solar System evolved and formed from. Therefore, these bodies show the evolutionary pathway from pre-solar grains to planetesimals, and finally completely formed planets. Also, collisions among protoplanets that led to the fragmentation of larger bodies, allow small bodies to have exposed core, mantle, or crustal material; and therefore, becoming the only accessible reservoir of extraterrestrial core material. [12]

As it can be seen in Figure 1.5, the exploration of SSSBs began in 1978 with the International Cometary Explorer mission, jointly conducted by NASA and ESA, which performed multiple flyby investigations of Halley's Comet and Comet 21P/Giacobini–Zinner. Since then, numerous small bodies exploration missions have been carried out by ESA, NASA, Japan, Russia, and China, often targeting multiple objects within a single mission. To date, approximately twenty successful missions have been completed, while four others remain active. As exploration technologies have advanced, mission architectures have evolved from flyby observations and impact experiments toward rovers, sample-return and in situ exploration missions. Among these, only three missions have successfully conducted contact sampling operations: the Japanese Hayabusa and Hayabusa2 missions, and NASA's OSIRIS-REx mission. All of which employed touch-and-go sampling techniques, where the spacecraft does not land on the body, but it comes in contact with the surface of the asteroid for only a brief moment to collect samples. In addition, ESA's Rosetta–Philae mission achieved in situ surface exploration, while China's Tianwen-2 mission aims to combine in situ exploration with a sample-return. Each exploration strategy offers distinct advantages and supports different scientific objectives; but with continuous advances in space technology, the focus of SSSB exploration has gradually changed from the general characterization of the body or its regolith physical and chemical properties toward a deeper understanding of the origin and evolutionary history of small solar system bodies.[13]

1.2.1. Rosetta

The Rosetta Mission was a very important mission in ESA's long-term program Horizon 2000. The main scientific objectives of the mission was studying the origin of the solar system by looking into the origin of comets. To achieve these goals Rosetta wanted to study the characteristics of the nucleus and the cometary coma, and the plasma environment of comet 67P/Churyumov-Gerasimenko. It consisted of two mission parts: the orbiter and the lander, depicted in Figure 1.6. The comet's evolution was investigated with decreasing heliocentric distance by the orbiter instruments, this was obtained by monitoring the physical and chemical properties of the nucleus and in situ analysis of the near-nucleus environment. On the other hand, the lander Philae objective was to analyze the nucleus material directly. [14]

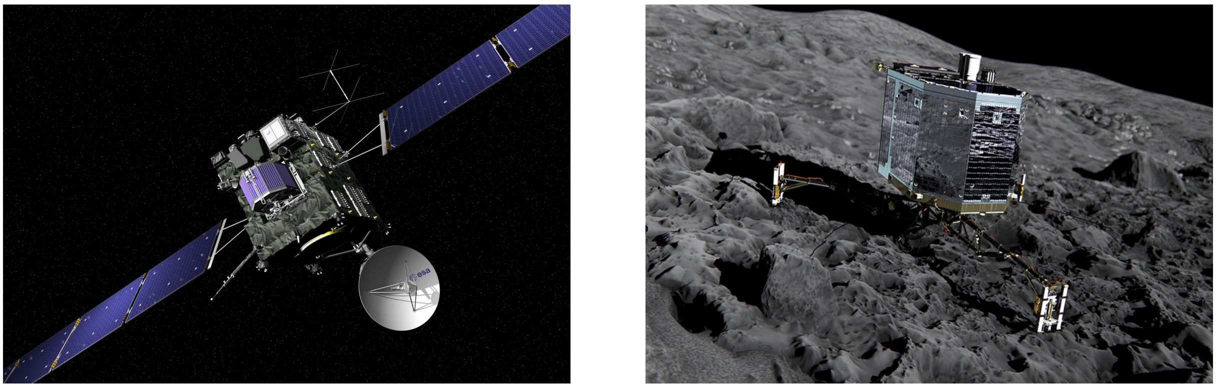

Figure 1.6: Rosetta mother spacecraft and PHILAE lander [15]

The lander system had a total mass of 97.9 kg including 26.7 kg worth of scientific payload. It also had 13.1 kg of parts which supported Philae on the orbiter: the Mechanical Support System and the Electrical Support System with part of the telecommunications system; those stayed there after separation. [16]

Philae itself consisted of an upper square main body with a mass of 86.5 kg and a three-legged landing gear with a mass of 11.1 kg and an unfolded diameter of 3.08 m. After separation from Rosetta at a velocity of 0.05–0.52 m/s, Philae descended to the 67P surface using only one reaction wheel. The main landing impact energy was supposed to be absorbed by the electro-mechanical damping device (EMDD) located on the landing gear, and by the top layer compaction of the cometary surface caused by footpads. As it can be seen in Figure 1.7, two footpads were arranged at the bottom of each landing leg, and an ice screw was installed between the two footpads to prevent the sideslip of the lander thorough their penetration. In addition, in order to prevent the rebounding caused by the initial landing impact, Philae had an Active Descent System (ADS) on the main body, and an anchoring harpoon located at the bottom of the landing gear. [17]

Philae was expected to anchor after the landing on the nucleus surface of comet 67P to complete an in-situ study of the materials on the surface and in the subsurface up to 0.2 m deep; but during the actual landing, the ADS failed and the anchoring harpoon was not fired, the EMDD did not work right away, and therefore, it was the top layer compaction that absorbed most of the impact energy. This caused Philae to land after rebounding twice, it came to rest in a crevice where only minor solar energy could be collected. [17]

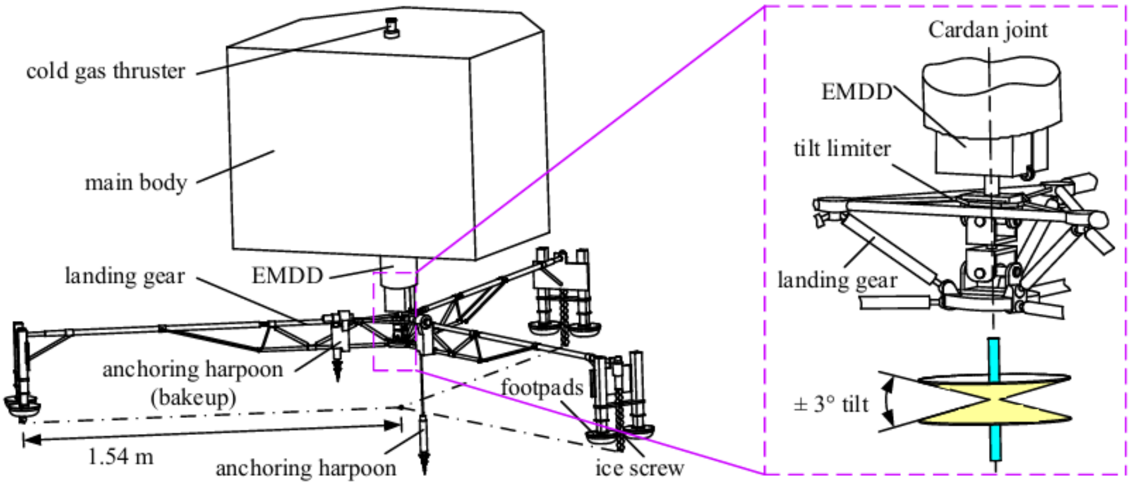

Figure 1.7: PHILAE model [17]

1.2.2. Hayabusa

Hayabusa was the first asteroid sample return mission, and it was also the first spacecraft to explore an asteroid that had dimension under a kilometer: the target was the S-type near Earth asteroid Itokawa, about 500 m in length. The project primarily objective was a technology demonstration for future sample-return attempts from bodies like comets and asteroids. Its voyage had many problems, most of which were not anticipated before launch, but Hayabusa successfully returned surface material from the asteroid. Even if the amount of sample from Itokawa was small, the analyses have been continued worldwide, and a lot of new information has been gained. [18]

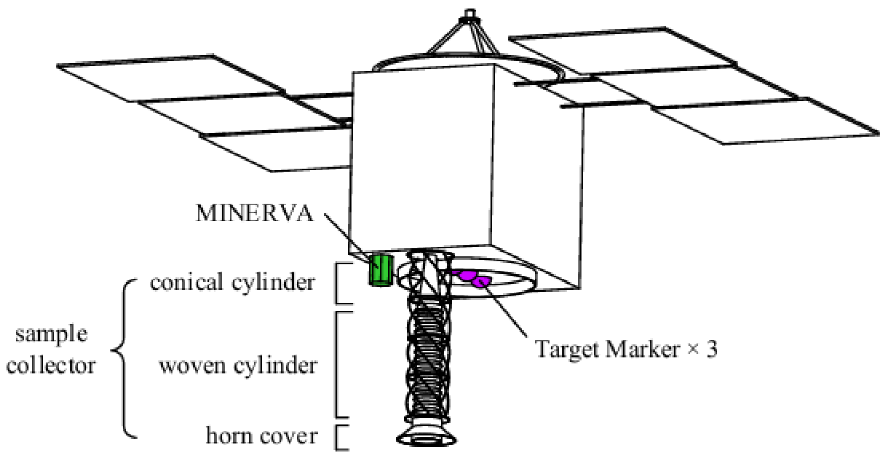

Figure 1.8: Hayabusa model [17]

The Hayabusa probe was a three-axis stabilized probe with a tetragonal-box shape represented in Figure 1.8. It had a total mass of approximately 500 kg, which contained 131.5 kg of propellant. Hayabusa sampling collector was cylindrical and located on the abdomen in order to cover the sampling site and sample the asteroid Itokawa by its own pioneering Touch And Go (TAG) approach. The outside of the sampling collector was connected by a conical cylinder, a woven cylinder, and a horn cover. The woven cylinder could be expanded to the configurations of launch or sampling. During the TAG process, the horn cover would touch the asteroid surface, and under that action of the contact force, the woven cylinder would deform and cause the displacement of the horn cover. A laser beam was used to trigger the projectile-shooting sampling operation based on the confirmed deformation. Hayabusa used a spherical illuminator called target marker, which is an optical descent navigation to ensure that it would not hit rocks. Hayabusa had several cushioning designs: for example, the woven cylinder in the sampling collector was made of flexible material and deforming could provide a certain degree of cushioning for the probe, it also had many small high polymeric beads within the spherical container of target marker to obtain a low elastic recovery coefficient when landing. [17]

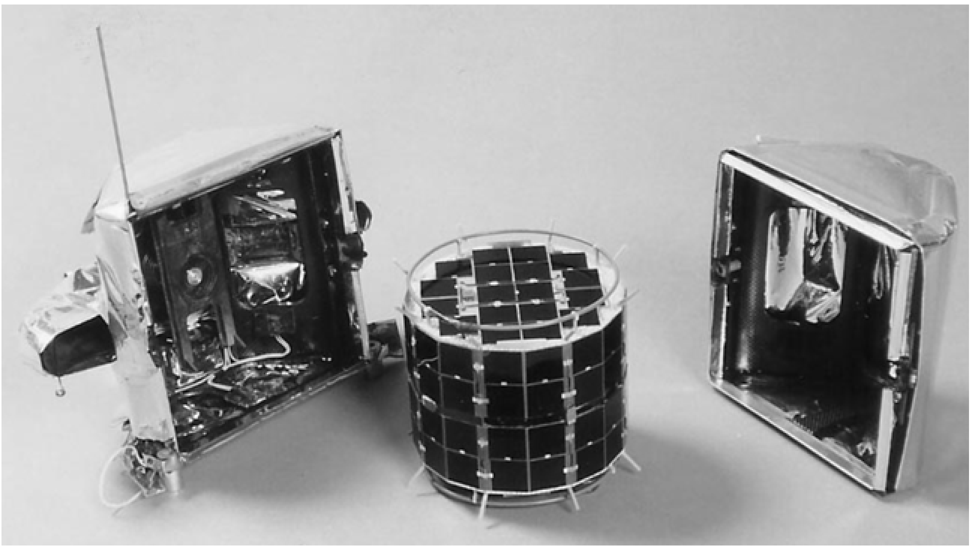

Figure 1.9: Minerva robot [19]

For the Hayabusa mission, an small robot for asteroid surface exploration was designed, called MINERVA (MIcro/Nano Experimental Robot Vehicle for Asteroid), shown in Figure 1.9. MINERVA was the first asteroid exploration rover to ever be developed and deployed. Its main objectives were establishing a novel mobility in micro gravity environment, demonstrating the autonomous exploration capability, and to perform the first-ever scientific observations on an asteroid surface. It is an octagon shaped cylinder with a diameter of 12 cm and a height of 10 cm, and a mass of 591 g. It was powered by solar energy, and it had two actuators inside in order to move, one of them is used as a torque, and by rotating the torque, a reaction force against the asteroid surface makes the rover hop. After hopping into free space, it moves ballistically. [19]

Hayabusa implemented two TAG operations: in the first one, Hayabusa fell on the asteroid surface and rebounded twice; on the other hand, the second TAG operation was successful in collecting thousands of Itokawa particles, even though the intended sampling mechanism of the sampler on the spacecraft did not work. With regard to MINERVA, the hopper was lost at an altitude of 200 m, because an automatic emergency ascent of Hayabusa was initiated to avoid hazards and the command for releasing MINERVA was already sent. [17]

1.2.3. Hayabusa 2

The Hayabusa2 mission was the successor of the first asteroid sample return mission ever, Hayabusa by JAXA. The Japanese agency planned this mission to understand the origin and evolution of materials in the early solar nebula and in the asteroid parent body, as well as to characterize the physical properties of planetesimals. The target of the study was conducting global-, local-, and micro-scale observations of carbonaceous-type NEA Ryugu, through remote sensing from the spacecraft, in situ surface measurements by landers, and returned sample analysis. [20]

The Hayabusa-2 probe was a three-axis stabilized probe with a tetragonal-box shape, similarly to Hayabusa, and it had a total mass of 609 kg. Hayabusa-2 inherited the majority of its technologies from Hayabusa, including the TAG method and the execution mechanism. The sampler horn extended beneath the spacecraft to conduct the sampled surface materials to a catcher inside the main body. The sampling was performed within the few seconds of the horn touching the asteroid's surface, before firing the thrusters to ascend. In order to collect sufficient amount of samples, a projectile was shot onto the asteroid's surface to produce impact ejecta, which were then collected into a chamber of the sample catcher through the horn. In addition to remote-sensing instruments and the sample acquisition system represented in Figure 1.10, a small carry-on impactor was designed in order to excavate an artificial crater to get subsurface samples. [17] [20]

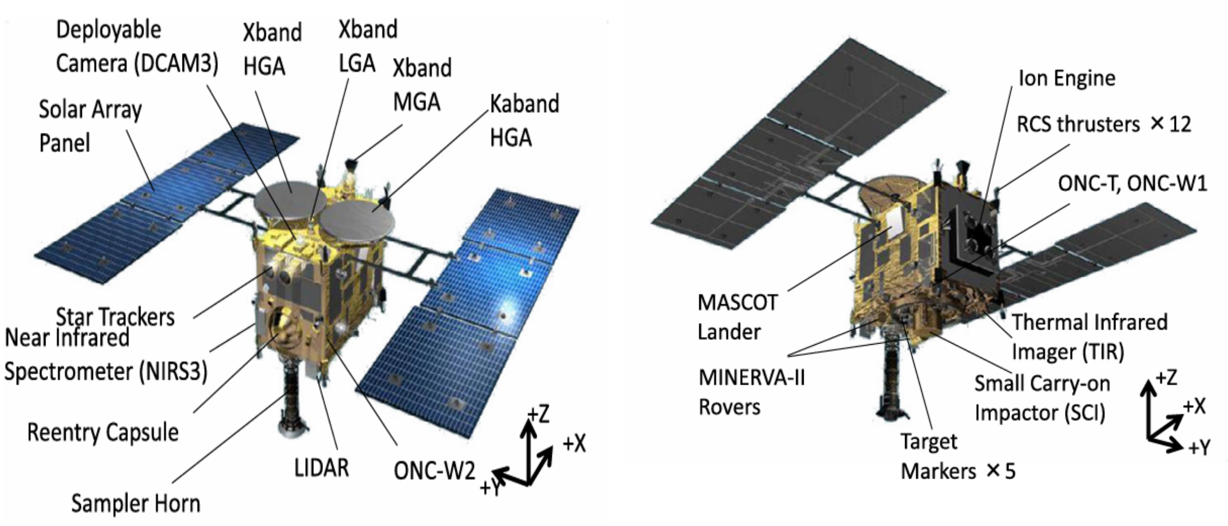

Figure 1.10: Hayabusa 2 model [20]

Hayabusa-2 also carried a group of small jumping robots called MINERVA-II, which consisted in MINERVA–II–1A (or HIBOU), MINERVA–II–1B (or OWL) and MINERVA–II–2, shown in Figure 1.11. MINERVA–II–2 was similar to MINERVA from the Hayabusa mission in shape and structure; while MINERVA–II–1A and MINERVA–II–1B were smaller in height, and both had only one motor inside to move. In addition, Hayabusa-2 had a cube-shaped lander MASCOT for in-situ detection, with a mass of 9.6 kg. MASCOT was also a jumping robot, and it realized hopping and self- righting on the Ryugu surface applying a momentum generated by a small brushless DC motor. It had a three-layer sandwich framework structure, principally used for carrying loads and to absorb part of the landing impact. MASCOT was released with spring mechanism at less than 100 m of altitude. [17]

The Hayabusa 2 mission was a success all around. MINERVA–II–1A and MINERVA–II–1B were released successfully reached the Ryugu surface, becoming the first hopping robots to land on an asteroid. MINERVA–II–2 was released and then successfully reached the surface after several bounces. Also MASCOT was ejected and came successfully to rest on Ryugu after four bounces; then it performed hopping and self-righting maneuvers three times. Hayabusa-2 successfully implemented both the first TAG operation and the second TAG operation in the artificial crater that had been bombarded by the impactor. [17]

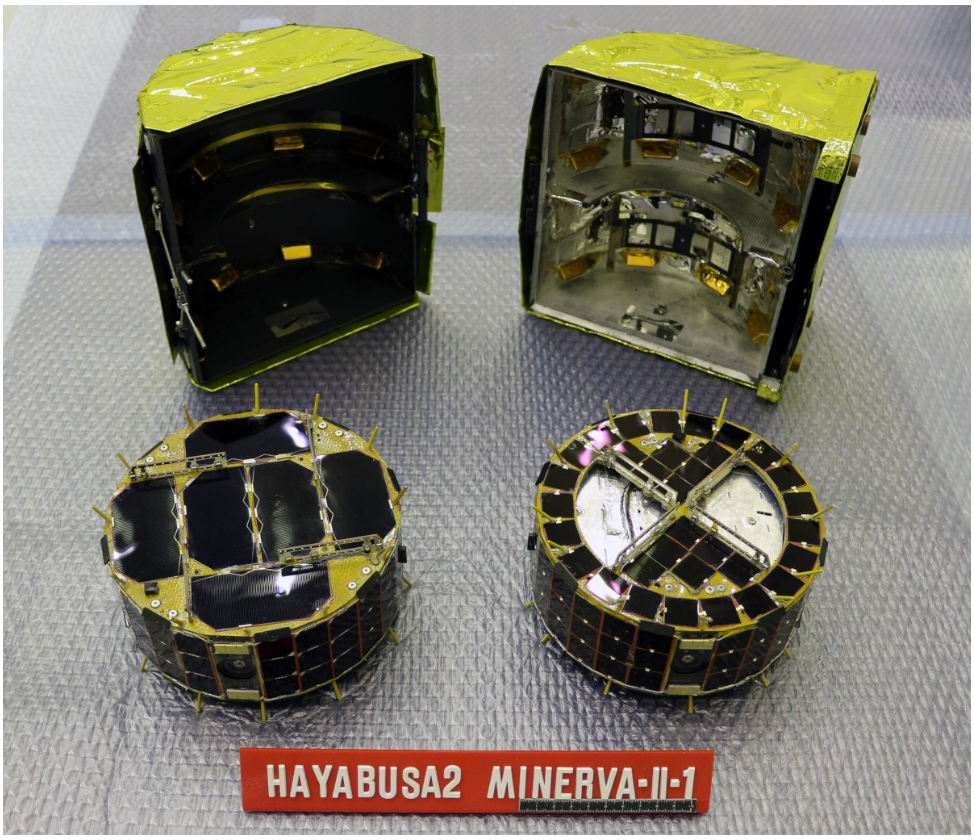

Figure 1.11: MINERVA II-1A and MINERVA II-1B [6]

1.2.4. Dawn

Dawn was the ninth mission in the Discovery program to explore the solar system. It was a unique scientific mission utilizing ion propulsion, which made it not only affordable, but also the least expensive of the Discovery missions. Dawn's targets were Vesta and Ceres, the most massive asteroids in the Main Belt, and chosen because they are intact and present during the events at the dawn of the solar system, and because they are very different too. Vesta underwent magmatic differentiation and began to solidify in the solar nebula. Ceres, on the other hand, contains much water ice and possibly subsurface liquid water, thus possibly leading to a different style of differentiation and a more dynamic surface. [21]

The spacecraft, represented in Figure 1.12, was three-axis stabilized and equipped with large solar arrays that provide the electrical power required to operate both the ion propulsion system, the onboard flight systems and the scientific payload. During the mapping phases at Vesta and Ceres, the spacecraft maintained continuous orientation of its scientific instruments toward the surface, while at the same time kept the solar arrays pointed toward the Sun for power generation. Scientific data collected during orbital operations were stored onboard and later transmitted to Earth; for these communication sessions, the spacecraft temporarily interrupted scientific observations and reoriented its high-gain antenna toward Earth. An important aspect of the mission to Vesta took into consideration was the extensive prior investigation of the howardite eucrite and diogenite meteorites, which are believed to originate from Vesta. This existing knowledge influenced the design of the scientific payload, which consisted of the framing camera, the visible and infrared mapping spectrometer, and the gamma ray and neutron detector. In addition, the spacecraft telemetry system provided radiometric tracking data that were used to characterize the gravitational field of the target bodies. The framing camera system was composed of two redundant cameras, although only one was operated during the mission thus far. The framing camera acquired images of the surface from multiple viewing geometries, enabling later the reconstruction of surface topography. During scientific observations, the instruments were directed toward the surface, while the three ion thrusters remained inactive. The visible and infrared mapping spectrometer acquired spectral measurements to produce hyperspectral surface images along a direction orthogonal to the spacecraft motion, or scanned the surface using an internal mirror to generate hyperspectral image cubes of selected regions. The gamma ray and neutron detector was designed to determine the elemental composition of the regolith to depths of several decimeters through measurements of gamma rays and neutrons emitted from the surface. [21]

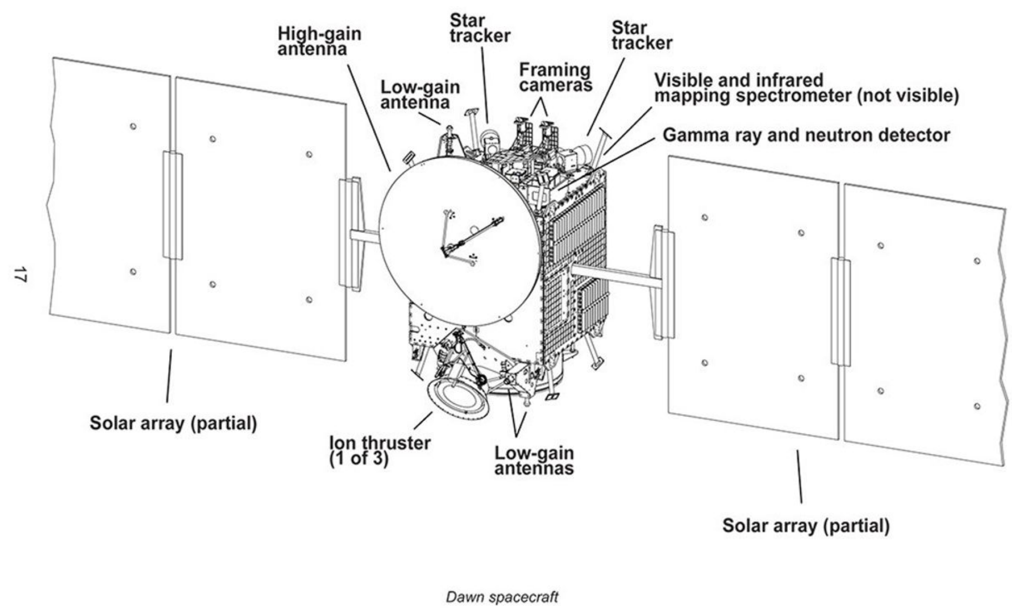

Figure 1.12: Dawn spacecraft model [7]

The Dawn spacecraft entered the gravitational sphere of influence of Vesta on July 16, 2011, and departed on September 5, 2012, remaining in orbit for more than 400 days. During this period, the spacecraft adjusted its orbital altitude and viewing geometry to conduct data acquisition across four principal orbital phases in order to satisfy the scientific requirements. The first phase consisted of 21 days in the Survey orbit at an altitude of approximately 2735 km above the surface. Followed by 34 days in the High Altitude Mapping Orbit 1 (HAMO1) at an altitude of 685 km. The spacecraft then transitioned to the Low Altitude Mapping Orbit (LAMO), located at an altitude of about 210 km, where it remained for 141 days. The final operational phase comprised 41 days in the second High Altitude Mapping Orbit (HAMO2). Different scientific instruments were prioritized during each orbital phase according to the mission objectives. During the Survey orbit, the primary instrument was the visible and infrared mapping spectrometer, which focused on acquiring spectral information of the surface. In HAMO1, the framing camera became the principal instrument, enabling detailed imaging and topographic reconstruction of the asteroid. During the LAMO phase, priority shifted toward measurements from the gamma ray and neutron detector and gravity-field investigations, while additional observations from VIR and the framing camera were also collected. [21]

1.2.5. MMX

Mars Moon eXploration (MMX) is a JAXA mission that will explore the Martian moons and return a sample from Phobos. The Martian moons Phobos and Deimos are important for understanding the origin and formation of Mars and the Solar System in general; for example, the exploration of the Mars system can also bring new information on how water was delivered to the rocky planets. Therefore, exploring the Martian system and returning samples from Phobos, the MMX mission would investigate the origin of the Martian moons, but also address significant questions on the formation of planetary systems and on the transport of material between the inner- and the outer Solar System.[22]

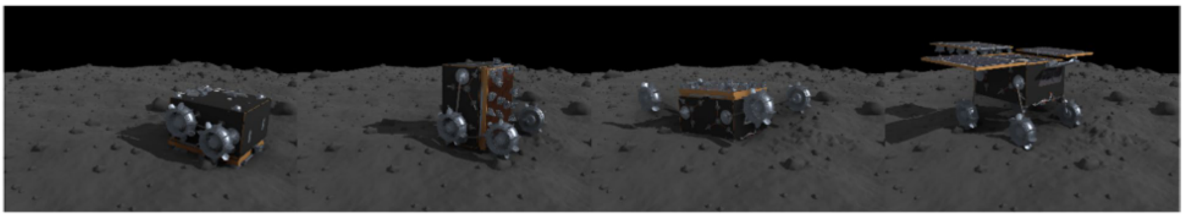

Figure 1.13: MMX uprightning sequence [23]

An important part of the MMX mission will be delivering the rover to the surface of

Phobos. The MMX Rover will perform in situ science, and also be a scout, preparing for the landing of the main spacecraft. The rover is set to be released from the mother spacecraft, before ballistically descending to the surface of Phobos and coming to rest in an unknown attitude after several bounces; after it will upright itself and deploy the solar panels, as represented in Figure 1.13. In addition to the many scientific objectives, the MMX Rover will have an important demonstration to achieve: the locomotion on wheels in a very low-gravity environment, since Phobos gravity is in the range of 0.3-0.7 mg. For this reason, no strict locomotion requirements have been set, and also because the distance reached by the rover on Phobos will strongly depend on the surface terrain and the soil is not yet known. The MMX mother spacecraft will act as a relay for all telemetry and commands between the Earth and the rover. [24]

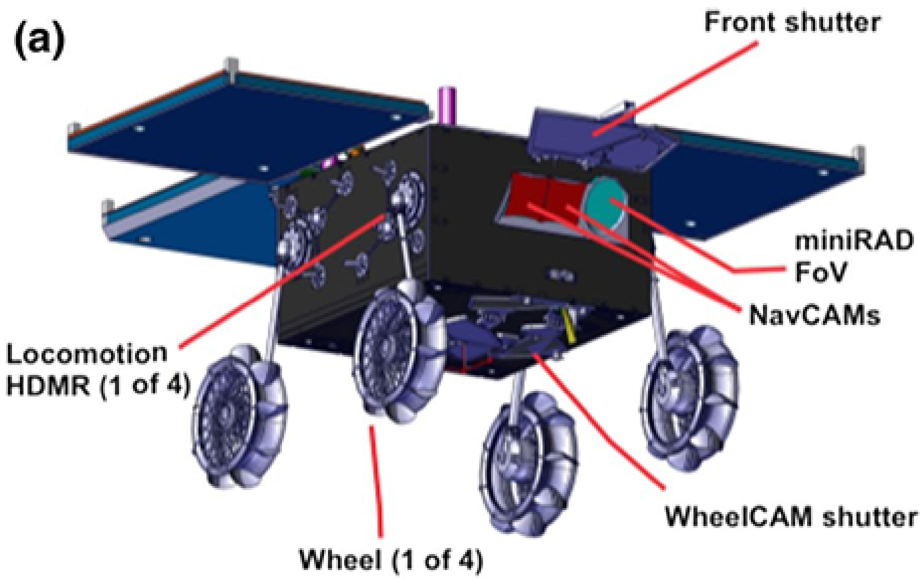

Figure 1.14: MMX rover model [24]

The MMX rover is a four-wheel autonomous system with a size of 41x37x30 cm and a mass of 25 kg, as shown in Figure 1.14. The body is a rectangular box and attached at the sides there are four legs with one wheel per leg [25]. The rover design accommodates four principal investigator instruments: the miniRAD instrument, the Raman spectrometer, the WheelCams and the navigation cameras. The miniRAD instrument will measure the thermal infrared surface emission to determine the surface brightness temperature. The compact Raman spectrometer was developed for in-situ mineralogical analysis, and is placed at the bottom side of the rover to measure downwards to the ground. The two WheelCams are also on the underside of the rover, each looking at a different rover wheel to capture in-situ images of Phobos' surface, to then examine the mechanical and dynamic properties of its regolith observing the interactions between the rover wheels and the surface terrain. Lastly, the navigation cameras consist of a stereoscopic pair of cameras that aim to answer the scientific questions about the surface geology of Phobos; in particular, the images will allow digital terrain models to be delivered with good ground sampling dimension. [23]

MMX is not an asteroid exploration mission but it was built on the experience of asteroid sample return spacecraft Hayabusa and Hayabusa 2, and it will set important achievements for the field.

2 | Mission

This chapter presents the mission concept for which the rover described in the following chapters has been specifically designed. It provides an overview of the target body, highlighting its scientific relevance within the context of small-body exploration. Lastly, the chapter outlines the primary scientific objectives of the mission.

2.1. Mission proposal

The proposed mission combines in situ exploration and sample return operations, both performed by a mobile rover deployed on the surface of asteroid Vesta. Building upon the scientific achievements of the Dawn mission, as well as the technological heritage of rover-based small-body exploration missions such as Hayabusa and Hayabusa2 with their hopping rovers, and the Martian Moons eXploration mission featuring a wheeled rover, the mission aims to advance both scientific understanding and surface mobility capabilities in low-gravity environments. As one of the largest differentiated bodies in the main asteroid belt, Vesta represents a unique target for investigating the early stages of planetary formation and evolution. Through detailed surface analysis, subsurface sampling, and the return of untouched material to Earth, the mission seeks to address prominent questions regarding the evolution, collisional history, and compositional diversity of protoplanetary bodies, ultimately contributing to a deeper understanding of the formation and dynamical evolution of the Solar System.

2.2. Vesta

Asteroid (4) Vesta (Figure 2.1) was discovered on 29 March 1807 by the German astronomer Heinrich Wilhelm Olbers and named after the Roman virgin goddess of home, hearth, and family. Vesta is the second most massive asteroid in the Solar System after Ceres and the third largest considering the volume, following Ceres and Pallas. Scientific interest in Vesta increased significantly after studies demonstrated that its spectral reflectance closely resembles that of the howardite–eucrite–diogenite (HED) meteorite group, the largest class of achondritic (igneous stony) meteorites currently available for study. The hypothesis that Vesta is the parent body of the HED meteorites has therefore provided an important framework for integrated geological, geophysical, and geochemical investigations of differentiated asteroids.[26]

Vesta has the shape of a triaxial ellipsoid with principal axes measuring 286.3 km, 278.6 km, and 223.2 km, corresponding to a mean radius of 262.7 ± 0.1 km. With an estimated mass of 2.59×10^{20} kg, the asteroid exhibits an average surface gravity of approximately 0.25 m/s^2. However, variations in internal density distribution and topography generate significant local differences in the gravitational field. Due to its relatively weak gravity, Vesta preserves pronounced topographic variations in elevation, with most surface slopes ranging between 5° and 10°, while some regions reach inclinations of up to 40°. [27]

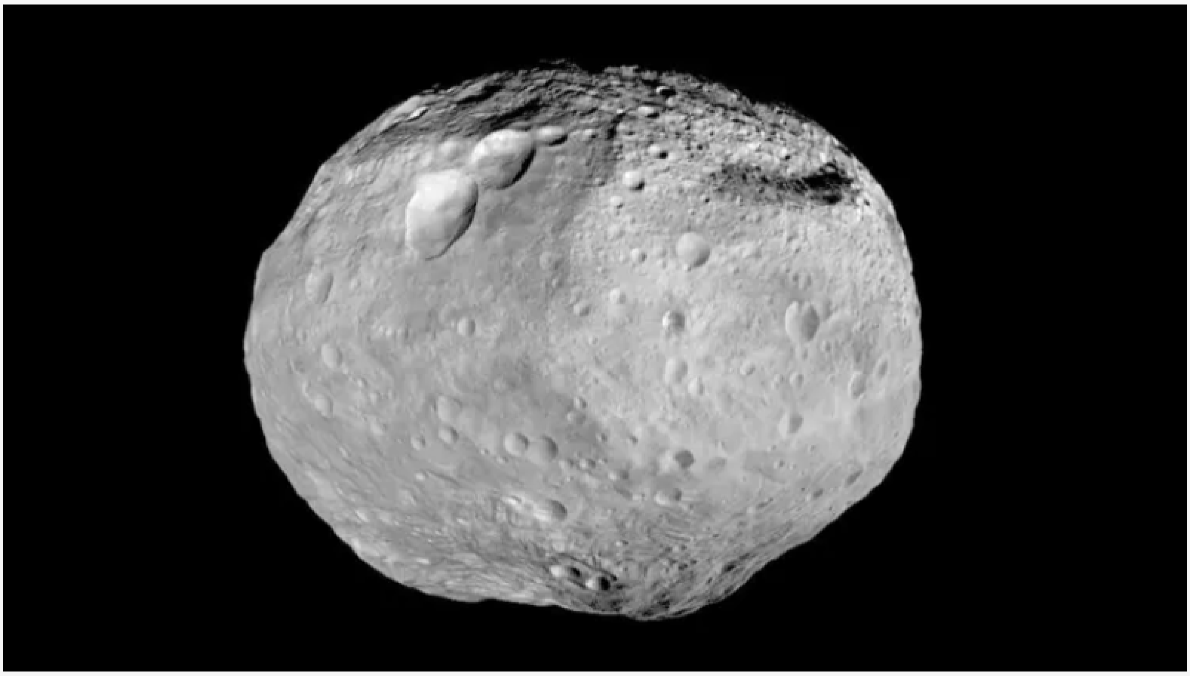

Figure 2.1: asteroid (4) Vesta [7]

The giant impact basin Rheasilvia, named after the mythical mother of Romulus and Remus, was first identified through observations by the Hubble Space Telescope. The basin, approximately 500 ± 20 km in diameter, is centered near Vesta's south pole; considering the size of its parent body, Rheasilvia is among the largest impact basins in the Solar System. One of the most remarkable structures within Rheasilvia is its central uplift, formed by the rebound of subsurface material following peak compression during the impact event. Central uplifts are characteristic features of large impact basins observed on

Earth, the Moon, Mars, Mercury, and several outer planetary satellites; however, its central peak rises nearly 20 Km above the surrounding terrain, making it the second-highest known mountain in the Solar System. [26][27]

Topographic mapping of Vesta also revealed a second major basin, Veneneia, named after one of the legendary Vestal Virgins. Veneneia has an approximate diameter of 400 km and a depth of about 12 km. The younger Rheasilvia basin partially overlaps nearly half of the older Veneneia structure, as it can be seen from Figure 2.2. In addition to these large basins, Vesta hosts at least ten other craters exceeding 50 km in diameter, including an older crater roughly 250 km wide that was also partially overprinted by Rheasilvia. The southern hemisphere displays a relative scarcity of craters, consistent with extensive resurfacing caused by the Rheasilvia and Veneneia impact events. In contrast, the heavily cratered northern terrains appear to represent older and more stable surfaces that were largely unaffected by ejecta deposits from the southern basins. [26][27]

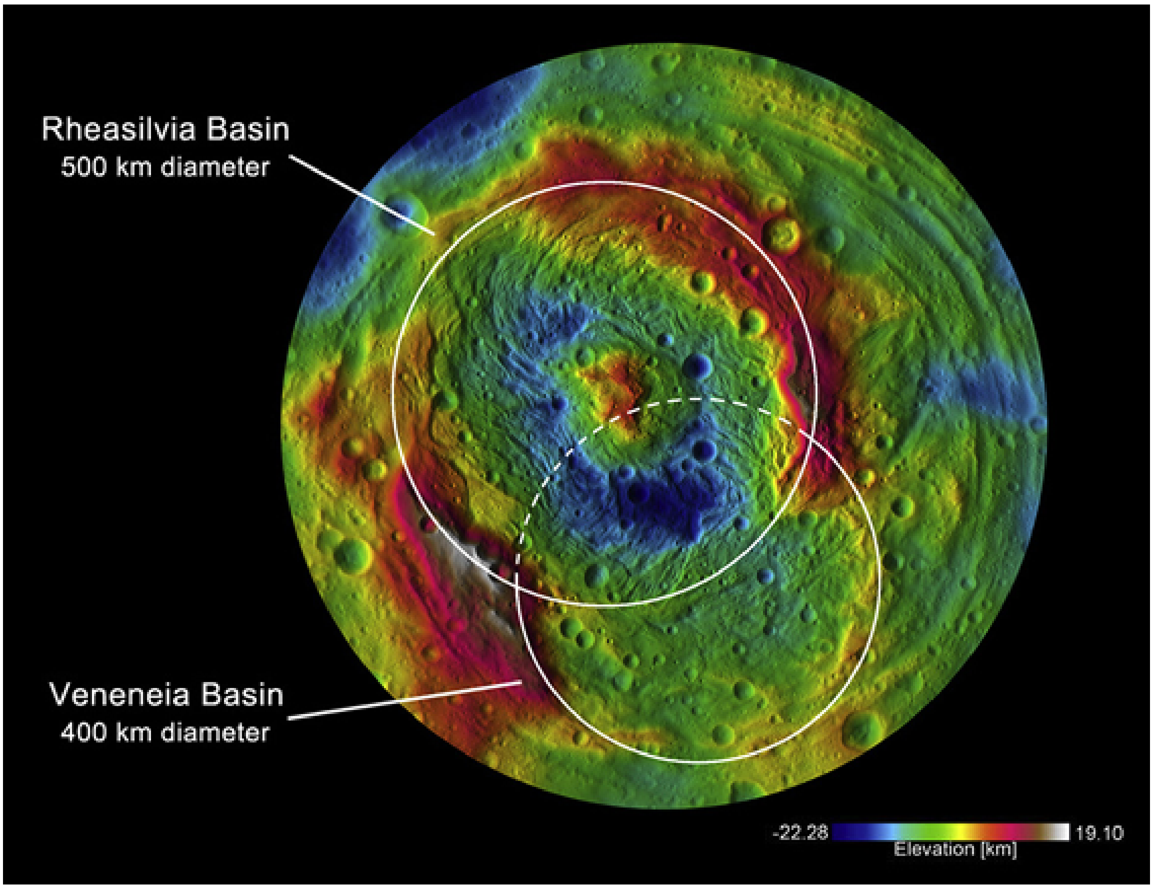

Figure 2.2: Rhaesilvia and Veneneia basins [26]

2.3. Scientific objectives

Based on the open questions left by the Dawn mission, this mission proposes a further exploration of Vesta with details that only in situ analysis and a sample return could offer. Returning pristine material from Vesta and studying it on Earth would provide new insights into fundamental questions related to the history of the asteroid and the solar system in general. The driving questions addressed are:

1. How did Vesta differentiate?
2. Is Vesta the parent body of the HED meteorites on Earth?
3. How did water get to Vesta?

Addressing the three scientific questions is essential for reconstructing the origin and evolution of both Vesta and the early Solar System. As the largest intact differentiated asteroid, Vesta preserves evidence of a fully differentiated internal structure, including a metallic core, making it a unique laboratory for investigating the primordial stages of terrestrial planet evolution. Understanding its differentiation provides insight into the igneous processes, which could also be represented in the HED meteorites. These meteorites, widely considered to originate from Vesta, constitute the most comprehensive samples available from any differentiated asteroid and therefore provide critical constraints on the parent body's chemical, mineralogical, and thermal evolution. In addition, studies of HED meteorites constrain the timing of Vesta's differentiation and crust formation, establishing a framework for interpreting its geological history. More broadly, studying differentiated planetesimals such as Vesta reveals the diversity of evolutionary ways experienced by early Solar System bodies and improves our understanding of the processes that governed rocky planet formation, planetary atmosphere formation, and the delivery of water to terrestrial planets. [28][29]

In order to answer the questions as completely as possible, the corresponding scientific objectives were drawn:

- Investigate the chemical composition of lower-albedo regions seen on Vesta
- Estimate the elemental abundance and isotopic composition of lower-albedo regions seen on Vesta
- Estimate the volatile content of lower-albedo regions seen on Vesta
- Thermal analysis
- Seismic analysis

- Return a mass of samples sufficient to perform the minimum necessary analysis on Earth

In order to address all scientific objectives as well to reduce the complexity of the overall mission, in-situ measurements would be performed. These measurements would ensure that all objectives of the mission can be achieved regardless of alteration of the volatiles during the return phase; and leaving to be done on Earth all the experiments that require large and extremely high precision instrumentation, which is not feasible to accommodate on a spacecraft.

To accomplish all the scientific objectives of the proposed mission, the implementation of a lander capable of movement is essential. A rover able to locomote on the surface can access multiple areas of interest, allowing in situ measurements and sample acquisition across diverse geological environments that would otherwise remain unreachable with a stationary platform. Mobility therefore represents a key characteristic for maximizing the scientific return of the mission. Hence, a few a high level requirements can be drown:

- the rover shall be able to move freely on the surface of Vesta;
- the rover shall move safely on the surface of Vesta;
- the rover shall be able to carry a sizable scientific payload;
- the rover shall perform multiple scientific experiments;
- the rover shall obtain a minimum quantity of surface sample to return to Earth.

In this context, the final objective of this thesis is to develop a preliminary design of the rover's locomotion subsystem for the mission proposed in this chapter, with particular focus on the mobility architecture and its adaptation to the operational and environmental constraints of the mission.

3 | Locomotion system technologies and trade-off analysis

In this chapter, the first part is dedicated to presenting the principal locomotion technologies developed for space exploration, defining their advantages, detriments and operational principles. In the second part, a trade-off analysis is carried out to find the best solution for the mission proposed, based on chosen parameters selected considering the type of expedition, its scientific objectives and the environment encountered.

3.1. Locomotion system technologies

Current locomotion concepts can be classified into the following groups according to their operating principle: classic wheeled systems, hopping rovers, multi-legged robots and modified wheeled technology [30]. A review of these main categories is presented, providing their working principles, advantages and limitations. The present analysis and consequent trade-off do not take into account newer technologies like tensegrity robots [31] and soft robots [32]; even though they are promising options, they are still emerging fields of research, currently subjects of initial studies.

3.1.1. Classic wheeled rover

Classic wheeled locomotion has been typically defined as travelling the environment by rolling using passive suspension, and it is intended for uninterrupted ground contact [30].

Wheeled locomotion is the oldest locomotion technology: it is very well understood and it has been researched and used extensively on numerous planetary exploration missions on the Moon and on Mars [33].

The classic wheeled rover design is essentially built on the principle of minimizing mechanical complexity and redundancy while maximizing efficiency and speed. This approach exploits the continuous rolling motion of the wheels to translate rotational energy into forward movement with low energy dissipation [34].

Wheeled locomotion relies its movement on traction obtained from friction, a force that is proportional to the normal force from the weight of the rover. The driving force for wheeled rovers is [35]:

$$f_w \leq \mu m_r g \tag{3.1}$$

Where μ is the friction coefficient between ground and wheel, m_r is the mass of the rover and g the acceleration of gravity. Therefore, the driving force is proportional to gravity, and on the surface of asteroids, where local gravity can be extremely low, traditional rovers have difficulties achieving mobility. The lower the frictional force, the smaller the traction must be; thus the rover's wheels should revolve slowly to make the rover translate, or the wheels would just continuously keep slipping [36].

On surfaces with loose soils, steep slopes, or in general significant irregularities, and also electrostatically charged regolith, wheeled systems may experience slippage, reduced traction, or damage. The rover could get stuck in sand dunes, and rocky terrains are inaccessible. This type of rover has limited climbing abilities: typically it's only able to overcome obstacles the size of their wheel diameter. Therefore, avoiding large obstacles or unsuitable terrain is necessary, but it also requires complex and slow path planning and it restricts the potential landing sites of research too [33].

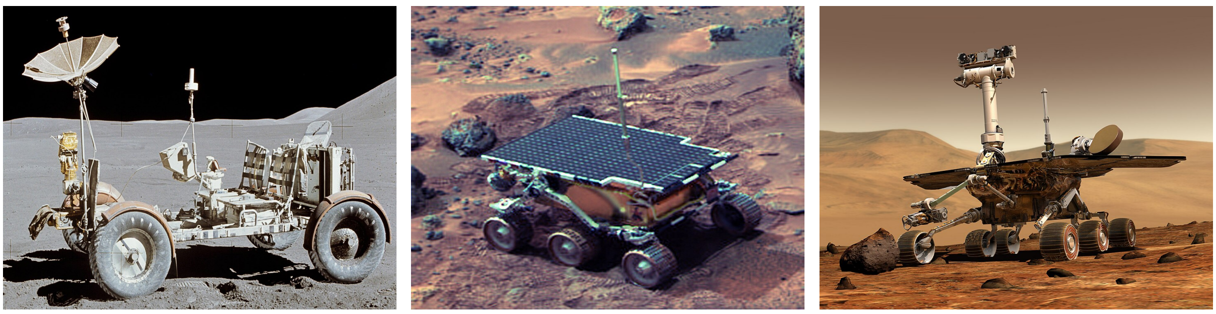

Figure 3.1: Classic wheeled rover examples; from left to right: Lunar Roving vehicle [7], Sojourner [37], Spirit rover [7]

This type of rover is very flexible to the mission, the size and weight of the design can be adapted depending on the task it is needed for and therefore on the scientific payload it transports. Figure 3.1 shows three classic rovers with very different sizes and payloads capacity. The Lunar Roving Vehicle used on the Apollo mission to transport a 440 kg payload (2 astronauts included) was 2.3x3x1.1 m and weighted 210 kg [7]. Sojourner of the Mars Pathfinder mission accomplished all its mission objectives with a mass of just 11 kg, and 65x48x30 cm [37]. The twin rovers Spirit and Opportunity completed many experiments on Martian soil, they had a mass of 180 kg and dimensions: 1.5 m high, 2.3 m wide and 1.6 m long [7].

3.1.2. Multi-legged rover

The multi-legged systems are the newest technology considered for the trade-off. The state of the art for terrestrial legged robots has reached maturity; and as the technology advances, the concept of legged locomotion expands to space explorations [33]. There is less field experience for legged rovers, since they have never been used on planetary or asteroid exploration missions, but they are largely considered the blueprint for future space exploration mission.

Legged systems offer increased versatility and flexibility in challenging environments; their capability of responding to the local features of the ground makes them perfect in missions involving detailed scientific exploration and sample collection and for operations where the terrain is unpredictable, too rough or too soft [34]. Multi-legged robots can climb steep slopes with loose soil, even though more traditional rovers are prone to sinkage in soft terrain. They can move more freely, their ability to walking in every direction, turning on the spot and climbing or jumping reduces the need for unnecessary manoeuvres to avoid obstacles.

Legged mobility is thought to be the future solution for scientific exploration missions on asteroids because of two main advantages over other moving systems. Legged systems can use inter-limb forces (or ground reaction forces) to actively anchor to the surface. This strategy minimizes the forces at each contact point, therefore maintaining a secure connection to the terrain despite the absence of significant gravitational forces. Also their movement does not depend on normal forces, that are usually generated by gravity. Multi-legged systems are designed to minimize the potential danger of interaction forces, that could accidentally cause the robot to lose contact with the terrain, or exceed the exit velocity of the small body [38].

Multi-legged rovers consume more power than other locomotion systems because of their extreme mechanical complexity. Planning and controlling the walking motion of a robot with multiple degrees of freedom is computationally intensive, and thus reduces energy efficiency.

Also, shock loads are an important drive parameter for some parts of this locomotion system. This types of loads during landing could lead to serious consequences. Examples of possible critical scenarios are: collision with the ground and the consequent damage of the scientific payload, the robot getting stuck in complex terrain and not able to go back to its standing state, a rebounce after landing that leads to escaping the gravitational field [39].

In recent years, many prototypes of multi-legged robots created for space exploration have been developed. Figure 3.2 presents few of them: the series of LEMUR robots from JPL; Olympus, a four legged rover for Mars exploration that recently experienced simulated microgravity at an ESA facility; MANTIS, a robot for lunar missions; and many others [40].

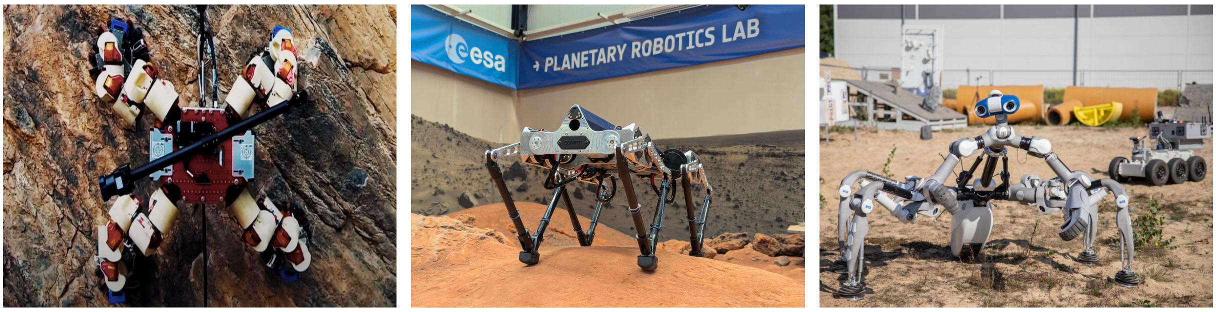

Figure 3.2: Multi-legged rover examples; from left to right: LEMUR [37], Olympus [15] and MANTIS [41]

3.1.3. Hopping rover

Hopping rovers are usually called hoppers. The hopping mechanism can be either internal (reaction wheel, DC motor) or external (a moving part that strike the surface), and it makes the robot push the small body's surface. This increases the contact force between the terrain and the rover's body, which makes the friction larger, and therefore, it can obtain higher horizontal speed than wheeled mechanism; once hopped into free space, the robot moves in a ballistic orbit. For this reason, hoppers are very useful on asteroids and small bodies in general, because under the influence of low gravity, they can travel long distances ballistically and can overcome high obstacles [19].

Jumping relies on high and short bursts of energy storage and release; that combined with renewable resources usage can potentially be a solution for the energy self-loading problem and also increase efficiency in extraterrestrial exploration. It usually requires such little mechanical energy that it is almost negligible to the overall power budget. However, the power required by the hoppers is directly proportional to the size and density of the small body; thus, energy requirements can become concerning for very large asteroids.

The physical properties of the surface, such as friction and cohesion, should be known and well understood for an accurate prediction of the hopping dynamic and its outcomes (velocity, angle, distance travelled, ecc.) [42]. Since the force transferred to the robot depends on the robot-terrain interaction, the dynamics of the surface are critical to obtain controlled landing and mobility [43]. The efficiency of hoppers on sandy surfaces is worse than on hard ground because this type of terrain can be deformed and it easily causes slips [44]. As for wheeled mobility, steep slopes are harder to traverse.

The hopping rover will typically land in an unpredictable configuration, thus, in order to manage the multiple possible landing scenarios, self-righting mechanisms are usually included into the design; as well as a way to protect the jumping mechanism and the scientific payload from the danger the crash of the landings can dispense [45].

Hoppers have been used frequently for research on small bodies, some successful examples designed for exploration are represented in Figure 3.3: MINERVA (0.6 kg, 12x12x10 cm) for the Hayabusa mission, MASCOT (10 kg, 30x30x10 cm) and MINERVA II, four hopping rovers (all four around 1 kg) developed for the mission Hayabusa 2 [6]. However, they are all designed in a small and light scale to maximize the hopping distance, and without a big scientific payload on board, therefore heavy experiments are typically not possible.

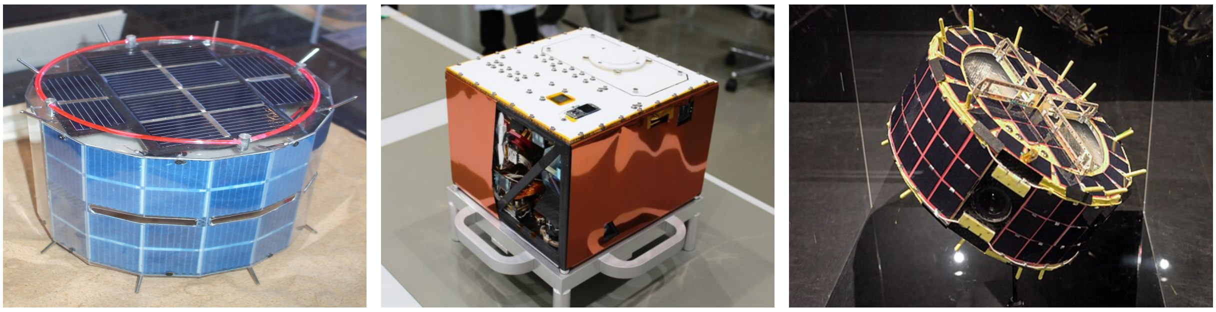

Figure 3.3: Hopping rover examples; from left to right: MINERVA [6], MASCOT [6] and MINERVA II [6]

3.1.4. Modified wheeled rover

Modified wheeled rovers apply changes to classic wheeled surface travel. The changes introduced may take several forms, such as actively modifying suspension characteristics through active or semi-active suspension, or changes in linkage aspects between the wheel and the chassis, such as not angle-fixed legs. However, ultimately the wheel is kept as the actuator, and the same way of generating the motion is applied, thus wheel rolling [30].

Similarly to classic wheeled travel, modified wheeled travel can generate motion through traction. Therefore, all the mobility problems in a microgravity environment presented in subsection 3.1.1 for traditional rovers can also be attributed to modified wheeled rovers. However, the modifications on classic wheeled rovers can result in the implementation of an additional locomotion mode, that can be referred to as wheel walking. This new mode of travel adds some of the advantages of legged locomotion to wheeled travel: modified wheeled rovers have improved tractive performance, they can generate a greater grip and climbing torques in challenging conditions, such as sandy terrains or high slopes. Exactly where the rolling motion of the wheels was subject to high slip ratios.[46]

The better performance adds complexity and degrees of freedom to the design, and also computational and mechanical power to the overall budget, but it is typically accepted as a trade-off to allow greater flexibility in the exploration and to avoid entrapment [30].

Comparably to classic wheeled travel, modified wheeled rovers are adaptable to the mission and the payload transported. Therefore, the technology continues to develop and improve, offering numerous prototypes that differentiate both in size and design, Figure 3.4 shows three of them. The IDEFIX rover designed for the JAXA mission MMX will be the first wheeled rover to move and execute multiple scientific observations on an celestial object that small; it weights 25 kg and has dimensions of 41x37x30 cm [6] and proposed an active leg technology. The Rosalind Franklin, created for the ExoMars mission, was 310 kg heavy and occupied 2x2.5x2.5 m [15]. The first ATHLETE prototype developed by JPL in the context of the study of heavy-lift utility vehicles to support human exploration of the lunar surface is 2.75 m wide and a maximum height of over 2m, the mass is approximately 850 kg, and the maximum payload capacity it can carry is 300 kg on Earth [37].

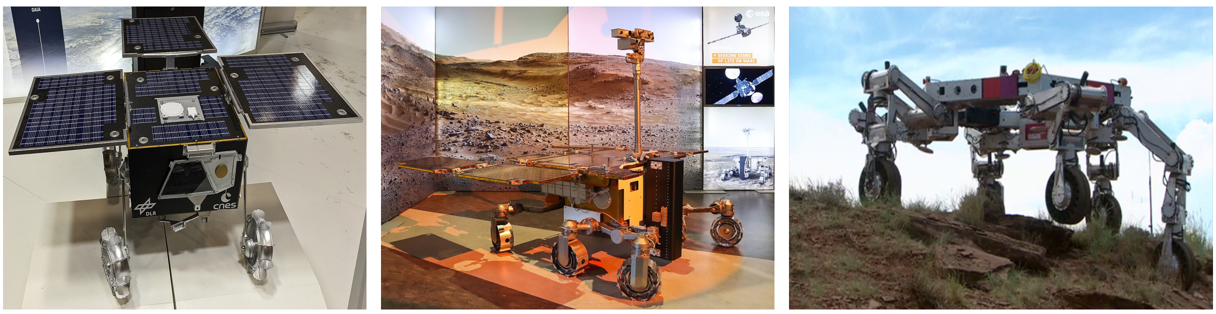

Figure 3.4: Modified wheeled rover examples; from left to right: MMX rover [6], Rosalind Franklin [15] and ATHLETE [37]

3.2. Trade-off analysis

A trade-off analysis is carried out between the four technologies outlined in the previous section: the classic wheeled rover, the hopping rover, the multi-legged rover and the modified wheeled rover. The goal is to select the best suited locomotion system for the mission proposed, determining the technology able to provide adequate traction on a large variety of surface conditions in a milligravity environment, while also minimizing spacecraft resources' use. Following, the method selected for the trade-off is explained, then a description of the chosen parameters is outlined and the results are illustrated in the end.

3.2.1. Analytical hierarchy process

The trade-off analysis is achieved through the Analytical Hierarchy Process (AHP), a well-established methodology to select the better among alternative solutions when multiple objectives and parameters need to be taken into consideration [47]. First, the candidate solutions have to be selected; then, the parameters have to be selected tacking into account the mission requirements stated in section 2.3. These parameters will guide the decision making process so their significance should be explained. All the steps of the AHP are applied twice, on the parameters and on the technologies. The initial phase is a pairwise comparison, applied to the parameters to express their relative relevance, and multiple times on the technologies, to evaluate their relative accomplishment with respect to each one of the parameters. The ultimate rating is achieved with the linear combination of the intrinsic weight of every parameter with the corresponding weight of each technology for that parameter. The AHP steps:

1. **Pairwise comparison:** construction of a square matrix $A = [a_{ij}]$, where each element a_{ij} describes how much the technology i is preferred to the technology j considering a certain parameter, or how much the parameter i is more important than the parameter j for the problem proposed. The diagonal is composed of ones. The elements above the diagonal are composed of values according to personal knowledge on the subject and the numerical scale by Saaty (1994) illustrated in Table 3.1. The elements below the diagonal are their reciprocals $a_{ji} = 1/a_{ij}$. By the end of this step there should be $N + 1$ square matrices: one $[NxN]$ to represent the importance of the parameters, and N matrices $[nxn]$ to represent the performance of the technologies for each parameter, where N is the number of parameters and n is the number of technologies.

The values assigned in the pairwise comparison matrix are primarily based on subjective knowledge and judgment, and therefore there could be inconsistencies and contradictions. In order to reduce this problem, a Consistency Ratio (CR) is computed for each matrix, to assess the consistency of all the comparisons for a parameter.

$$CR = \frac{\lambda - n}{(n-1)RI} \tag{3.2}$$

where λ is the maximum eigenvalue of the matrix, n the size of the matrix and RI is the Random Index, a tabulated number dependent on the size of the matrix. The usual threshold is 0.1, thus if $CR < 0.1$ the matrix is considered consistent in its entirety.
The matrices built with this procedure and their CR value are reported in Appendix A, while the obtained weights and the final technology ranking can be found in subsection 3.2.3.

Value	**Definition**	**Explanation**
1	Equal importance	Two technologies contribute equally to the objective
3	Weak importance	Experience and judgement slightly favour one technology over the other
5	Strong importance	Experience and judgement strongly favour one technology over the other
7	Demonstrated importance	One technology is strongly favoured and demonstrated in practice
9	Extreme importance	The evidence favouring one technology over the other is of the highest possible order
2,4,6,8	Intermediate values	When compromise is needed between two adjacent judgements

Table 3.1: AHP numerical scale developed by Saaty [48]

2. **Weight vector:** the matrix obtained in the previous step is normalized columnwise:

$$||a_{ij}|| = \frac{a_{ij}}{\sum_i^n a_{ij}} \tag{3.3}$$

Then the weight is extracted:

$$w_i = \frac{1}{n}\sum_{j}^{n} ||a_{ij}|| \tag{3.4}$$

The sum of all weights should be equal to one and they can be converted into percentages by multiplying the weight by one hundred. When this step is done, each parameter has an intrinsic weight that represents its relevance in the problem, and each technology has a relative weight for each parameter illustrating its efficiency for that criterion.

3. **Final ranking:** the overall rating for each technology is computed with a linear combination of the intrinsic weight of every parameter with the corresponding weight of each technology for that parameter.

3.2.2. Trade-off parameters

Following, the parameters used in the trade-off are defined and for each one of them the technologies explained in section 3.1 compared to each other.

- **Volume:** it represents the volume occupied by the locomotion system. The volume should be small enogh to reduce costs, while also maximizing the allocation of scientific instruments. Hopping is the most compact system, usually stowed inside the body of the rover. The wheeled systems follow with their size adaptability; while the multi-legged rover mechanical complexity prevents them to extremely reduce their size.
- **Mass:** it is the total mass of the locomotion system. It should be minimized in order to have lower costs and be able to accommodate more scientific payload. As for the volume, hopping is the best solution to reduce mass budget, followed by wheel locomotion and multi-leg.
- **Power:** it is the electric power consumed by the locomotion system. Again, it should be minimized to decrease costs, but also mass and volume reserved to power generation. A classic wheeled rover minimizes power usage thanks to its simplicity; while a modified wheeled system is slightly more complex, hence requires larger power. Hopping is usually very efficient but large asteroids like Vesta can be a power budget concern. Lastly, multi-legged systems are mechanically intensive and also need to process higher volumes of data.

- **Gravity:** this parameter describes the competence of a locomotion system to function in a milli-gravity environment. The least impacted by low gravity is the multi-legged rover. The second best way of moving in a low gravity environment is hopping since it does not rely on traction. The wheeled rovers have more difficulties in this condition, but a modified wheel can accommodate the walking mode.

- **Surface characteristics:** it expresses the capacity of a locomotion system to operate on a wide variety of surfaces. The multi-legged rover is the most versatile system since they can walk both on hard rock and soft granulate. It is followed by the modified wheeled rover with its possibility for wheel-walking. Hopping is mainly suited for hard surface usage, and a classic wheel rover could have problems both on very rocky terrains and on loose regolith.

- **Reliability:** it indicates the ability of the system to provide a stable and reliable locomotion, for this purpose it is extensively based on level of knowledge and practical field experience. Wheeled rover technology is very well understood and has been used extensively in missions for decades. Hopping has been the main topic of study regarding how to move on asteroids for years with some successful missions. The multi-legged rovers have just recently become the principal subject of research, with no active space mission yet.

- **Safety:** this parameter represents the capability of the locomotion system to operate without putting the rover in danger. Regarding risks like tipping over, getting stuck or other conditions that could potentially break or impede the rover to completely continue with its mission, the modified wheeled locomotion system is the least concerned. The classic wheeled rover possesses similar locomotion characteristics, but the absence of a walking mode makes the rover more prone to cut the mission short. Multi-legged systems are more complex and fragile, and hopping rovers involve a landing scenario for each step.

- **Complexity:** it assesses the simplicity of the system, considering the number of components and the control logic needed. The classic wheel rover design aims to maximize simplicity; hopping too does not rely on an excessive amount of components and complex control logic. The modified wheeled rover needs a more elaborated control for the multiple moving modes, and the multi-legged rover has the highest degree of mechanical complexity and control logic sophistication.

In Table 3.2, every parameter is assigned a value to show its importance in the mission, to guide the comparison procedure for the pairwise matrix and compute the weights. Small values are linked to higher importance, and high values to minor relevance. When multiple parameters are assigned the same value is because they contribute similarly to the global viability of the mission, and therefore, must be satisfied at the same time. Gravity and surface characteristics are considered the most critical parameters. The mechanical properties of the surface of Vesta are mostly yet unknown, therefore, the locomotion system should be able to operate on many types of terrain. Low gravity creates an environment where it is extremely difficult to function, as a consequence, the technology must be able to move in this condition. Safety and power are next in the ranking: safety because the locomotion system shall not compromise the integrity of the rover; power because the power budget in space missions typically poses an important constraint on the design. Following, mass and reliability, where the advantages of having a low mass budget and a system with field experience are obvious; however, a slightly heavier mass and less expertise can be accepted for an assured greater performance. Complexity is a less critical parameter, in fact, higher mechanical and control complexity is admissible if it leads to better locomotion capabilities. Volume ranks the lowest, because all technologies can be sized, however some can scale more than others.

Parameter	**Value**
1	Gravity
1	Surface characteristics
2	Power
2	Safety
3	Mass
3	Reliability
4	Complexity
5	Volume

Table 3.2: Trade-off parameters and corresponding value

3.2.3. Trade-off results

The results of the trade-off, the weights of the parameters, and the performance of the four locomotion technologies with respect to each parameter, are all reported in Table 3.3. In the final ranking, the technology that better satisfies most of the parameters has the highest percentage.

The results are divided into two groups. The first group is composed by technologies that score less than 23%, and it is constituted by the hopping rover and the classic wheeled rover. The hopping rover shows consistently a poor performance, ranking second lowest for many parameters. On the other hand, the classic wheeled technology, even considering good results in numerous criteria, it presents significant drawbacks for the most important parameters. For these reasons, they are not considered suitable baseline solutions for the locomotion system. The second group has scores higher than 27%, and it is formed by the multi-legged rover and the modified wheeled rover. Both technologies are highly promising, but the multi-legged rover is strongly penalized by its complexity and being an emergent technology in its early stages of development. Eventually, the modified wheeled rover offers the most robust and adaptable performance, serving as a solid foundation for a locomotion system on Vesta.

Technology	**Surface characteristics**	**Gravity**	**Safety**	**Power**
Classic wheeled	6.301%	7.178%	25.535%	51.882%
Multi-legged	46.878%	53.059%	12.795%	4.613%
Hopping	14.934%	24.446%	6.493%	12.029%
Modified wheeled	31.886%	15.314%	55.176%	31.475%
Weights	23.389%	23.389%	14.004%	14.004%

Technology	**Mass**	**Reliability**	**Complexity**	**Volume**	**Results**
Classic wheeled	23.470%	45.844%	48.458%	20.089%	**22.939%**
Multi-legged	8.202%	7.009%	5.629%	7.886%	**27.638%**
Hopping	44.857%	15.406%	28.434%	51.934%	**20.071%**
Modified wheeled	23.470%	31.739%	17.477%	20.089%	**29.351%**
Weights	8.291%	8.291%	5.158%	3.471%	

Table 3.3: Trade-off results for the chosen technologies

4 | Locomotion system design

This chapter presents the design of the locomotion system for the modified wheeled rover intended to operate within the mission scenario described in chapter 2. The chapter is structured into three main sections: the first focuses on the wheel design, while the second presents the suspension system. For both subsystems, the trade-off analyses used to identify the final design solutions are discussed. Lastly, the chapter concludes with a section dedicated to a comprehensive characterization of the complete locomotion system.

4.1. Wheels' design

This section presents the wheel design process and the corresponding trade-off analysis. It begins with the selection of the appropriate number of wheels for the rover configuration. Subsequently, the wheel technologies considered during the trade-off study are introduced, and their operating principles, advantages, and limitations are discussed. A comparative trade-off analysis is then performed to identify the most suitable solution according to the selected evaluation criteria, and its results are discussed. Lastly, the wheel CAD model and the Finite Element Method (FEM) analysis are presented, leading the characterization of the final wheel design.

The present trade-off analysis takes into account only two types of wheel design: one developed for the MMX rover and the other created for the Rosalind-Franklin rover of the ExoMars mission. These two configurations were selected because they represent fundamentally different design approaches, thus comprehending a wide range of possible wheel characteristics. Furthermore, the rovers on which they are implemented are regarded as important examples of modified wheeled rover systems.

4.1.1. Wheels' number

All successful missions with a rover had variations regarding the suspension of the locomotion system or the wheel design itself, but every one of them started from the blueprint of a 4 or 6 wheeled vehicle.

The trade-off study in Apostolopoulos (2001) [49] compares the simulations of a six-wheeled vehicle with the wheel diameter of 20 cm and a four-wheeled vehicle with the wheel diameter of 30 cm. The six-wheeled vehicle results in greater sinkage, more resistance, less drawbar pull, and shallower maximum slope ascension than the four wheeled one. Hence, this type of vehicle tends to sink deeper into soft ground, requires more effort to move, generates less useful pulling force, and cannot climb slopes that are as steep, therefore it is easier to stop completely the mission because the rover can not move anymore. The results favored the four wheeled vehicle for the lower weight and amount of components, derived from having two wheels less. However, the six wheeled rover used in the study also had a rigid suspension, and the best asset of the six wheeled approach is the flexible suspension, that allows the vehicle to keep as many wheels in contact with the ground as possible to maintain tractability [30]. This permits greater stability and redundancy and to have a better distribution of the rover's load among all the wheels, and it allows this configuration to be suitable for high mobility performance on rocky surfaces. It is usually seen as an acceptable compromise. However, the slightly increased rolling resistance, additional complexity, more actuator parts, thus supplemental resource consumption need to be considered as well. [30] [50]

Considering every aspect just brought forward, a six wheeled vehicle was selected as the best possible solution for the mission proposed. Tacking into account a flexible suspension, a six wheeled rover was thought to deliver a better performance on the type of environment that the mission will encounter.

4.1.2. MMX wheel

The MMX locomotion system was designed taking into consideration that the terrain on Phobos was for the majority unknown. Therefore, one important driver during the design was robustness, in order to create a rover capable of operating on multiple types of terrain: from soft and granulate soil like regolith, to hard and rocky surfaces. The soft and powdery soil has been found to be the most dangerous, since sinkage of the wheels could happen in this type of terrain and permanently immobilize the rover, putting an end to the mission. [51]

Wheels for exploration rovers are usually relatively large in order to reduce soil pressure below them and consequently the probability of high sinkage. They also usually have grousers on the rim, small raised bars attached to the surface of a wheel that act as a shovel. They are frequently employed since it has been demonstrated that they improve traction of rigid wheels especially on loose soft soil. The dimensions and shape of these features depends on the mission environment, and thus a dedicated study is needed. [51]

The MMX wheel design was optimized in a multi-disciplinary way to take into account numerous parameters: the demanding environmental conditions of Phobos, landing requirements, terrain characteristics chosen as worst-case assumption, interfaces with other subsystems. The aim of the optimization was mechanical strength, easy manufacturability, the best traction obtainable, which means minimum slip, and as always, the lowest mass possible. The final result can be seen in Figure 4.1: 4 rigid wheels with width of 5.3 cm and a radius of 10.4 cm; these values have been chosen as large as the storage space on the MMX spacecraft allowed. The number of grousers is nine to keep the strong grouser base at the release mechanism interface and the grouser height is 35 mm. The grouser shape has a light curvature to increase strength and stiffness. Other wheel features were improved, such as the shape of the grouser tips, the spoke structure and the side struts, since they increase the design's structural strength and traction on harder surfaces and obstacles. [52]

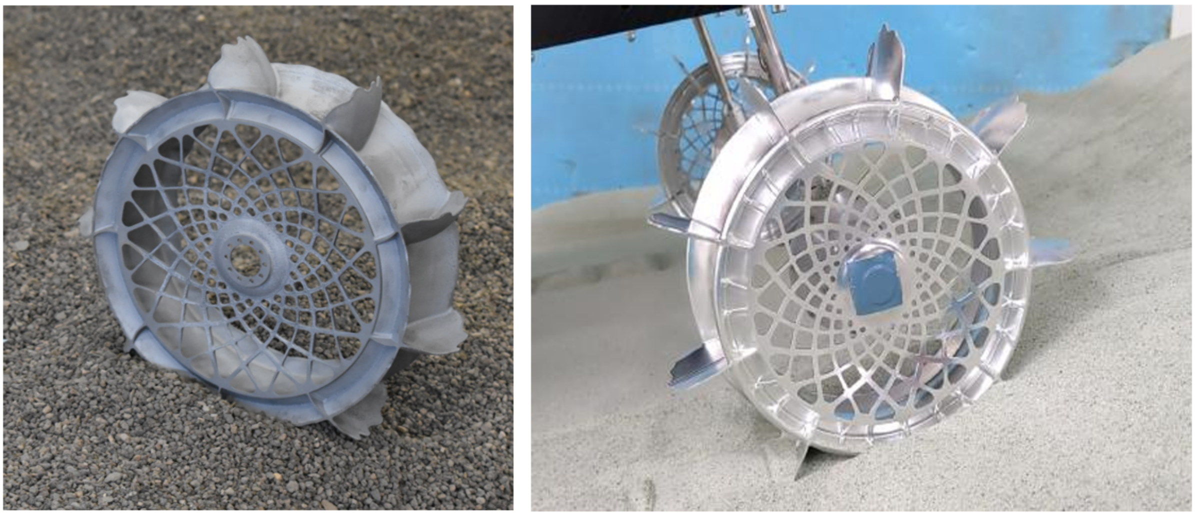

Figure 4.1: MMX wheel: prototype (left)[25] and as manufactured (right)[52]

The traction shape is asymmetric, since driving backwards is not an usual mode of operations, and considered only in extraordinary situations. The soil is displaced backward by the wheel, forming tracks that are later traversed multiple times, thereby enabling a more complete utilization of the displaced material to generate traction. Because a smaller volume of material is displaced toward the sides of the wheel, the resulting wheel tracks exhibit lower levels of compaction, and are therefore more easily cut during steering maneuvers. Moreover, the geometry reduces the extent of bulldozing effects, which in turn decreases resistive forces while enhancing overall tractive efficiency. [25]

This compromise between traction and structural characteristics, and also the usage of a high strength aluminum alloy was fundamental in keeping the wheel's mass as low as 190 g [52]. The aluminum chosen has hardening effects in cold temperatures, this means having a uniform thermal behavior at the interfaces. Furthermore, aluminum is electrically conductive, hence helpful in avoiding clogging of soil due to electrostatic effects, which could deteriorate the traction of the wheel. [25]

4.1.3. ExoMars wheel

The nature of the terrain to be traversed during the ExoMars mission imposed various constraints to be included in the locomotion system design for its successful operations.

The wheel design trade-off had two stages: firstly, the performances of several rigid and flexible wheel's ideas were compared; then, the best performing wheel concept was optimized in a second step. Rigid wheels are the ones where the portion in contact with the ground remains fixed and circular, even considering some radial compliance from the spokes. On the other hand, in flexible wheel designs the running surface deforms under normal loads during operations. Hence, it provides a bigger effective wheel diameter, and thus more contact with the ground than the rigid counterpart with the same diameter. Since they potentially provide a better traction performance on soft and granulated terrains, they were the selected design. This way, a better wheel performance could be achieved with a smaller wheel, that could also be carried in the available volume. [53]

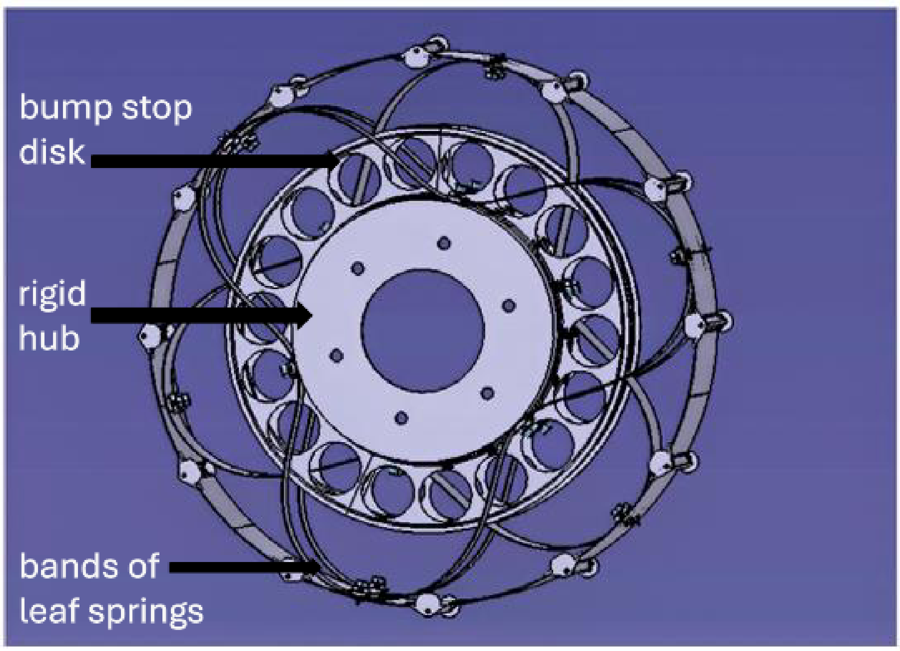

Figure 4.2: Detailed model of ExoMars wheel

Figure 4.2 shows the model of the wheel. Three parallel leaf springs bands provided elasticity to the wheel.Their length is 0.4 mm and they are made with stainless steel, and arranged in a sinusoidal configuration to achieve an elevated effective stiffness, and that provide support to the tire at six evenly distributed circumferential locations. The design ensures that, at the maximum nominal wheel load of 500 N, the elastic running surface and the associated spring elements come in contact with the bump-stop discs integrated within the wheel assembly. These discs are mounted to the rigid hub, which also serves as the interface with the actuator housing. This configuration limits further deformation beyond the design maximum load and prevents the springs from entering the plastic deformation regime under dynamic overloads, even if transient. Under nominal operating loads, no contact occurs between the spring elements and the bump-stop discs.[54]

Grousers were added to increase traction, and thus slope and obstacle traverse capability. The grouser height was limited for two reasons: the first was the stowage volume constraints, and the second was to take into consideration the risks coming from the deflated airbag fabric during lander initiation. On the other hand, the minimum grouser spacing on the wheel circumference took mainly into account the loss of effectiveness when the spaces become stuck with granular soils. Side-grousers were also identified as an important feature to provide lateral resistance and to stop side-slip when traversing soft soil slopes. [53]

Figure 4.3: Exomars wheel [15]

Figure 4.3 represents the final wheel solution, where the diameter was constrained to 0.25

m and the wheel width measures 100 mm, which was the maximum volume that could be used to accommodate the rover in stowed configuration inside the lander. The optimum grouser configuration identified comprises 12 grousers with a height of 4 mm. Mass per wheel is 2.5 kg.[53]

4.1.4. Wheel trade-off

The trade-off analysis of the wheel is achieved with the Analytical Hierarchy Process, the same methodology used to choose between the different types of locomotion, and whose steps have been explained in section 3.2.1. The matrices built for the pairwise comparison procedure are reported in Appendix B.

The parameters selected to perform this trade-off are the mass and the surface characteristics. The mass represents the mass of the wheel, that shall be minimized: the design for the MMX rover's wheel is much lighter than the wheel designed for the ExoMars rover. On the other hand, the surface characteristics parameter assesses the wheel capability to operate on the terrain that will be encountered on Vesta, since it is mostly unknown, this means that the wheel should be able to operate on a wide variety of terrains, from rocky surfaces to soft granulate soils. Considering these criteria, the flexible wheel created for the Rosamund-Franklin rover can achieve a better performance than the rigid wheel designed on the MMX rover. Similarly as in section 3.2.2, in Table 4.1 the parameters adopted to define the wheel design are given a value to show their importance, and to guide the comparison procedure for the pairwise matrix. The mass is considered the most critical parameter, since both designs were created taking into account the worst case scenario possible, thus soft soil.

Parameter	**Value**
1	Mass
2	Surface characteristics

Table 4.1: Trade-off parameters for the wheel design and corresponding value

The results of the trade-off, the weights of the parameters, and the performance of the two wheel technologies with respect to each parameter, are all reported in Table 4.2. The MMX wheel design results being the better suited for the mission thanks to its light-weight mass.

Technology	Mass	Surface characteristics	Results
MMX	12.5%	83.33%	**36.11%**
ExoMars	87.5%	16.67%	**63.88%**
Weights	66.67%	33.33%	

Table 4.2: Trade-off results for the wheel technologies

4.1.5. Wheel CAD model and FEM

The wheel was modeled using SOLIDWORKS. Two distinct configurations were initially developed, and subsequently evaluated through the Finite Element Method (FEM).

Both configurations share identical rim and grouser geometries, they are presented in Figures 4.4 and 4.5. The rim has a diameter of 16 cm and a width of 4.9 cm, featuring a concave profile with a radius of 2.9 cm measured from the tip of the grousers, which extend an additional 4 cm radially outward from the rim. The wheel includes nine grousers, equally spaced along the circumference, each with a thickness of 0.75 mm. These components are manufactured from aluminum alloy EN 7075 (Ergal). As it can be seen in Figures 4.4 and 4.5 , the two models differ only in the design of the wheel disk.

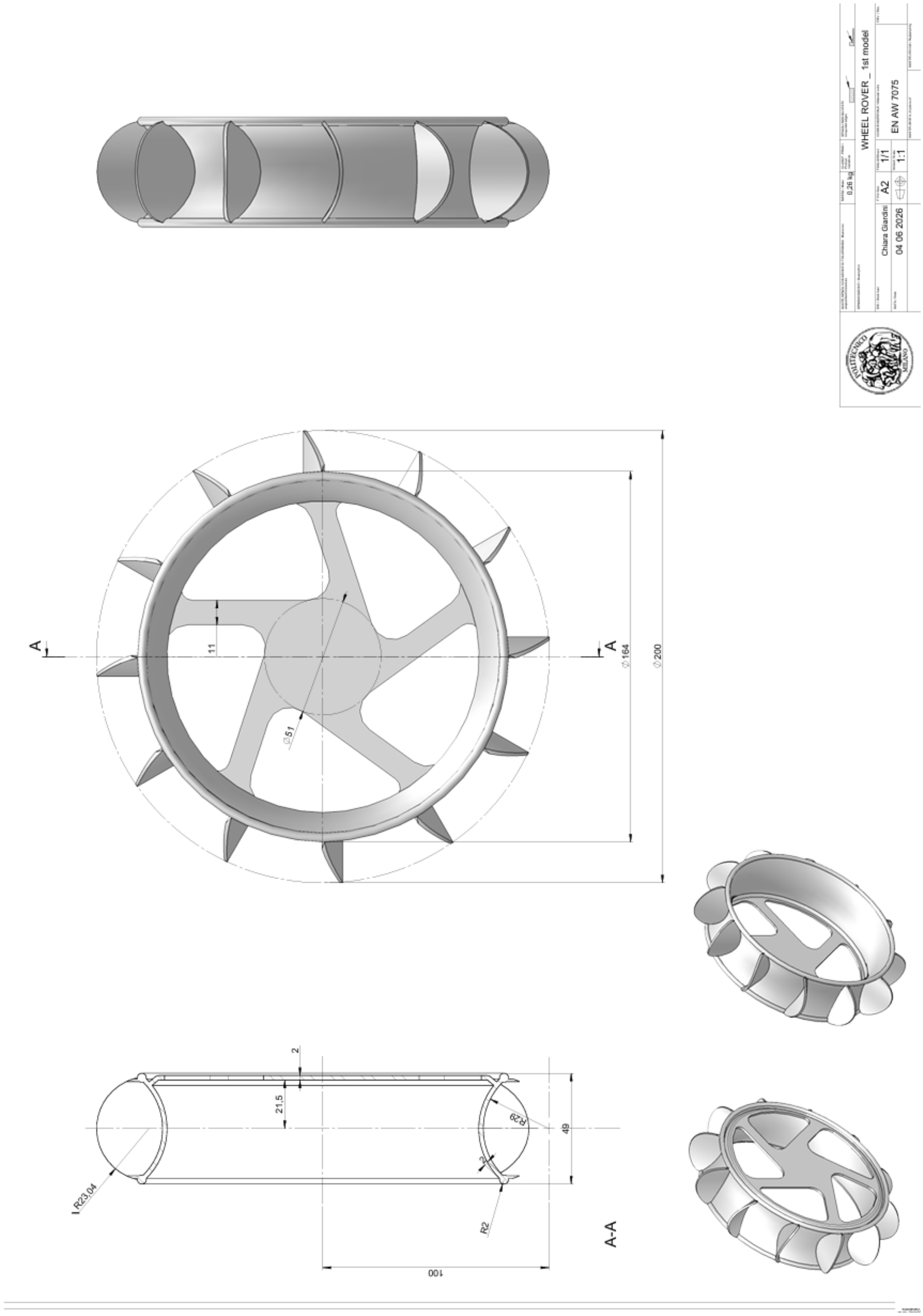

Figure 4.4: The CAD model of the first configuration of the wheel

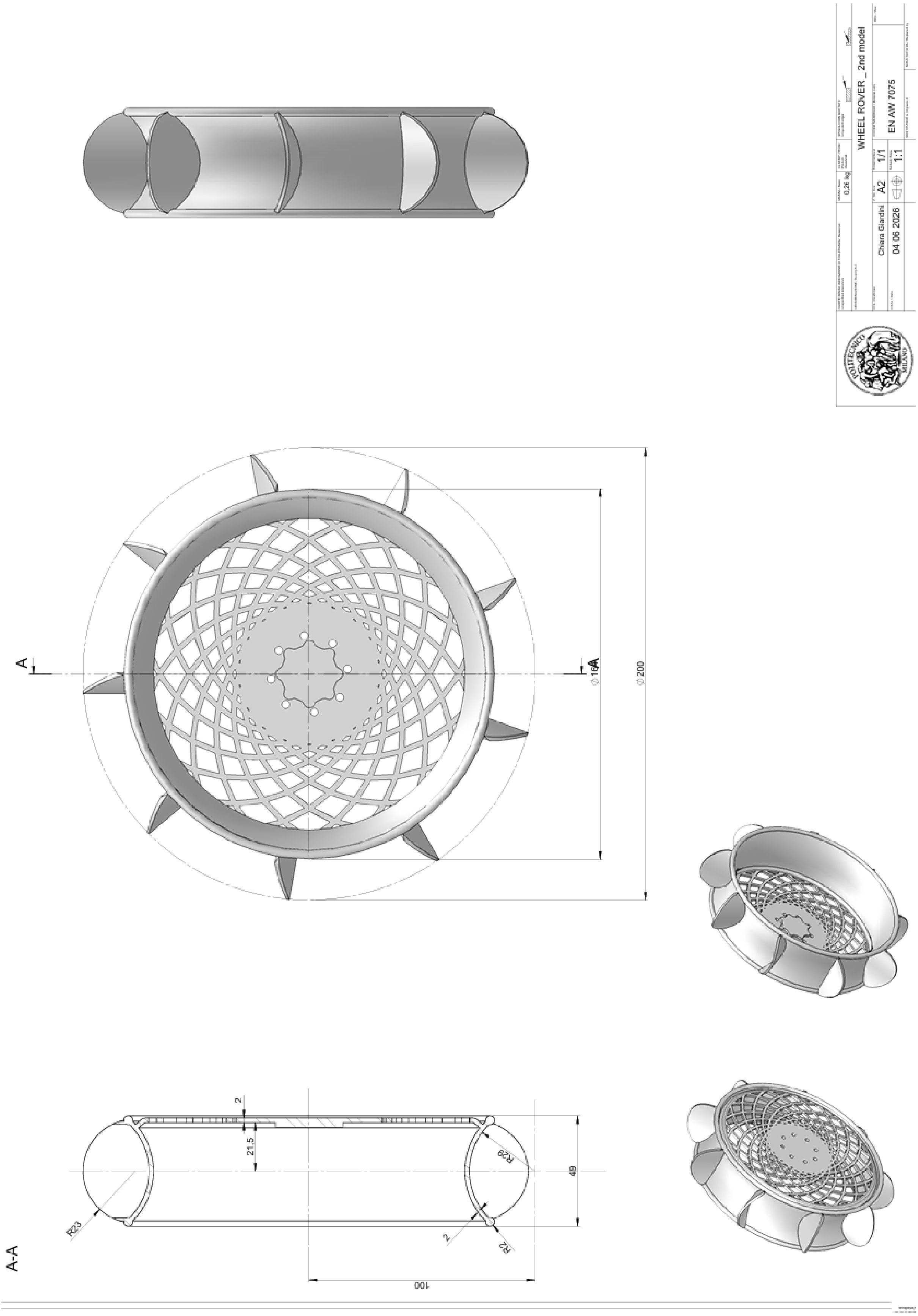

Figure 4.5: The CAD model of the second configuration of the wheel

The FEM analysis consists of a static structural evaluation of the rim and disk for both configurations. Boundary conditions were defined by constraining completely the wheel on the ground. As shown in Figure 4.6, a load of 250 N, that represents one quarter of the total rover weight under Earth gravity, was applied at the center of the rim width, aligned with the disk center, that corresponds to the interface with the leg assembly. The load applied represents a worst case scenario that could happen during operation on Vesta, where only four of the six wheels are in contact with the ground, and therefore the total weight of the rover is carried by only four wheels. Additionally, the weight was considered under Earth gravity because the gravitational pull of the asteroid is very weak. The effect of using the asteroid's actual gravity would be so small that the difference between the results of the two models would not be noticeable, even if in terms of stresses or displacements the configurations differ considerably.

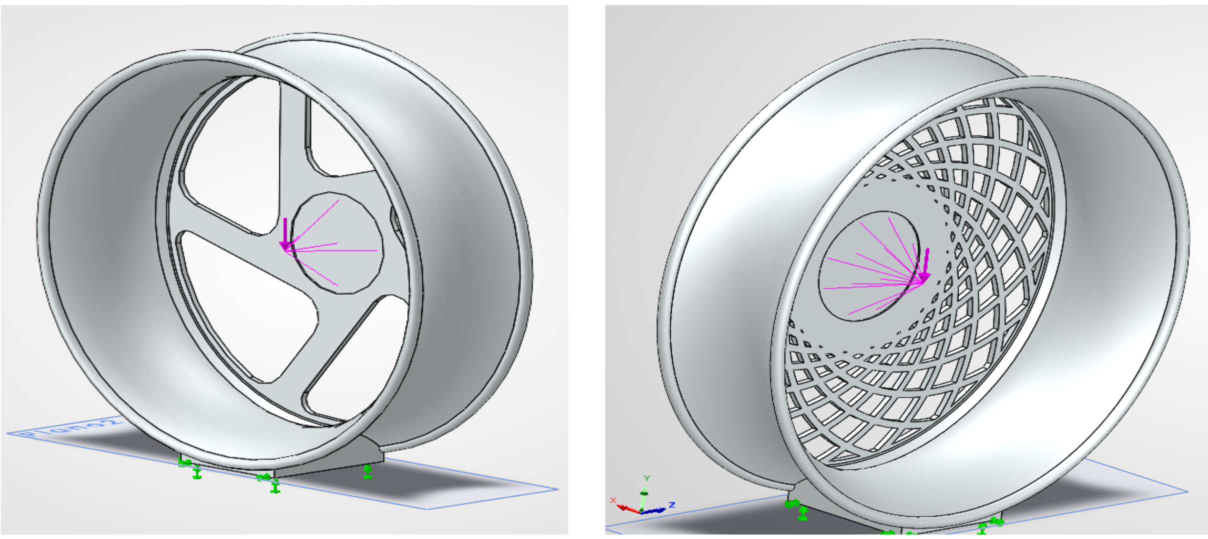

Figure 4.6: The two models of the wheel with the load and constraint applied

The first model mass is 0.28 kg. Figure 4.7 shows the Von Mises stresses on the wheel. The area with highest concentration of stress is the disk of the wheel, since the entire rim is subject to only 3.705×10^{-2} MPa. On the disk the worst stresses are around $(7.640\text{-}9.548) \times 10^{1}$ MPa but are constrained to very small portions in particular positions. On the other hand the majority of the disk is characterised by a stress of 5.731×10^{1} MPa. Figure 4.8 shows that the vertical displacements worst concerns are located on the right side of the disk and are around 0.01 mm. The displacements relating to the axis perpendicular to the plane of the disk are slightly more concerning, since on the upper part the disk is pulled backward of 0.54 mm, while on the bottom part is pulled forward 0.42 mm, creating a torque on the disk of the wheel.

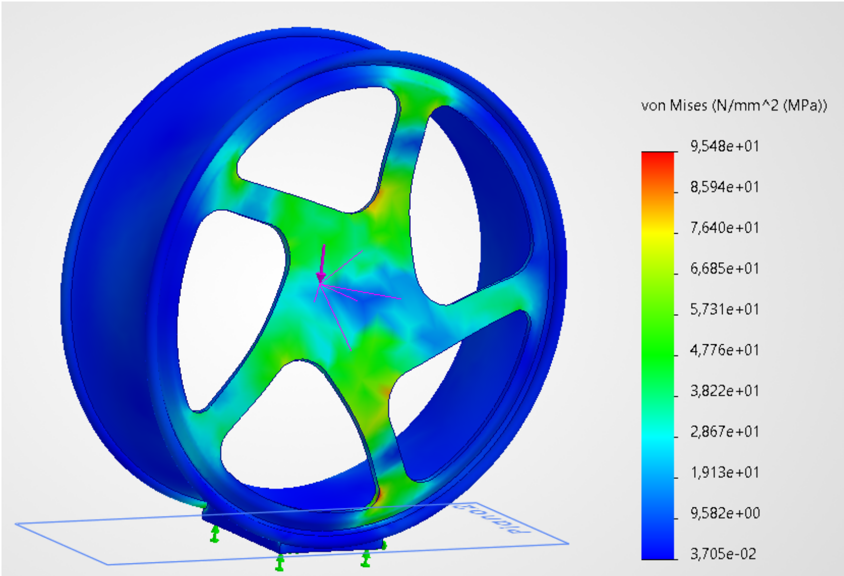

Figure 4.7: Von Mises stresses diagram for model 1

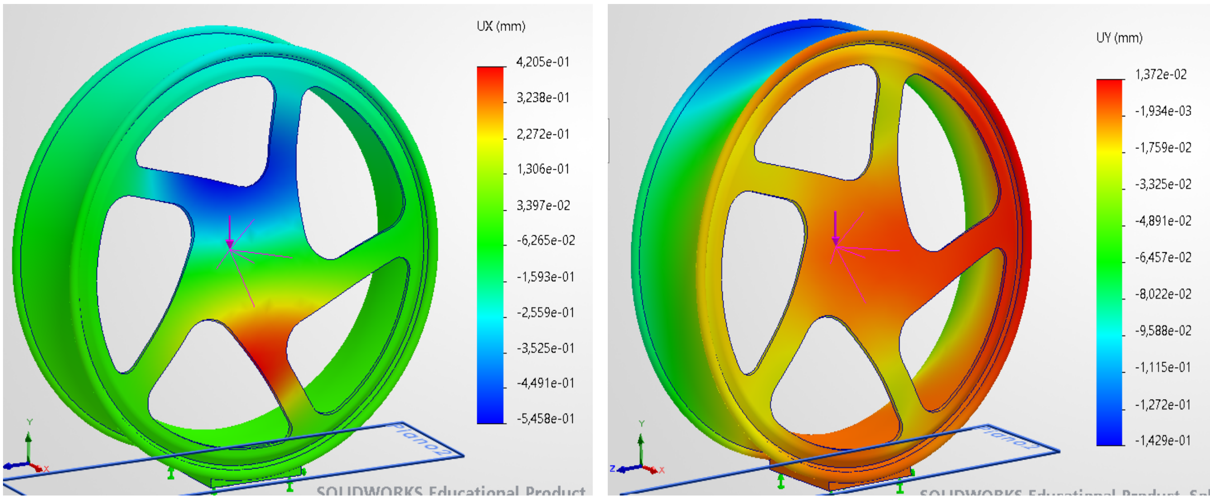

Figure 4.8: Displacements diagrams for model 1, on the left x-displacement and on the right y-displacement

The second model mass is 0.3 kg. Figure 4.10 shows the Von Mises stresses on the wheel. The area with highest concentration of stress is the disk of the wheel, since the entire rim is subject to only 2.383x10^{-2} MPa; on the disk the worst stresses are around (5.105-6.380)x10^{1} MPa but are constrained to very small portions in particular positions, while 3.829x10^{1} MPa is a more uniform stress on the disk. The vertical displacements worst concerns are all over the disk, but the peak is 0.0063 mm. Figure 4.9 indicates that the displacements relating to the axis perpendicular to the plane of the disk are less concerning then in model one, since on the upper part the disk is pulled backward of 0.37 mm, while on the bottom part is pulled forward 0.20 mm, still creating a torque on the disk of the wheel.

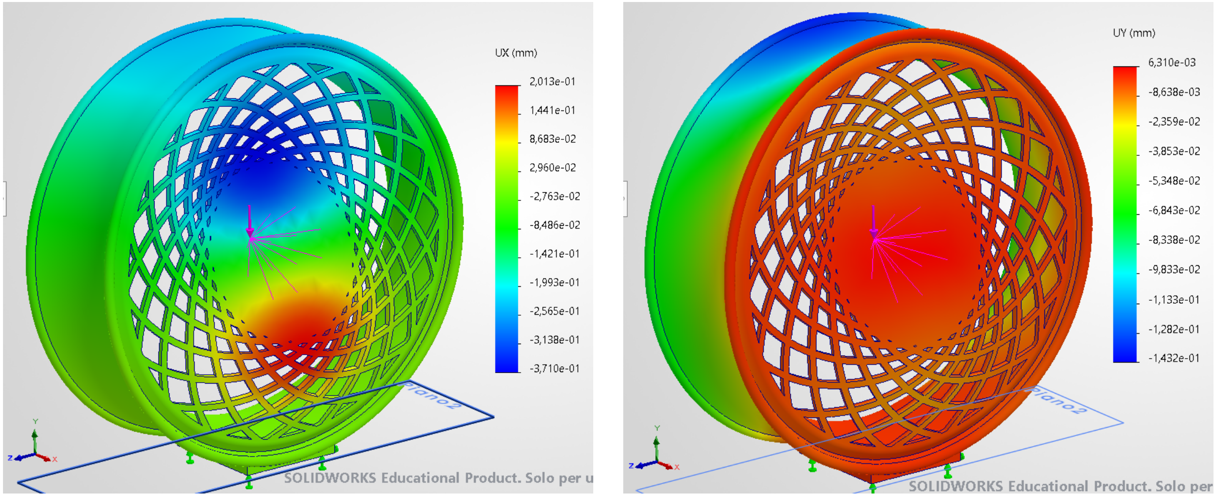

Figure 4.9: Displacements diagrams for model 2, on the left x-displacement and on the right y-displacement

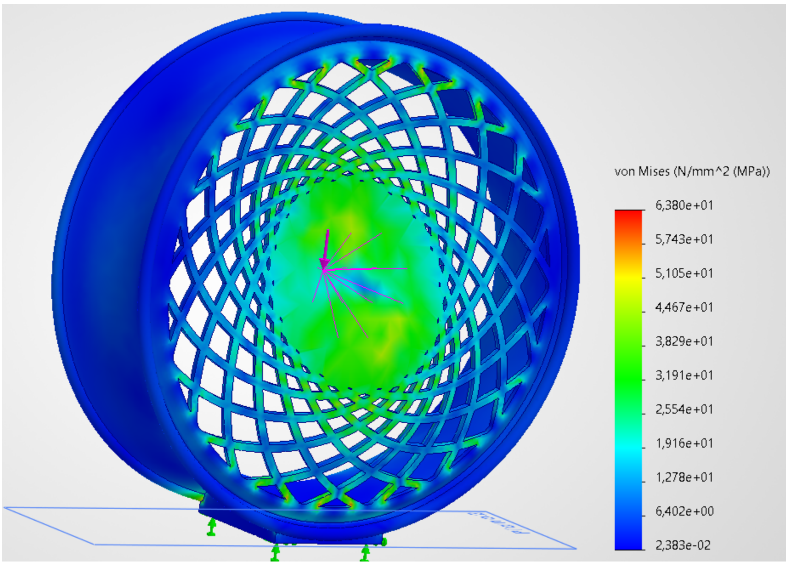

Figure 4.10: Von Mises stresses diagram for model 2

From the static analysis results, it is clear that the second model is the best one, even considering a minimal increase in mass.

4.2. Suspension system's design

This section presents the suspension system design process and the corresponding trade-off analysis. It begins with the introduction of the suspension technologies considered during the trade-off study and their operating principles, advantages, and limitations are discussed. A comparative trade-off analysis is then performed to identify the most suitable solution according to the selected evaluation criteria, and its results are discussed. Lastly, the suspension CAD model and the Finite Element Method (FEM) analysis are presented, leading the characterization of the final suspension design.

The present trade-off analysis takes into account four types of suspension design: one developed for the MMX rover, another created for the Rosalind-Franklin rover of the ExoMars mission, the third is the classic rocker-bogie configuration, and lastly the tri-star system. These configurations were selected because they represent fundamentally different design approaches, thus comprehending a wide range of possible suspension characteristics. While, the tri-star system and the MMX suspension type are relatively new designs, on the other hand, the rocker-bogie configuration is a veteran in the space exploration, but still subject to improvements and changes on the typical design.

4.2.1. MMX suspension system

One of the critical parts of the MMX rover is its locomotion subsystem (LSS), consisting of four locomotion modules represented in Figure 4.11, each composed by the shoulder, the 275 mm leg and the wheel. The entire locomotion subsystem of the IDEFIX rover showed in Figure 4.12 weights 4.52 kg. [23]

The shoulder assembly constitutes a highly integrated subsystem that incorporates multiple electromechanical and sensing components. Specifically, it houses two electric motors along with two angular position sensors and a torque sensor; of the two motors, one is dedicated to the wheel actuation, and that allows skid steering, and the other is committed to the rotation of the leg. In addition, the assembly includes embedded electronics, thermal management hardware, an accelerometer, and several temperature sensors, thereby enabling comprehensive monitoring and control of its operational state. [52]

During the launch phase, cruise, and the descent onto Phobos, a hold-down and release mechanism (HDRM) is employed to secure the legs and wheels against the sides of the chassis, ensuring structural stability and mitigating the risk of mechanical damage under dynamic loading conditions. [52]

Within the rover's internal compartment, the locomotion electronics box (E-box) serves as the central unit for locomotion control. It contains all motor drivers, analog-to-digital conversion interfaces for sensor data acquisition, and a field-programmable gate array responsible for managing the locomotion subsystem. The E-box is governed by the Locomotion Software, which is a C-language software partition operating within the hypervisor framework of the rover's onboard computer system. [52]

Finally, the locomotion subsystem is interconnected through a network of 20 electrical harnesses. These provide connectivity between the eight motors, four sensor interfaces, four cruise heater connectors, and four HDRMs, linking them to the locomotion E-box, the primary spacecraft interface connector, and the rover's power conversion and distribution unit. [52]

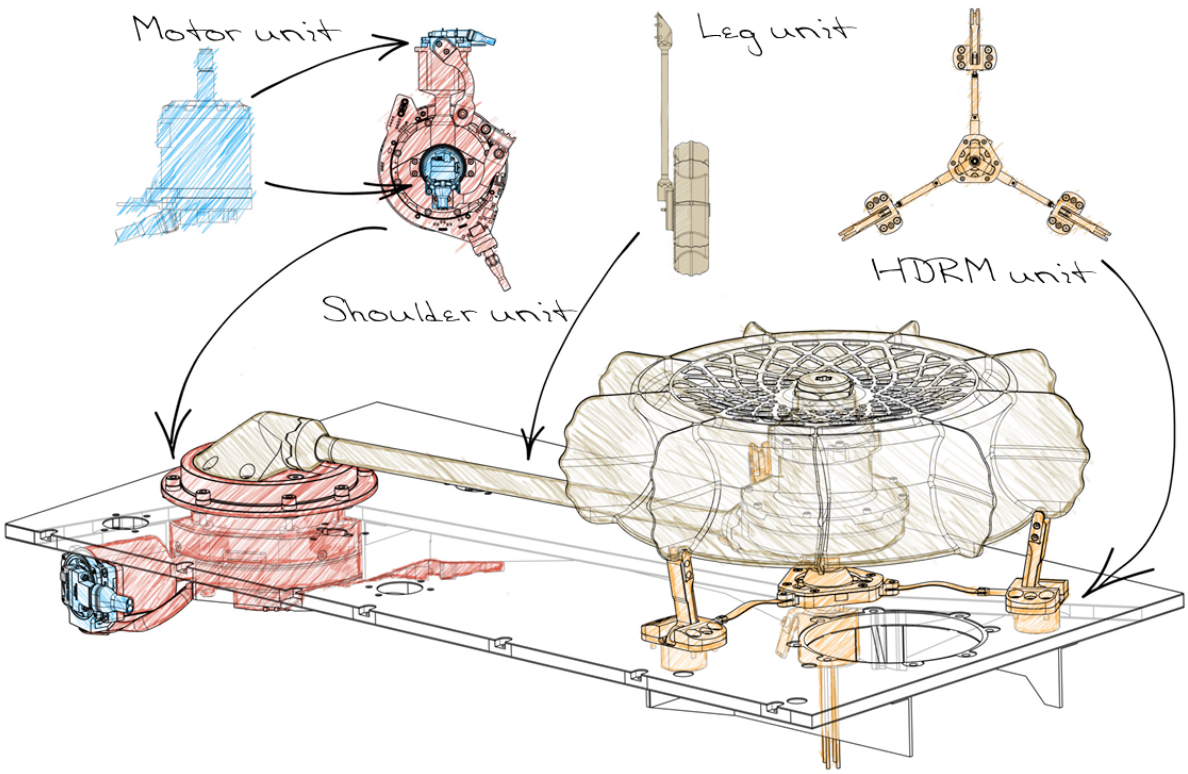

Figure 4.11: MMX rover overview of the components [55]

The requirements set by the mission can be met with the four locomotion modes implemented on the on-board computer:

- **Uprighting mode:** it is the process of getting the rover from the cruise stowed position into an inertial placement where the solar panels can be unfolded. This procedure is the first assignment that the locomotion system of the MMX rover will have to accomplish on Phobos. Depending on the configuration the rovers lands, a specific sequence starts where using precomputed leg angles the locomotion control system commands the wheel and shoulder motors.[56] [25]

- **Drive mode:** the rover needs to be able to drive forward, make curves and accomplish point turns on itself. These movements are realized through a geometric skid steering approach, since the wheels are not steerable. Considering this approach, the wheels must be capable of turning with coordinated speeds, therefore, in order to prevent undesired rotations of the legs, the leg motors are always kept active, even if no action is required at the moment.[56] [25]
- **Alignment mode:** the aim of this mode is to alter the orientation and height of the rover adjusting the leg angles. It computes the coordinated angles to achieve the new required orientation and height, and it gets there through the rover kinematics. All four wheels are needed to be on one plane for stability reasons.[56] [25]
- **Inching locomotion mode:** this mode is implemented on hazardous terrains to obtain an improved performance. The aim is to maximize the traction and minimize the slip, thus to lower the risk of sinkage. It is intended to be used on very soft sand and steep slopes, and the rover should move only in a straight direction. The two front and back wheel pairs move alternatively and the rover body, that should stay parallel to the reference plane, moves up and down. [56] [25]

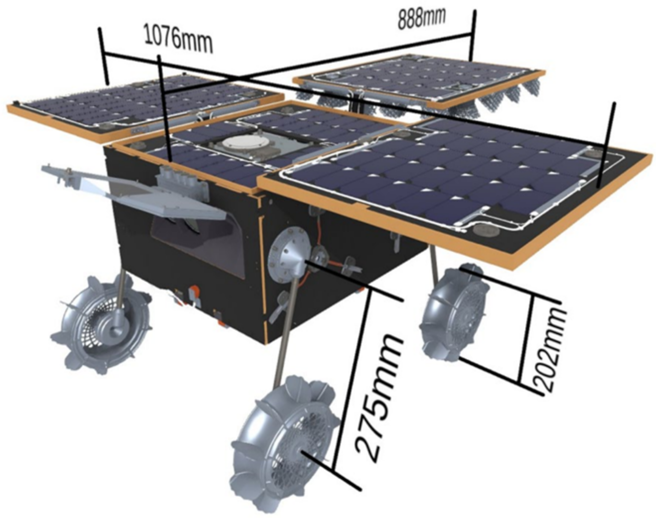

Figure 4.12: MMX rover [23]

4.2.2. ExoMars suspension system

The ExoMars suspension is the so called " triple bogie". This arrangement is based on three bogies, two of them are located at each side of the rover and the last one on the rear. These three points of attachment permit to keep all wheels in contact with the ground, since they can passively rotate around the axes perpendicular to the planes of the body structure in those points; they also provide platform stability. For each bogie there are two levers, that connect to two wheel modules. [57] [58]

The ExoMars rover has a wheel base of 1.26 m and wheel track of 1.31 m. Titanium was chosen to minimize the structural mass and give a good thermal expansion. The estimated mass of the locomotion subsystem (excluding electronics) is 47 kg; therefore, since each wheel is 2.5 kg, the entirety of the suspension system weights 32 kg.[53]

Figure 4.13 presents the locomotion architecture, which follows the configuration 6×6×6 with 6 wheel–walking, comprising six supporting wheels, six driven wheels (DRV), six steered wheels (STR), and six wheel-walking actuators (DEP). In total, the system has 18 degrees of freedom (DOFs), each actuated by an independent brushed DC motor coupled with a gearbox.

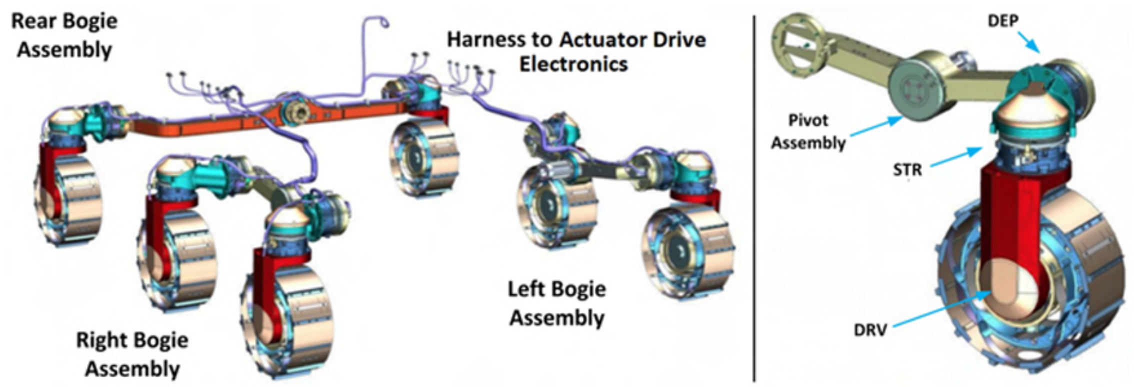

Figure 4.13: Exomars rover suspension parts [57]

From a kinematic perspective, the chain associated with each wheel, considered from the suspension attachment outward, consists sequentially on the wheel-walking, steering, and driving stages. The wheel drive actuators, which incorporate harmonic drive mechanisms, are integrated within rigid wheel hubs. Notably, the steering axis is oriented vertically and passes through the center of the wheel–ground contact patch, ensuring a precise directional control. The steering actuators are positioned in the upper section of the leg and utilize worm gear transmissions (type of mechanical gear system consisting of a screw-like shaft and a gear, that permits to transmit motion and torque at a right angle); this configuration is specifically designed to fit within the constrained volume available. Similarly, the wheel-walking actuators employ right-angle drivetrain arrangements combined with worm gears, enabling their longitudinal integration within the hollow-section bogie beams. An additional advantage of the worm gear implementation is its inherent high resistance to back-driving torque. Hence they do not allow torque to be transmitted from the output shaft back to the input shaft, thereby eliminating the necessity for supplementary braking systems. [53]

The rover has two configurations represented in Figure 4.14. The stowed configuration consists in the wheel legs rotated around the walking axes and locked against the lander base plate with hold-down and release devices. The deployment requires operations from the 6 wheel-walking actuators and 6 wheel drives in synchronicity. [53]

Figure 4.14: Exomars rover deployed and stowed configuration[53]

Wheel walking is one of the rover locomotion modes: it synchronizes the motion of the wheel driving motor with another motor. This synchronization can be used to swing the wheel back and forth, and it increases traction on soft soils. [53]

The requirement for the locomotion subsystem energy is to limit its consumption to 160 Wh for a 100 m traverse over a reference terrain specified in terms of soil type, slope, statistical rock size and frequency distribution. [53]

4.2.3. Tri-star suspension system

The tri-star system is a modularly designed system created to better adapt and obtain the required driving force on rough terrains. All the components of the ensemble, i.e.

the driving motor, the reducer, the control unit, the driver unit and the tri-star wheel combination are all integrated together as one single system, showed in Figure 4.15. [59]

The tri-star modular wheel is formed by three wheels arranged as a triangle, two of them are on the ground and one is above them. The configuration consists of a planet carrier, where the solar gear is mounted in the center, then for each arm, a first planet gear and a second planet gear connected to a wheel. It has two possible movements: rotation when the wheels rotate on their axis all at the same speed, or revolution where is the planet carrier to rotate on its axis. The second mode is used if any of the wheels in contact with the soil gets stuck, or there is an obstacle to climb. It makes this type of system very adaptable in rocky, uneven terrains. [59]

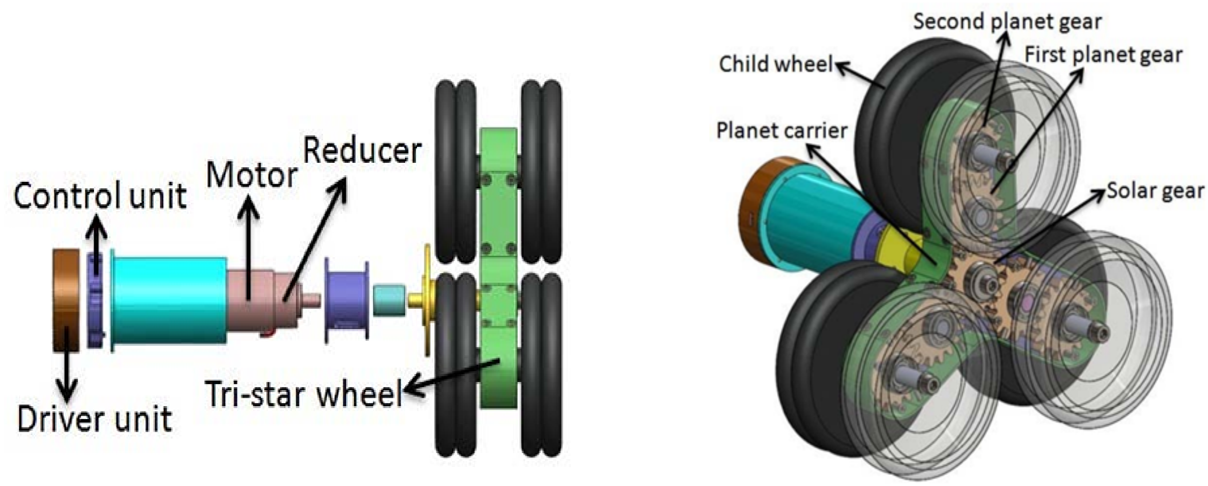

Figure 4.15: Tri-star modular wheel [59]

The other major part of this structure, besides the modular wheel system, is the articulated mechanism of the chassis represented in Figure 4.16. The chassis is composed of two sections, the main and auxiliary bodies, that are connected through the articulated mechanism. This mechanism fulfills three principal functions:

- mechanically linking the two chassis sections with a single passive degree of freedom;
- enabling the variation of the relative angle between them;
- providing a buffering effect during operations.

Structurally, a shaft passes through two hinges, while torsion springs connect the two chassis segments; these torsion springs introduce a linear damping behavior between the bodies. A limit plate, actuated by two linear servo motors, regulates the relative angular displacement. In particular, extension of both actuators induces a clockwise rotation of the limit plate, therefore reducing the inter-chassis angle; on the other hand, retraction produces rotation in the opposite direction, increasing the angle. Additional springs are incorporated to further enhance the buffering capacity between the main and auxiliary chassis. The inclusion of the articulated mechanism enhances the system's flexibility and adaptability to uneven terrain, while also allowing real-time mechanical adjustment of the rover's center of mass, which ensures continuous ground contact of the six wheels and enables the generation of important traction forces. [59]

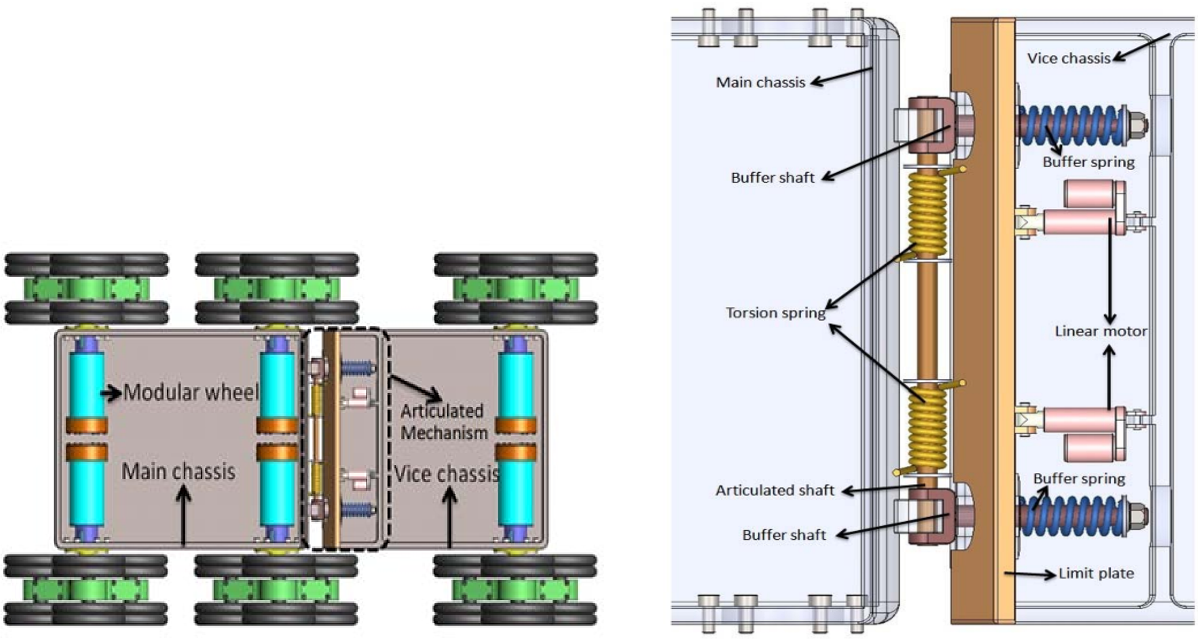

Figure 4.16: Tri-star chassis and articulated mechanism [59]

All the aforementioned components and design choices result in a system that, while structurally simple and capable of operating under a constrained power budget, is characterized by significant mass and lacks an active steering capability. [59]

4.2.4. Rocker bogie suspension system

The rocker bogie suspension design is an asymmetrical suspension structure: as it's possible to see in Figure 4.17 in the frontal part there is a rigid construction with assembled two wheels known as "the bogie", that is connected to the wheel in the rear with a bar: this mechanism is "the rocker" [60].

The term "rocker" refers to the rocking action of the bigger constructions of the suspension system with respect to the chassis: when one rocker rises, the other falls; they are connected to the vehicle chassis through a differential showed in Figure 4.18. The term "bogie" refers to the links that have a drive wheel at each of the two ends. Both sides of the chassis are symmetric, each side has three wheels that are linked together. [61]

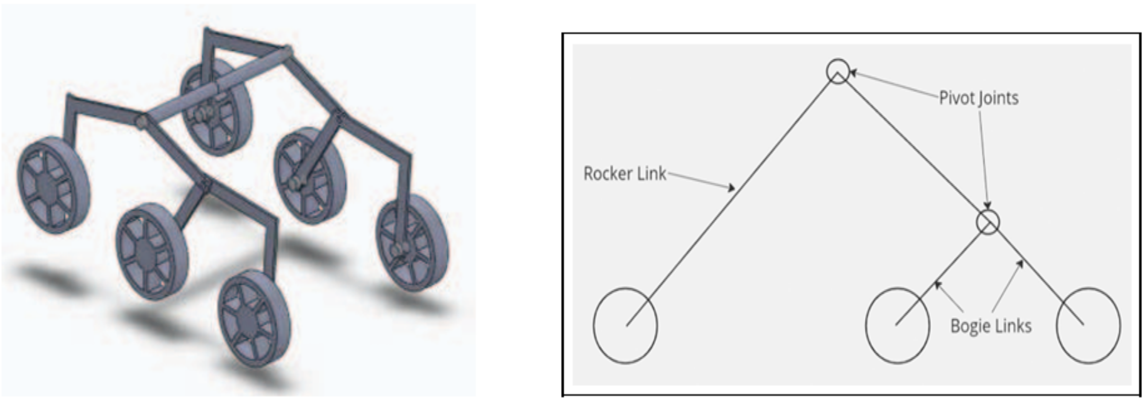

Figure 4.17: On the left a rocker-bogie CAD model [60], on the right a line diagram of the rocker-bogie mechanism [61]

The rocker-bogie suspension enables all six wheels of the vehicle to passively keep contact with the surface even when driving on hazardous and uneven terrain. The other main advantage of this configuration is that the wheels' pressure on the ground will be equilibrated, since the weight of the vehicle is distributed over the 6 wheels, thus reducing the risk of the vehicle sinking on soft soil. These are important features that develop good ground traction resulting in an highly mobile rover. [62] [63]

Another key characteristic of the rocker bogie suspension is the ability to absorb significant driving loads, and reduce the vibrations transmitted from the interaction between wheels and terrain to the main body. This can be credited to the free pivot joints added at the suspension-body interface and at the junction of the rocker-bogie links, they enable independent rotation of each link around them and actively damp the mechanism preventing direct contact between the links. The dampening effect attenuates the danger for the scientific instruments that the rover could carry as payload and that were not designed to withstand large loads in their science-gathering configuration. Therefore, one of the design requirements is to create a soft suspension to limit the accelerations experienced by the payload, but not too soft that could result in such large deflections that the rover's body may come in contact with the surface in an uncontrolled manner. [62] [61]

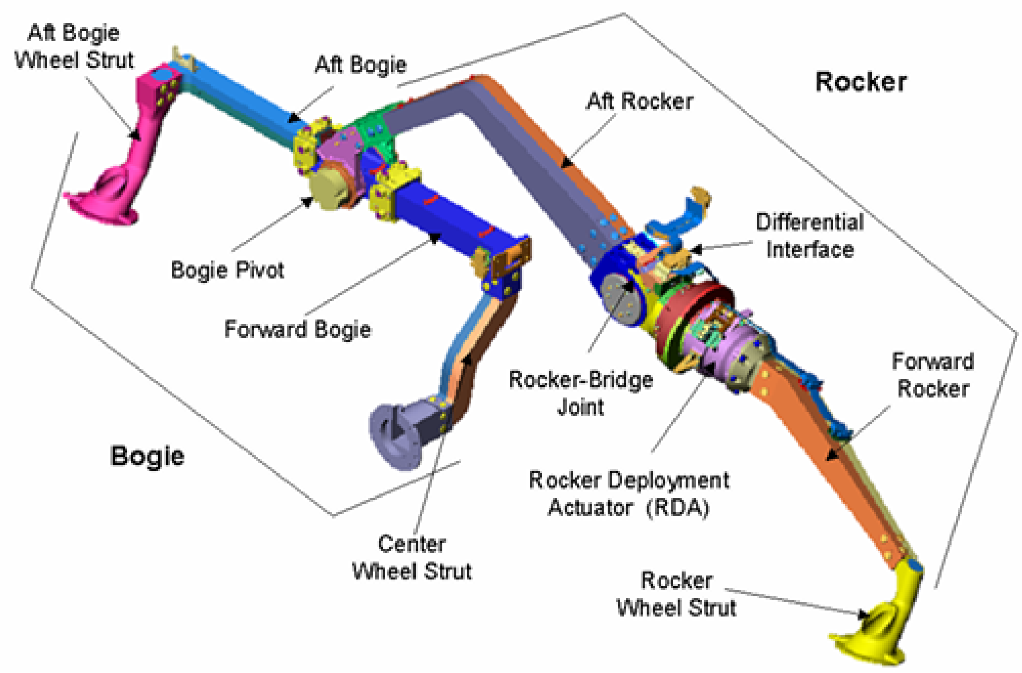

Figure 4.18: Rocker-bogie suspension parts [62]

4.2.5. Suspension system trade-off

The trade-off analysis of the suspension is achieved with the Analytical Hierarchy Process, the same methodology used to choose between the different types of locomotion and wheel designs, and whose steps have been explained in section 3.2.1. The matrices built for the pairwise comparison procedure and their CR value are reported in Appendix B.

The parameters selected to characterize this trade-off are mass, power, surface characteristics and complexity:

- The mass represents the mass of the suspension system, that shall be minimized and capable of compacting. The MMX rover has the least heavy suspension system, followed by the one designed for Rosamund-Franklin, then the rocker bogie that cannot be stowed, and last the tri-star system with the most weight and not compactable.
- The power describes the electric power consumed by the system, that should be minimized. The tri-star suspension system minimizes power usage thanks to its simplicity; the rocker-bogie systems and the ExoMars suspension have comparable but more complex mechanics that tends to consume more power resources; and lastly, the MMX system is computationally and mechanically intensive considering

all the modes described and the skid steering technique.

- The surface characteristics parameter assesses the suspension capacity to operate on the terrain that will be encountered on Vesta, and since it is mostly unknown, this means that the suspension should be able to operate and keep all wheels in contact with the ground at all times on a wide variety of terrains, from rocky surfaces to soft granulate soils. The rocker-bogie system comes in second after the triple-bogie suspension, since the system designed for the ExoMars rover was created as an improvement of the rocker-bogie suspension. Then the MMX system, and finally the tri-star suspension accounting for the two chassis.
- The complexity parameter represents the simplicity of the system, considering the number of components and the control logic needed. The tri-star design aims to maximize simplicity; the triple-bogie system of the ExoMars rover simplifies the rocker-bogie suspension removing the differential interfaces, and the MMX system has the highest degree of mechanical complexity and control logic sophistication.

As in section 3.2.2, in Table 4.3 the parameters adopted to define the suspension design are given a value to show their importance, and to guide the comparison procedure for the pairwise matrix. The mass is considered the most critical parameter with the power following next: the power and mass budgets in space missions typically pose important constraint on the design, and the advantages of having a suspension system with low mass and low power usage are obvious. Following the surface characteristics, a better performance is always appreciated, but all the models taken into consideration were created for better results on hazardous terrains. Complexity is the least critical parameter, in fact, greater mechanical or control elaborateness is admissible if it leads to better locomotion capabilities, less mass and lower power consumption.

Parameter	**Value**
1	Mass
2	Power
3	Surface characteristics
4	Complexity

Table 4.3: Trade-off parameters for suspension design and corresponding value

The results of the trade-off, the weights of the parameters, and the performance of the four suspension technologies with respect to each parameter, are all reported in Table 4.4. The rocker-bogie presents drawbacks and a consistent poor performance for most parameters. Conversely, the tri-star suspension system, even considering good results in some criteria, it presents significant impediments for the most important parameters. For these reasons, they are not considered suitable baseline solutions for the locomotion system. On the other hand, both the MMX system and ExoMars suspension technologies are highly promising, but the MMX suspension is strongly penalized by its sophistication and non-indifferent power usage. On the contrary, the Rosalind-Franklin system offers the most robust and adaptable performance, serving as a solid foundation for the suspension system required.

Technology	**Mass**	**Power**	**Surface characteristics**	**Complexity**	**Results**
MMX	40.993%	12.251%	18.574%	9.596%	**26.404%**
ExoMars	29.396%	22.718%	46.556%	27.714%	**30.148%**
Tri-star	7.043%	42.311%	6.911%	46.581%	**20.590%**
Rocker-bogie	22.565%	22.718%	27.957%	16.107%	**22.856%**
Weights	46.581%	27.714%	16.107%	9.596%	

Table 4.4: Trade-off results for the chosen suspension technologies

4.2.6. Suspension system CAD model and FEM

The suspension system was modeled using SOLIDWORKS. Two distinct configurations have been developed, as can be seen in Figures 4.19 and 4.20. Then, the structural performance of each of them has been assessed via Finite Element Method (FEM).

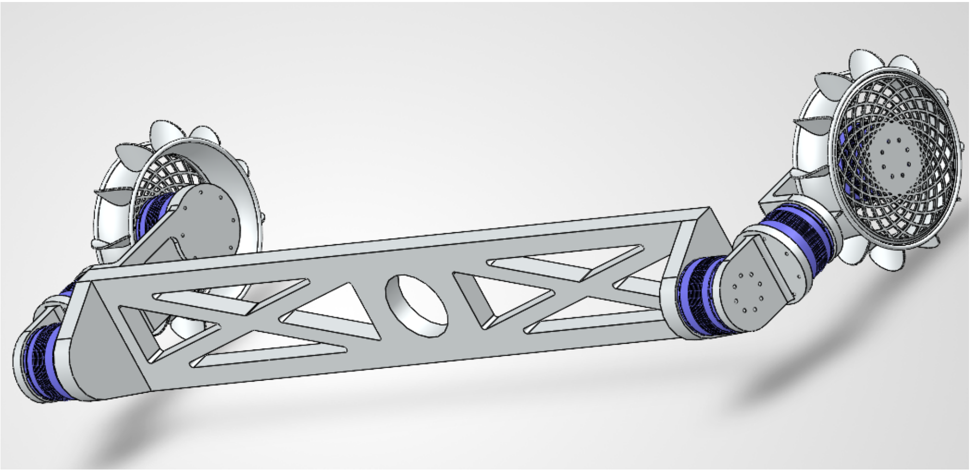

Figure 4.19: Suspension model 1

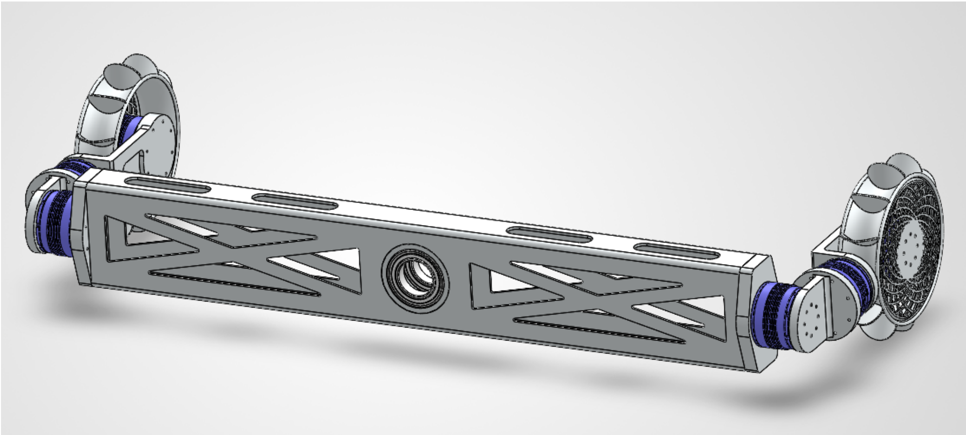

Figure 4.20: Suspension model 2

Both configurations share identical dimensions and leg assembly geometries. As can be seen in Figures 4.21 and 4.22, the rear beam is 80 cm long and 12 cm high, while the lateral beams are 60 cm long and 12 cm high too. The central extrusions for the bearings have a diameter of 8 cm: they are the attachments of the locomotion system to the chassis of the rover. These components are manufactured from aluminum alloy EN 7075 (Ergal). The two models differ only in the design of the beams: model one is designed as a single board, while model two is created as a tubular structure.

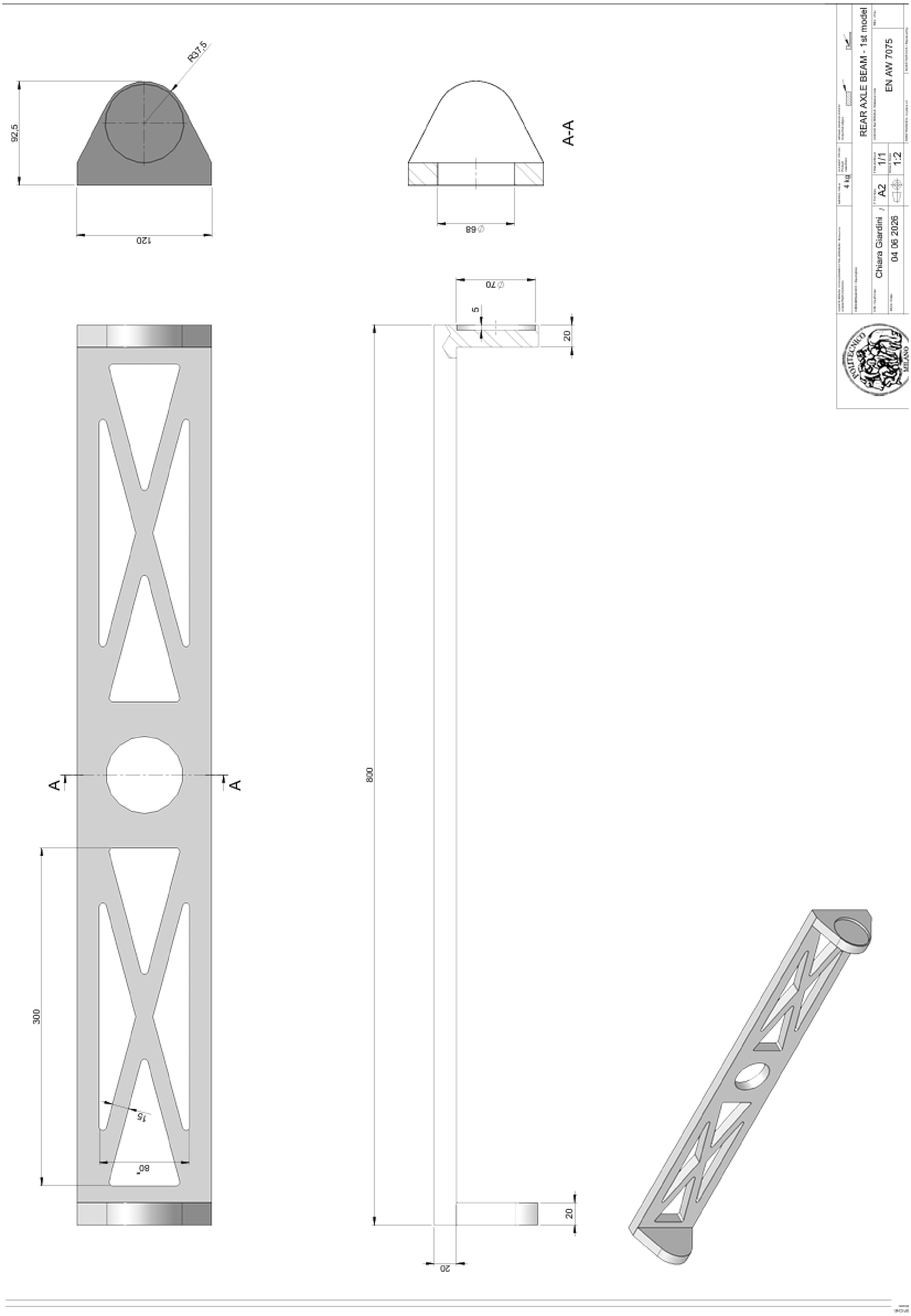

Figure 4.21: Suspension model 1

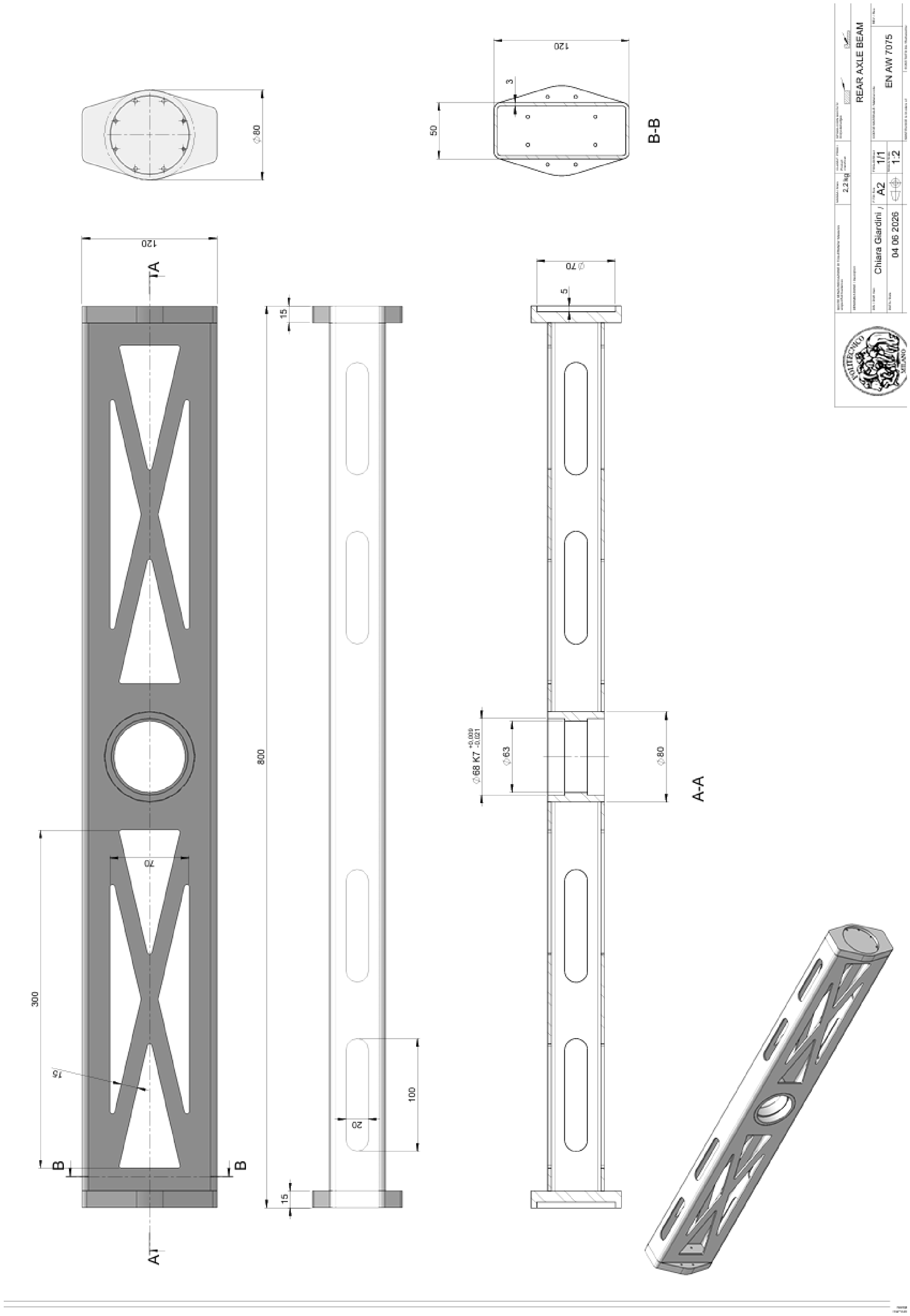

Figure 4.22: Suspension model 2

Table 4.5 shows that the FEM analysis consists of two static structural evaluations of the rear beam for both configurations. Boundary conditions were defined by fixing the beam on the bearing lodgment, so that it cannot rotate. In the two evaluations two loads of 250 N, each representing one quarter of the total rover weight under Earth gravity were applied. The difference between the evaluations rests in the location of the applied load. In both evaluations, the loads are applied in correspondence of the wheel position with respect to the beam, but in one evaluation the rover is considered in open configuration (Figure 4.23), while on the other evaluation the rover is in stowed configuration (Figure 4.24). The load applied represents a worst case scenario that could happen during operations on Vesta, where only four of the six wheels are in contact with the ground, and therefore the total weight of the rover shall be managed with two contact point less. Also the weight was considered under Earth gravity because the gravitational pull of the asteroid is very weak.The effect of using the asteroid's actual gravity would be so small that the difference between the results of the two models would not be noticeable, even if in terms of stresses or displacements the configurations differ considerably.

	Type of beam
Configuration 1	single board
Configuration 2	tubular structure

	Rover position
Load 1	operating
Load 2	stowed

Table 4.5: FEM analysis configurations and loads

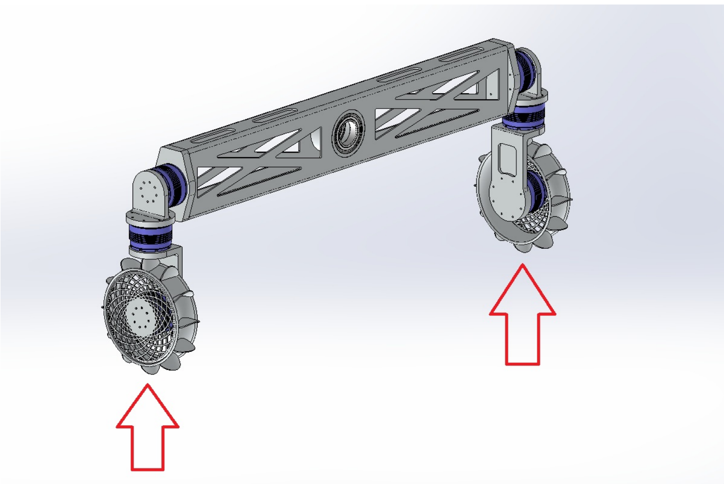

Figure 4.23: Suspension model 2 with load 1

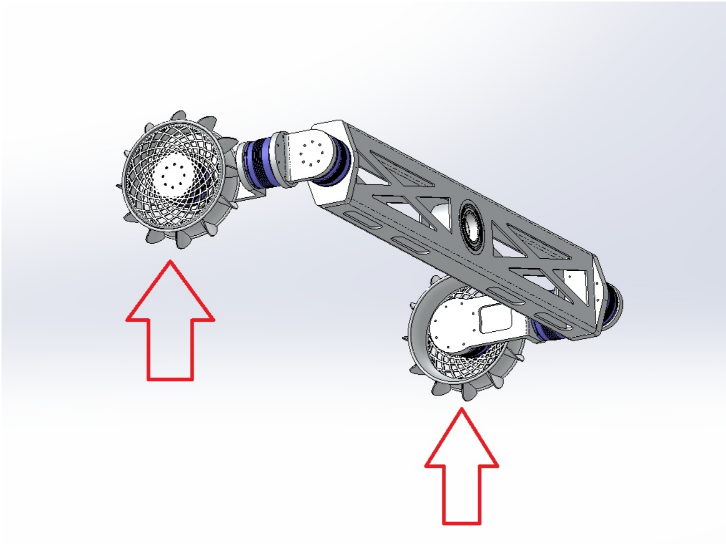

Figure 4.24: Suspension model 1 with load 2

The first model mass is 4 kg for the rear beam only. Considering the rover in open configuration, in Figure 4.25 the Von Mises stresses worst peaks are around (7.019-8.772)MPa, but are also constrained to very small portions in particular positions; stresses in most of the beam fall in the range 2.637-5.226 MPa. The worst vertical displacements are located at the very end of the leg attachment and are around one decimal of a millimeter, as shown in Figure 4.26. Figure 4.27 represents the displacements relating to the axis perpendicular to the plane of the beam, that are slightly more concerning, since on the upper part the beam is pulled forward of 0.074 mm, while on the bottom part is pulled backward of a similar amount, creating a torque on the beam.

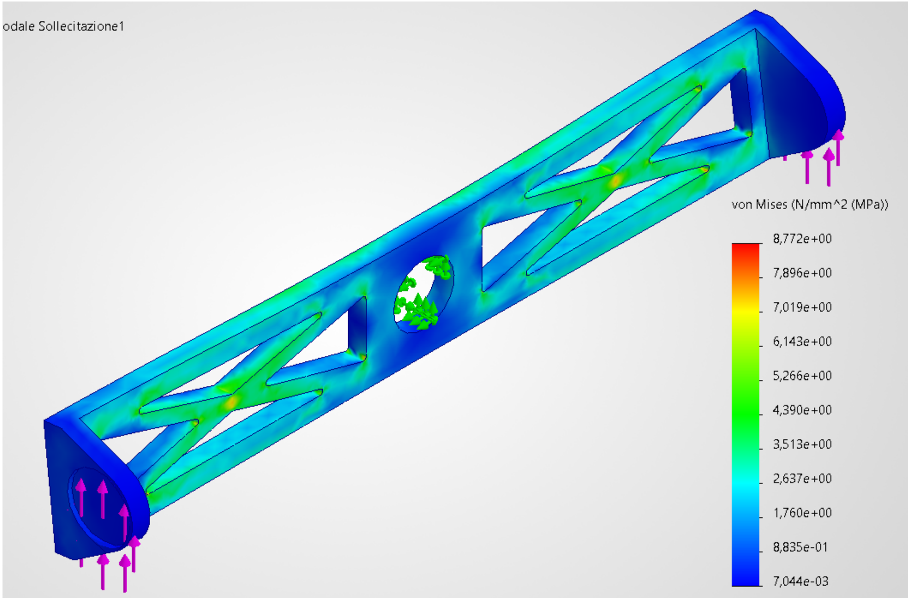

Figure 4.25: Von Mises stress for suspension model 1 with load 1

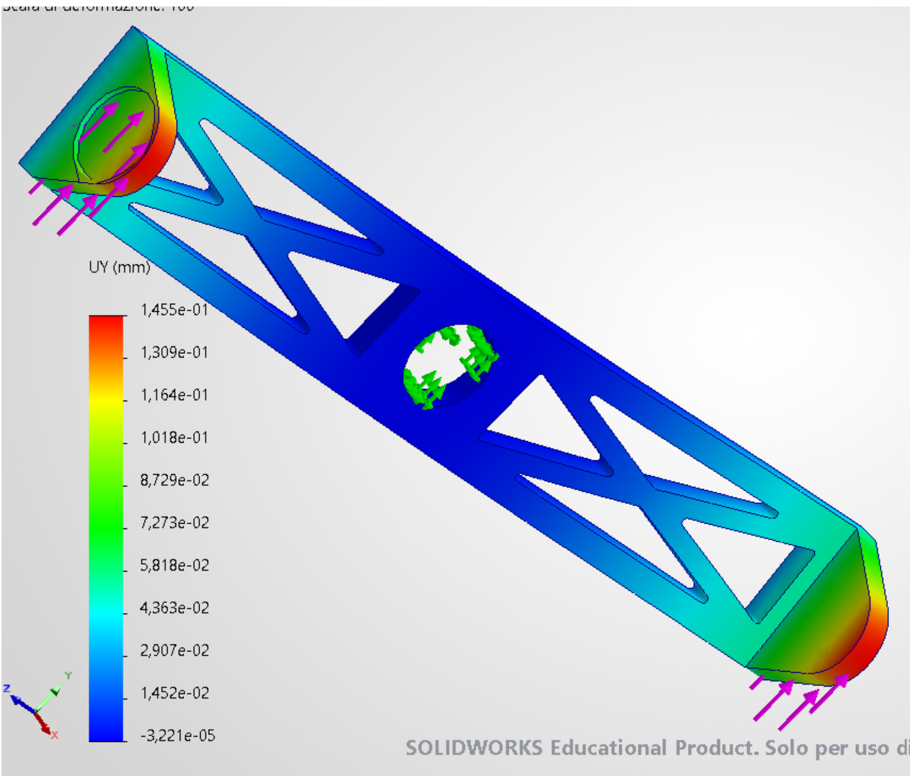

Figure 4.26: Displacement y-axis suspension model 1 with load 1

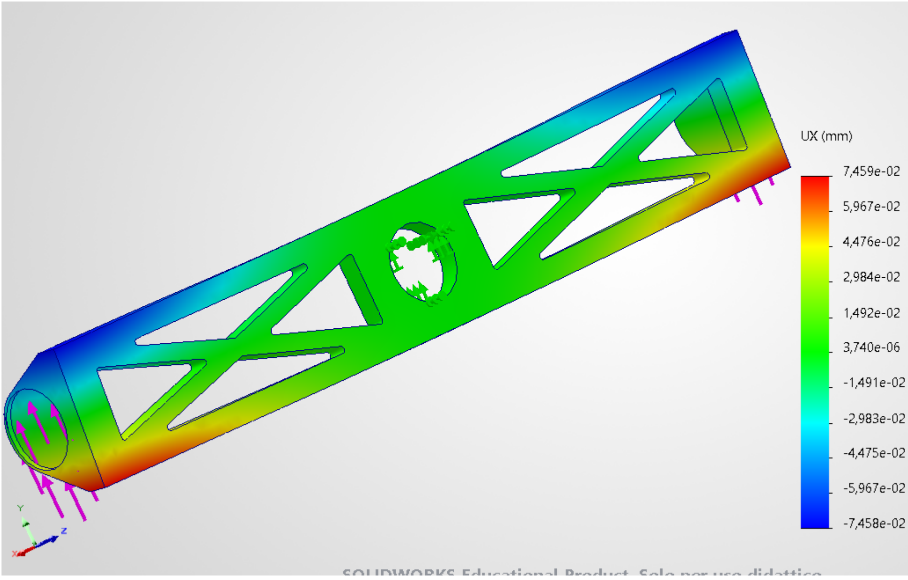

Figure 4.27: Displacement x-axis suspension model 1 with load 1

Considering the rover in stowed configuration, in Figure 4.28 the Von Mises stresses worst peaks are around (1.311-1.637)x10^1 MPa, but are again constrained to very small portions in particular positions; stresses in most of the beam fall in the range 4.945-9.842 MPa. The worst vertical displacements are again located at the very end of the leg attachment and are around two and a half decimal of a millimeter as shown in Figure 4.29. Figure 4.27 represents the displacements relating to the axis perpendicular to the plane of the beam, that are slightly more concerning, because also in this case a torque is created, since on the upper part the beam is pulled forward of 0.191 mm, while on the bottom part is pulled backward of a similar amount.

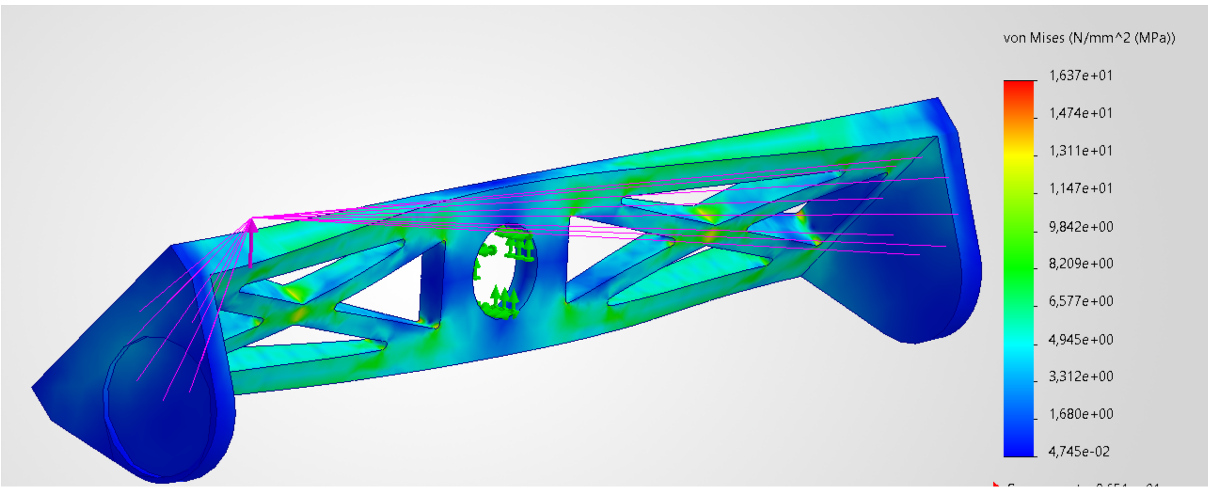

Figure 4.28: Von Mises stress for suspension model 1 with load 2

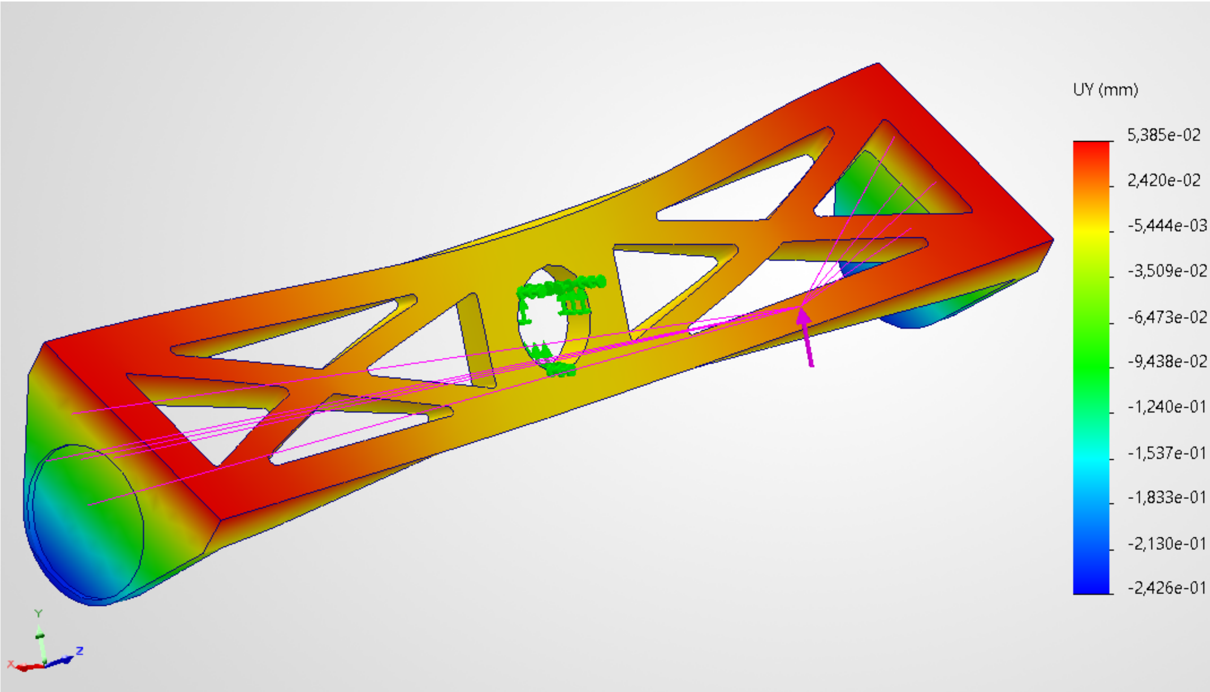

Figure 4.29: Displacement y-axis suspension model 1 with load 2

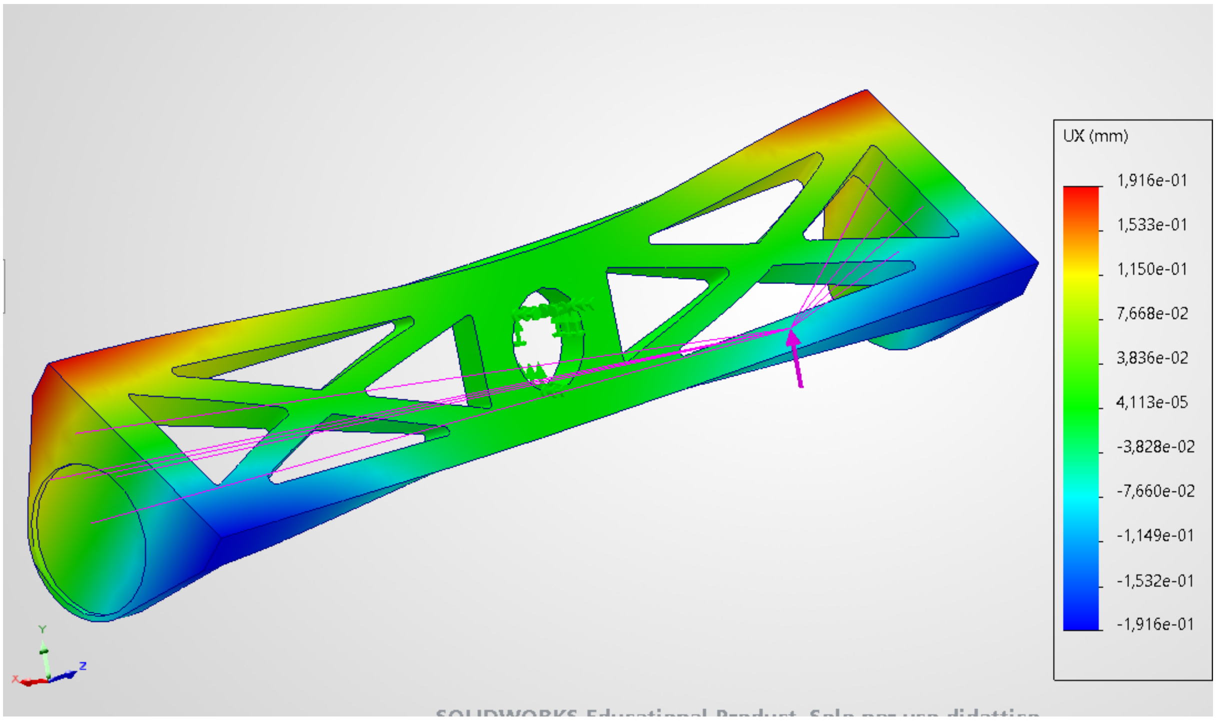

Figure 4.30: Displacement x-axis suspension model 1 with load 2

The second model mass is 2.17 kg for the rear beam only. Considering the rover in open configuration, in Figure 4.31 the Von Mises stresses worst peaks are around $1.505\text{x}10^1$

MPa, but are always constrained to very small portions in particular positions that are not visible; 1.509 MPa is the most generalized stress on the beam. The vertical displacements worst concernments are located at the very end of the beam where the leg attachments are located and are around 0.04 mm as shown in Figure 4.32. Figure 4.33 represents the displacements relating to the axis perpendicular to the plane of the beam, that are definitely not concerning, since the only peaks present are due to little deformations of the plane surface of the beam, and are around 0.01 mm, while the rest of the beam is subject to 10^{-5} mm deformations.

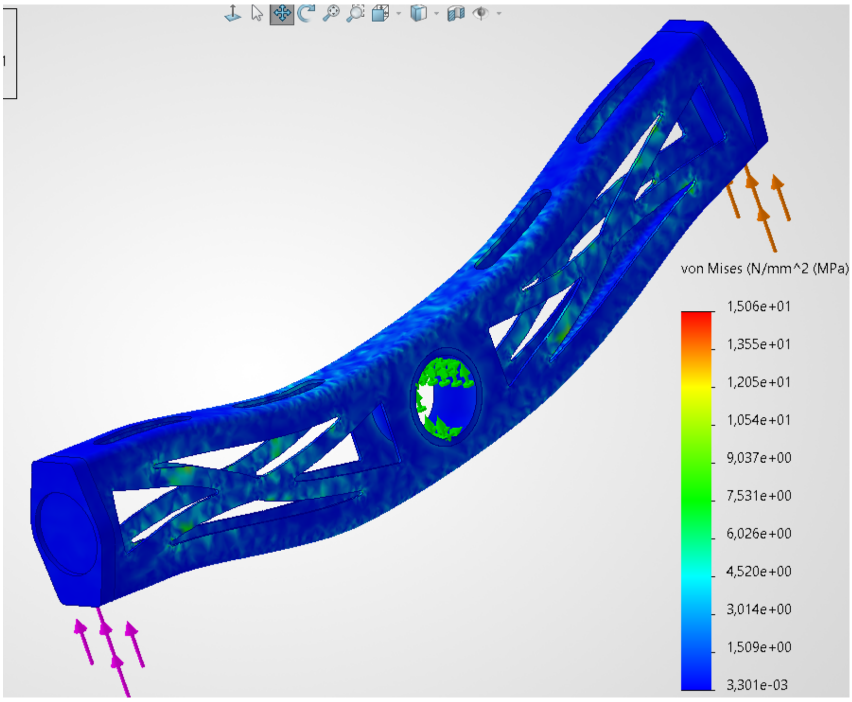

Figure 4.31: Von Mises stress for suspension model 2 with load 1

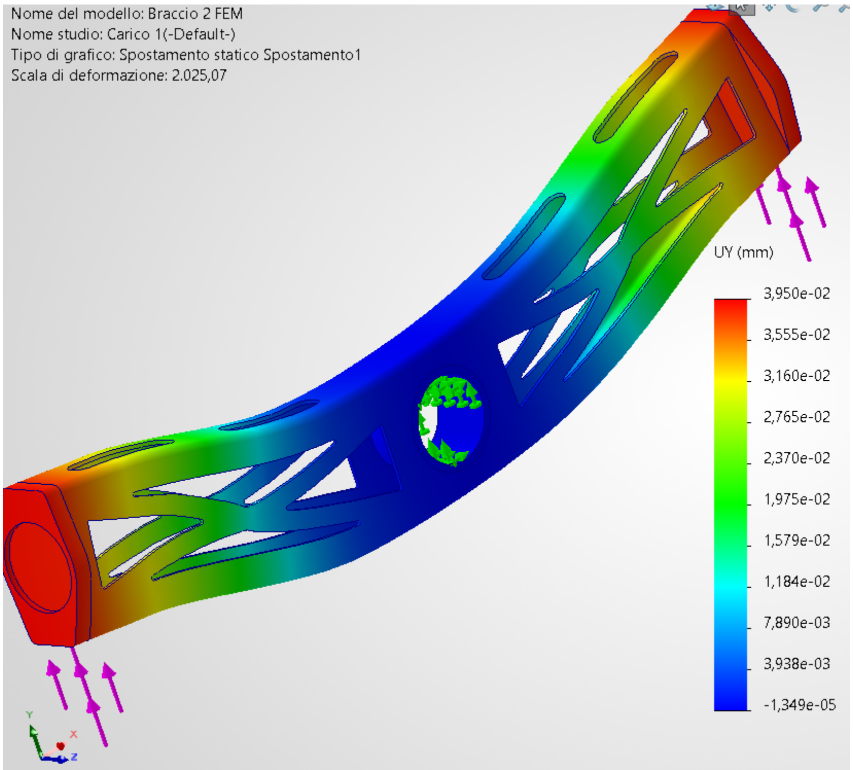

Figure 4.32: Displacement y-axis suspension model 2 with load 1

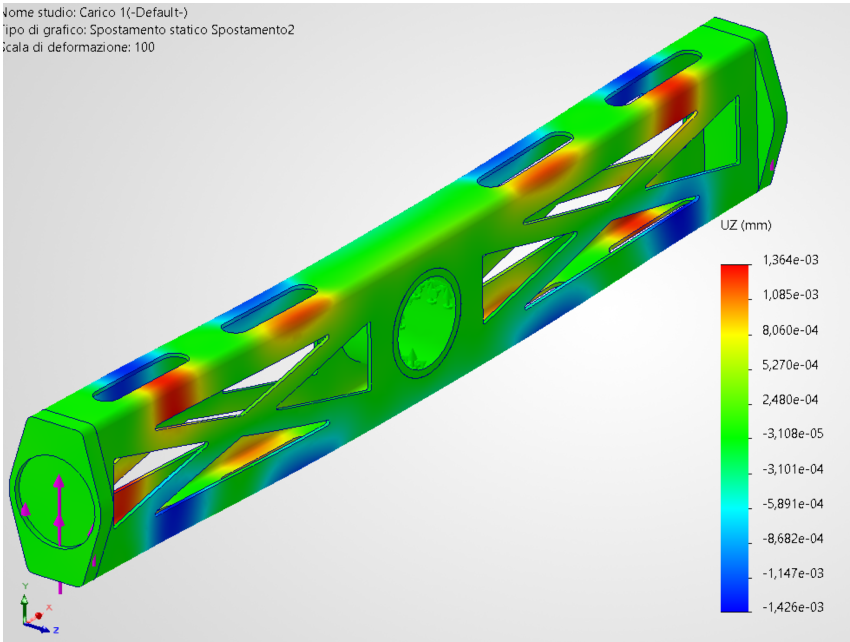

Figure 4.33: Displacement x-axis suspension model 2 with load 1

Considering the rover in stowed configuration, in Figure 4.34 the Von Mises stresses worst peaks are around 3.512×10^1 MPa, and are also constrained to very small portions in particular positions that are not visible; 3.519 MPa is the most uniform stress on the beam. The worst vertical displacements are again located at the very end of the leg attachments and are around one and a half decimal of a millimeter as shown in Figure 4.35. Figure 4.36 represents the displacements relating to the axis perpendicular to the plane of the beam, that are slightly more concerning, since on the upper part the beam is pulled forward of 0.165 mm, while on the bottom part is pulled backward of a similar amount, creating a torque on the beam.

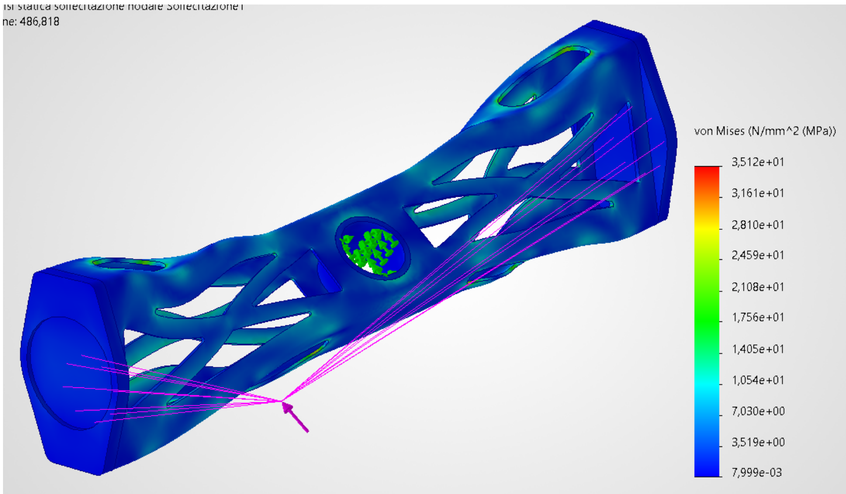

Figure 4.34: Von Mises stress for suspension model 2 with load 2

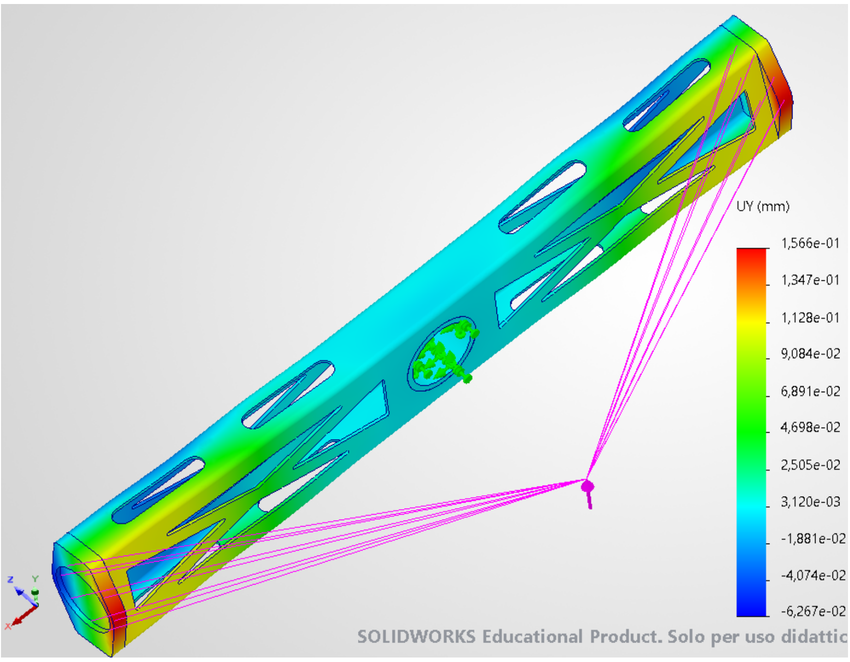

Figure 4.35: Displacement y-axis suspension model 2 with load 2

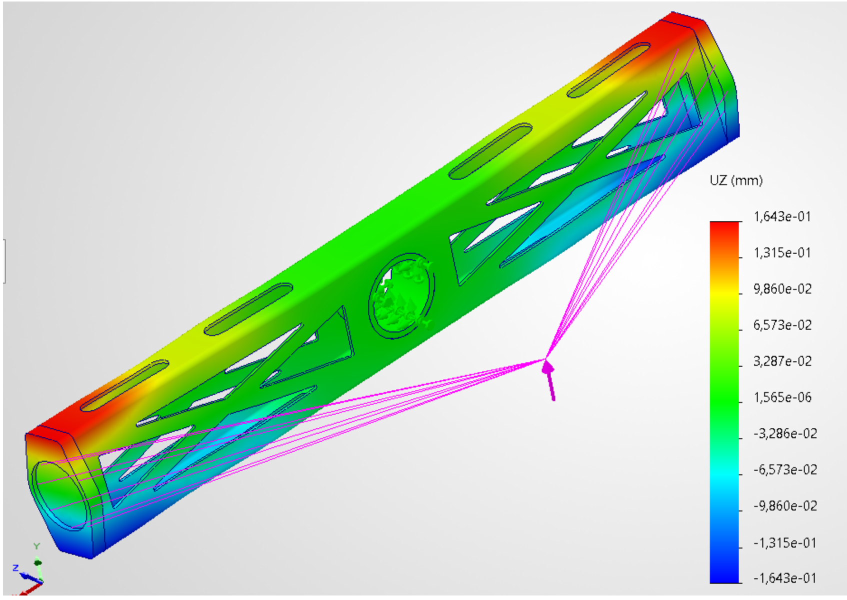

Figure 4.36: Displacement x-axis suspension model 2 with load 2

From the static analysis results, it is clear that the second model is the better one, taking into account both weight and performance.

4.3. Complete design

The entire locomotion system shown in Figures 4.38 and 4.39 was designed to be manufactured with the aluminum alloy EN 7075 (Ergal), a light weight and high strength alloy frequently used in aerospace applications. Its main characteristics are listed in Table 4.6.

Density	**Breaking load**	**Yield strenght**	**Elongation at break**
2.8 Kg/dm^3	540-560 N/mm^2	500-510 N/mm^2	7-8 %

Table 4.6: Ergal properties

To attach the locomotion system to the chassis of the rover 6 deep groove ball bearings have been used. Two bearings were employed for each connection to ensure the least amount of solicitation possible.

18 BCSA V4 motors from the series RI of Bonsystems were adopted. The model chosen is BCSA 070-049-I, whose parameters are displayed in Table 4.7. This model was selected because it is the smallest and lightest of series, also it has the highest reduction ratio and highest rated torque of the series, which allows for lower velocities.

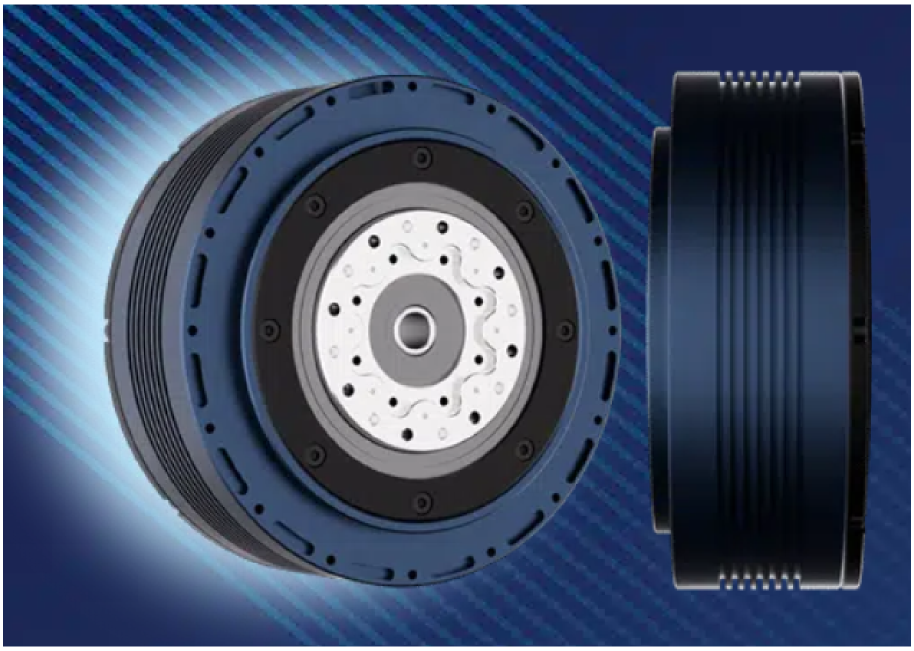

Figure 4.37: BCSA V4 motor series RI of Bonsystems [64]

Reduction ratio	Outer dimension	Thickness	Motor input voltage	Motor rated current
49	70 mm	50 mm	48 V	5.6 A

Motor maximum current	Motor rated torque	Motor rated input speed	Reducer output speed	Rated torque
16.8 A	0.57 Nm	3.19 RPM	65 RPM	13 Nm

Peak torque	Backlash	Input shaft hollow diameter	Offset both LC	Weight
38 Nm	10 arcmin or less	7.4 mm	5.5 mm	0.68 kg

Table 4.7: Motor characteristics [64]

Similarly to the ExoMars rover, the locomotive architecture follows the configuration 6×6×6 with 6 wheel–walking: so 6 motors drive the wheels, 6 steer them and the last 6 are applied to move the entire leg. Therefore, all 6 wheels can be driven and steered, and used in the wheel-walking mode, where the motion of the wheel driving motor with the leg motor are synchronized, and the wheel can be swinged back and forth to increase traction. The final mass of the complete system is 24.96 kg. It has two configurations: the stowed configuration occupies a volume of 1060 x 947 x 200 mm, while the operating configuration reaches a height of 400 mm.

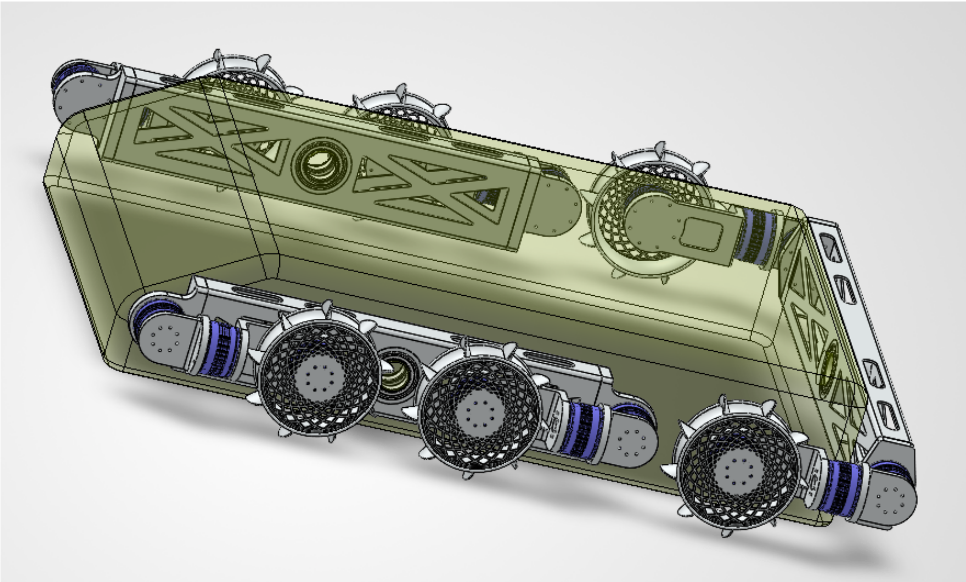

Figure 4.38: Rover in stowed configuration

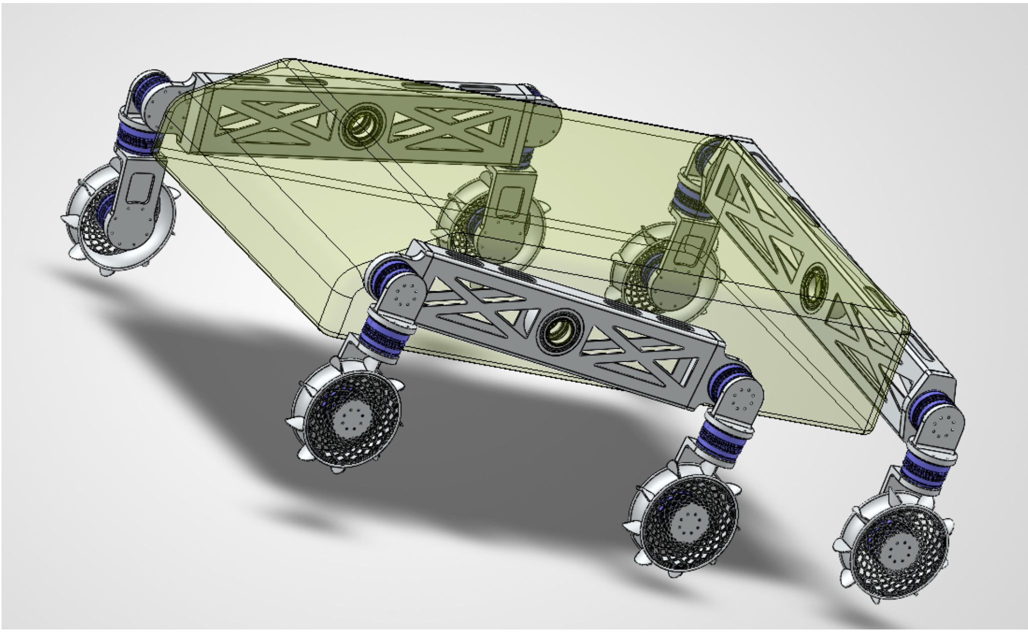

Figure 4.39: Rover in operating configuration

Considering the dimensions of the wheels, each motor would need 268.8 W to move the rover at the maximum speed possible, which is 68 cm/s. Though, this velocity is far too high for the environment the rover will operate in. Therefore, tacking into account a more reasonable driving speed of 1 cm/s, the power each motor would require is 2.17 W. Table 4.8 shows that the power budget is heavily influenced by the number of motors employed and for how much time, hence by the scientific operations the rover aims to do.

Mode of operation	**Driving**
Power	2.17 Wh x 6 wheel motors x time of driving in h

Mode of operation	**Steering**
Power	2.17 Wh x 6 wheel motors x time of steering in h + 2.17 Wh x n° steering motors x time of steering in h

Mode of operation	**Deploying**
Power	2.17 Wh x 6 leg motors x time of deploying in h

Mode of operation	**Deploying**
Power	2.17 Wh x 6 wheel motors x time of walking in h + 2.17 Wh x n° leg motors x time of walking in h

Table 4.8: Power budget

Some examples of the power budget could be:

- 30 minutes of driving without any maneuvers, thus only the 6 driving motors are being used: 6.5 Wh
- 15 min to deploy the rover, passing from the stowed to the operating configuration, so only the 6 leg motors are applied: 3.25 Wh
- 100 m of wheel walking, where all the driving and leg motors are employed: 72.34 Wh

4.3.1. Performance

Regarding the performance of the rover designed, it could be comparable with the MMX rover, because on granular loose soil in milli-g it depends heavily on the type of wheel.

terrain & slope	slip [%] forward	backward	inching
olivine 0°	5.4(0.4)	−9.7(0.1)	−6.5(2.6)
olivine 10°	16.4(2.6)	-	16.0(1.6)
olivine 20°	36.5(1.0)	-	32.5(0.7)
lava sand 0°	1.5(1.3)	−8.3(2.1)	-
plate 0°	−18.2(0.9)	−17.4(0.3)	-

Figure 4.40: Performance of MMX test campaign [56]

A locomotion test campaign performed on the MMX rover revealed the performance of the rover on different types of soil simulants and slope angles showed in Figure 4.40 [56]. In straight driving conditions on level terrain, slip remained below 10% on both sand simulants, indicating good traction performance due to the selected wheel design. On hard ground, negative slip values showed that the rover traveled farther than expected. During backward driving, when sinkage is low, slip also became negative on sandy terrain because the convex grousers lift the wheel instead of shoveling into the soil; while in softer sands with greater sinkage, the forward shoveling effect improves traction. On hard ground, forward and backward slip values were nearly identical, since the rover drives on the grouser tips in both directions with the same effective dimension. Compared to conventional driving, the inching locomotion mode showed similar performance on flat terrain and moderate slopes, but lower slip at a 20° slope. [56]

The MMX wheel design was developed considering a worst-case scenario, mainly due to the limited knowledge of the properties of Phobos regolith; similarly the uncertain soil characteristics of Vesta would be an important design driver. In terms of terrain morphology, the maximum slopes observed on Phobos can reach up to 45°, even though the majority of the surface presents inclinations below 15°. Similarly, on Vesta, most slopes are between 5° and 10°, with specific regions that reach gradients of 40°. Also, since traction performance on loose granular soils is very much influenced by the local gravitational environment, the great difference in gravity between the two bodies is quite relevant: Phobos has an extremely low gravity of approximately 1/2000 of Earth's gravity, on the other hand, Vesta's gravity is about 1/40 of Earth's gravity. Therefore, if the wheel design is capable of ensuring good mobility and traction performance on Phobos, it is reasonable to assume equal or improved performance under Vesta's conditions.

5 | Conclusion and future developments

In this study, the preliminary design of the locomotion system for a modified wheeled rover was proposed, as it is considered a potential locomotive technology for future missions to SSSB.

The AHP methodology has been adopted multiple times, combining an initial evaluation of different concepts, followed by a trade-off analysis. In the first place, the methodology was applied to determine which type of locomotion technology was better suited for the exploration mission proposed on asteroid Vesta; four different locomotive concepts were evaluated, and the subsequent trade-off analysis identified the modified wheeled rover as the best type of system for the expedition, due to its robust and adaptable performance. Furthermore, the methodology was employed during the design phase, to resolve the kind of wheel and suspension technology to adopt. The rigid wheel of the MMX rover was recognized as the better candidate for its light mass; on the other hand, the suspension system chosen was the 3-bogie suspension adopted by the ExoMars rover, due to its capability to operate across a broad range of surface conditions.

The specific design of the wheel disc and the specific structure for the beams of the suspension were later studied with static FEM analysis, considering worst case scenarios for the boundary conditions and the loads applied; in both cases the final solution selected was the one with the most strength and the least weight.

Afterward, the CAD model of the complete locomotion subsystem was presented, together with the corresponding volume, mass, and power budgets. The final preliminary design results in a rover capable of operating in two distinct configurations and featuring an architecture that supports three operational modes: driving, steering, and wheel-walking. Thanks to the adoption of an aluminum alloy structure, the total subsystem mass is maintained at approximately 25 Kg. In addition, the selected motors require relatively low power to achieve the target velocity, resulting in a moderate overall power demand that varies according to the scientific mission plan.

Lastly, the rover's performance was assessed through a literature review, where the results of a test campaign conducted on a prototype of the MMX rover were discussed. It could be used since mobility in low-gravity environments and on loose soil is strongly influenced by wheel design. The results indicate improved traction on the lava sand simulant compared to the olivine sand simulant, as well as better than expected performance during backward motion and forward motion on hard ground. Furthermore, the wheel-walking mode was found to reduce slip compared to conventional driving on sloped terrain.

5.1. Future developments

Several directions remain open for further investigation. First, a preliminary prototype could be developed according to the design guidelines presented in this work. Once a functional prototype is available, an experimental campaign employing different soil simulants could be conducted to evaluate the rover's locomotion performance and provide valuable insights for subsequent design iterations.

To complement the experimental campaign and obtain a predictive estimate of the mobility capabilities of the rover, an analytical model should be implemented. If validated, such a model could support future testing campaigns and mission concepts involving modified wheeled rover configurations by providing preliminary performance assessments.

The present work relied exclusively on static FEM analyses during the design phase. A more complete set of FEM analysis, comprehensive of modal, buckling, dynamical and optimization analyses in a microgravity environment that resembles the one on the target asteroid of the mission, could further improve the understanding of the rover's structural and locomotive behavior.

Further research on locomotion systems also requires an accurate characterization of regolith behavior in low-gravity environments. Therefore, methodologies and techniques for determining the relevant physical properties of the soil should be investigated, together with the practical expertise necessary for their effective application in experimental campaigns and numerical modeling activities.

Lastly, the remaining rover subsystems could be designed and integrated with the locomotion system in order to achieve a more complete and representative mission architecture.

Bibliography

[1] M. A. Barucci, et al. Space missions to small bodies: asteroids and cometary nuclei. *Astron Astrophys Reviews*, page 19–48, 2011. doi: 10.1007/s00159-011-0048-2.

[2] D Hestroffer, et al. Small solar system bodies as granular media. *The Astronomy andAstrophysics Review*, 2019. doi: https://doi.org/10.1007/s00159-019-0117-5.

[3] J de Le´on, et al. Finding the compositional diversity of the solar system. IX Scientific Meeting of the Spanish Astronomical Society, 2010. URL `https://www.sea-astronomia.es/sites/default/files/archivos/proceedings9/CIENCIAS%20PLANETARIAS/INVITADAS/deleonj-invitada/F-deleonj.pdf`.

[4] R. A. N. Araujo. Dynamics of minor bodies in the solar system. *THE EUROPEAN PHYSICAL JOURNAL SPECIAL TOPICS*, 234:7815–7828, 2026. doi: https://doi.org/10.1140/epjs/s11734-025-01981-6.

[5] Quanzhi Ye. Minor planets, asteroids, comets and interplanetary dust within 30 au. 2024. doi: 10.48550/arXiv.2409.09540.

[6] JAXA. Japanise space agency. URL `https://global.jaxa.jp`.

[7] NASA. National aeronautics and space administration. URL `https://www.nasa.gov`.

[8] Anita L. Cochran, et al. The composition of comets. *Space Science Review*, 197: 9–46, 2015. doi: DOI10.1007/s11214-015-0183-6.

[9] Julio A. Fernández. Origin of comet nuclei and dynamics. *Space Science Review*, 138:27–42, 2008. doi: DOI10.1007/s11214-007-9274-3.

[10] Gonzalo Tancredi. A criterion to classify asteroids and comets based on the orbital parameters. *Icarus*, 234:66–80, 2014. URL `http://dx.doi.org/10.1016/j.icarus.2014.02.013`.

[11] Haseeb Ashfaq. Experimental investigation of an choring performance on asteroid analog materials. Master's thesis, Politecnico di Milano, 2025.

[12] Seth Jacobson, et al. Small bodies tell the story of the solar system: A scientific rationale for a multi-target small body sample return program including the earth-based laboratory analysis of returned samples. *Planetary Science and Astrobiology Decadal Survey*, 2023. URL `https://doi.org/10.48550/arXiv.2007.08603`.

[13] Tingzhang Wang, et al. Progress in the development of small-celestial-body anchoring robots. *nature astronomy*, 7:380–390, 2023. URL `https://doi.org/10.1038/s41550-023-01926-w`.

[14] KARL-HEINZ GLASSMEIER, et al. The rosetta mission:flying towards the origin of the solar system. *Space Science Reviews*, 128:1–21, 2007. doi: 10.1007/s11214-006-9140-8.

[15] ESA. European space agency. URL `https://www.esa.int`.

[16] J P BIBRING, et al. The rosetta lander(“philae”)investigations. *Space Science Reviews*, 128:205–220, 2007. doi: 10.1007/s11214-006-9138-2.

[17] Canhui Yin, et al. Technical progress in landing mechanisms for exploring small solar system bodies. *Progress in Aerospace Sciences*, 122, 2021. URL `https://doi.org/10.1016/j.paerosci.2021.100697`.

[18] Makoto Yoshikawa, et al. Hayabusa sample return mission. *Asteroids IV*, pages 397–418, 2015. doi: 10.2458/azu_uapress_9780816532131-ch021.

[19] Takashi Kubota and Tetsuo Yoshimitsu. Intelligent rover with hopping mechanism for asteroid exploration. 6th International Conference on Recent Advances in Space Technologies, IEEE, 2013. doi: 10.1109/RAST.2013.6581357.

[20] Sei-ichiro Watanabe, et al. Hayabusa2 mission overview. *Space Science Reviews*, 208: 3–16, 2017. doi: 10.1007/s11214-017-0377-1.

[21] C T RUSSELL, et al. Dawn completes its mission at 4 vesta. *Meteoritics Planetary Science*, 48:2076–2089, 2013. doi: 10.1111/maps.12091.

[22] Stefano Campagnola, et al. Mission analysis for the martian moons explorer (mmx) mission. *Acta Astronautica*, 146:409–417, 2018. URL `https://doi.org/10.1016/j.actaastro.2018.03.024`.

[23] Stephan Ulamec, et al. Science operations of idefix, the mmx phobos rover. *Progress in Earth and Planetary Science*, pages 12–97, 2025. URL `https://doi.org/10.1186/s40645-025-00771-x`.

[24] Patrick Michel, et al. The mmx rover: performing in situ surface investigations

on phobos. *Earth, Planets and Space*, 74, 2022. URL `https://doi.org/10.1186/s40623-021-01464-7`.

[25] Hans-Juergen Sedlmayr, et al. Mmx - development of a rover locomotion system for phobos. 2020 IEEE Aerospace Conference, IEEE, 2020. doi: 10.1109/AERO47225.2020.9172659.

[26] Timothy J. McCoy, et al. Asteroid (4) vesta ii: Exploring a geologically and geochemically complex world with the dawn mission. *Chemie der Erde*, 75:273–285, 2015. URL `http://dx.doi.org/10.1016/j.chemer.2014.12.001`.

[27] Katharina A. Otto, et al. Mass-wasting features and processes in vesta's south polar basin rheasilvia. *JOURNAL OF GEOPHYSICAL RESEARCH: PLANETS*, 118: 2279–2294, 2013. doi: 10.1002/2013JE004333.

[28] Michelangelo FORMISANO, et al. The heating history of vesta and the onset of differentiation. *Meteoritics Planetary Science*, 48:2316–2332, 2013. doi: 10.1111/maps.12134.

[29] Harry Y. Jr. McSween, et al. Hed meteorites and their relationship to the geology of vesta and the dawn mission. *Space Science Reviews*, 163:141–174, 2011. doi: 10.1007/s11214-010-9637-z.

[30] A. Thoesen and H. Marvi. Planetary surface mobility and exploration: A review. *Current Robotics Reports*, 2:239–249, 2021. URL `https://doi.org/10.1007/s43154-021-00056-3`.

[31] Valentin Gomez-Jauregui, et al. Tensegrity applications to architecture, engineering and robotics: A review. *Apllied Sciences*, 13, 2022.

[32] Yongchang Zhang, et al. Progress, challenges, and prospects of soft robotics for space applications. *Advanced Intelligent Systems*, 5, 2022.

[33] H Kolvenbach, et al. Scalability analysis of legged robots for space exploration. 68th International Astronautical Congress, IAF, 2018. URL `https://doi.org/10.3929/ethz-b-000183684`.

[34] Haitish V. Gandhi and Cagri Kilic. Planetary locomotion systems for enhanced-mobility through hybrid and adaptive methods. 2025. URL `https://doi.org/10.2514/6.2025-98207`.

[35] K Takahashi, et al. A study of locomotion mechanism based on gravitational en-

vironment. International Conference on Intelligent Robots and Systems, 2004. doi: 10.1109/IROS.2004.1390040.

[36] G Wilburna, et al. Development and testing of an engineering model for an asteroid hopping robot. 2019. URL `https://doi.org/10.48550/arXiv.1910.03831`.

[37] JPL. Jet propulsion laboratory. URL `https://www.jpl.nasa.gov`.

[38] Daniel Helmick, et al. Small body surface mobility with a limbed robot. International Conference on Intelligent Robots and Systems, IEEE, 2014. doi: 10.1109/IROS.2014.6942879.

[39] Ji Qi, et al. Integrated attitude and landing control for quadruped robots in asteroid landing mission scenarios using reinforcement learning. *Acta Astronautica*, 204:599–610, 2022. URL `https://doi.org/10.1016/j.actaastro.2022.11.028`.

[40] Gargi Das, et al. From nature to robots: a comprehensive survey on lizard-inspired robotics for ground and space exploration. *Bioinspiration Biomimetics*, 2026. doi: 10.1088/1748-3190/ae2b18.

[41] S Bartsch, et al. Development and control of the multi-legged robot mantis. *47st International Symposium on Robotics*, 2022. URL `https://ieeexplore.ieee.org/abstract/document/7559142`.

[42] Greg Wilburn, et al. Development and testing of an engineering model for an asteroid hopping robot. 2019. URL `https://doi.org/10.48550/arXiv.1910.03831Focustolearnmore`.

[43] Kosuke Sakamoto, et al. A mechanical design for efficient hopping of planetary rover on soft soil. International Conference on Advanced Intelligent Mechatronics (AIM), IEEE, 2018. doi: 10.1109/AIM.2018.8452427.

[44] Bin Chen, et al. Numerical simulations of the controlled motion of a hopping asteroid lander on the regolith surface. *Monthly Notices of the Royal Astronomical Society*, 485:3088–3096, 2019. URL `https://doi.org/10.1093/mnras/stz633`.

[45] Subir K Saha, et al. Landing mechanisms for hopping robots: Considerations and prospects. 2006. URL `https://www.researchgate.net/publication/265068067_LANDING_MECHANISMS_FOR_HOPPING_ROBOTS_CONSIDERATIONS_AND_PROSPECTS`.

[46] Martin Azkarate, et al. Design, testing, and evolution of mars rover testbeds: European space agency planetary exploration. volume 29, pages 10–23, 2022. doi: 10.1109/MRA.2021.3134875.

[47] E. H. FORMAN and S. I. Gass. The analytic hierarchy process - an exposition. *Operation Research*, 49.4:469–486, 2001. URL `doi:10.1287/opre.49.4.469.11231.`

[48] T. L. Saaty. How to make a decision: The analytic hierarchy process. *AESTIMUM*, 24:19–43, 1994. URL `doi:10.13128/Aestimum-7138`.

[49] Dimitrios S. Apostolopoulos. Analytical configuration of wheeled robotic locomotion. Master's thesis, Carnegie Mellon University, 2001.

[50] J. Kim and J. Ahn. Multi-disciplinary and multi-objective design optimization of a lunar rover system with operational considerations. *International Journal of Aeronautical and Space Sciences*, 23:192–206, 2022. URL `https://doi.org/10.1007/s42405-021-00415-6`.

[51] Leon Stubbig and Roy Lichtenheldt. Optimizing the shape of planetary rover wheels using the discrete element method and bayesian optimization. International Center for Numerical Methods in Engineering, 2021. URL `https://elib.dlr.de/148275/`.

[52] Stefan Barthelmes, et al. Mmx rover locomotion subsystem - development and testing towards the flight model. 2022 IEEE Aerospace Conference, IEEE, 2022. doi: 10.1109/AERO53065.2022.9843723.

[53] Nildeep Patel, et al. The exomars rover locomotion subsystem. *Journal of Terramechanics*, 47:227–242, 2010. URL `https://doi.org/10.1016/j.jterra.2010.02.004`.

[54] C G-Y Lee, et al. Design and manufacture of a full size breadboard exomars rover chassis. Swiss Federal Institute of Technology (ETHZ), 2006. URL `https://doi.org/10.3929/ethz-a-010043415`.

[55] Viktor Langofer, et al. Mmx locomotion subsystem: mechanics for extraterrestrial low gravity drive. 2023 IEEE Aerospace Conference, IEEE, 2023. doi: 0.1109/AERO55745.2023.10115807.

[56] Juliane Skibbe, et al. Locomotion control functions for the active chassis of the mmx rover. 2021 IEEE Aerospace Conference, IEEE, 2021. doi: 10.1109/AERO50100.2021.9438423.

[57] Martin Azkarate, et al. Concept, development and testing of mars rover prototypes for esa planetary exploration. 2022. doi: 10.1109/MRA.2021.3134875.

[58] Stéphane Michaud, et al. Development of the exomars chassis and locomotion sub-

system. 9th International Symposium on Artificial Intelligence, Robotics and Automation in Space, 2008. doi: https://doi.org/10.3929/ethz-a-010034575.

[59] Yong Yang, et al. A novel design of tri-star wheeled mobile robot for high obstacle climbing. 2012 IEEE/RSJ International Conference on Intelligent Robots and Systems, IEEE, 2012. doi: 10.1109/IROS.2012.6385776.

[60] John Faber Archila, et al. Simulation of rovers for precision agriculture. 2014 Joint Conference on Robotics: SBR-LARS Robotics Symposium and Robocontrol, IEEE, 2014. doi: 10.1109/SBR.LARS.Robocontrol.2014.30.

[61] S Rajath, et al. Rovers with rocker-bogie mechanisms: Areview of progress and innovations in design, manufacturing, and control. *Mechanical Engineering Science*, 238:6560–6583, 2024. doi: 10.1177/09544062231224541.

[62] Brian D. Harrington and Chris Voorhees. The challenges of designing the rocker-bogie suspension for the mars exploration rover. 37th Aerospace Mechanisms Symposium, NASA, 2004. URL `https://ntrs.nasa.gov/citations/20040084284`.

[63] Hacot Hervé. Analysis and traction control of a rocker-bogie planetary rover. Master's thesis, Massachusetts Institute of Technology., 1998.

[64] Bonsystems. Bcsa v4 series ri. URL `https://en.bonsystems.com/product/robot-actuator-bcsa-v4-ri/`.

[65] Ross Jones. The muses cn rover and asteroid exploration mission. 2000. URL `https://www.researchgate.net/publication/2524695_The_MUSES-CN_rover_and_asteroid_exploration_mission`.

[66] Institute of high energy physics chinese academy of sciences.

A | Appendix A

In this appendix, the pairwise comparison matrices for the Analytical Hierarchy Process procedure for the locomotion technologies' trade-off, and explained in subsection 3.2.1 are presented with their consistency ratio.

Parameters comparison

In Table A.1, the comparison matrix for the parameters explained in subsection 3.2.2 is presented. For a matrix with 8 elements, the random index is $RI = 1.40$. The consistency ratio is $CR = 0.009$.

Parameters	Surf.	Grav.	Saf.	Pow.	Mass	Rel.	Comp.	Vol.
Surf.	1	1	2	2	3	3	4	5
Grav.	1	1	2	2	3	3	4	5
Saf.	1/2	1/2	1	1	2	2	3	4
Pow.	1/2	1/2	1	1	2	2	3	4
Mass	1/3	1/3	1/2	1/2	1	1	2	3
Rel.	1/3	1/3	1/2	1/2	1	1	2	3
Comp.	1/4	1/4	1/3	1/3	1/2	1/2	1	2
Vol.	1/5	1/5	1/4	1/4	1/3	1/3	1/2	1

Table A.1: Pairwise comparison matrix for the locomotion trade-off parameters

Technologies comparisons

In the following tables, the comparison matrices of the technologies with respect to each parameter are presented with their consistency ratio. For matrices with 4 elements, the random index is $RI = 0.89$.

	CW	ML	H	MW
CW	1	1/6	1/3	1/5
ML	6	1	3	2
H	3	1/3	1	1/3
MW	5	1/2	3	1

Table A.2: Surface characteristics; $CR = 0.029$

	CW	ML	H	MW
CW	1	1/5	1/4	1/3
ML	5	1	3	4
H	4	1/3	1	2
MW	3	1/4	1/2	1

Table A.3: Gravity; $CR = 0.044$

	CW	ML	H	MW
CW	1	3	4	1/3
ML	1/3	1	3	1/5
H	1/4	1/3	1	1/6
MW	3	5	6	1

Table A.4: Safety; $CR = 0.055$

	CW	ML	H	MW
CW	1	9	5	2
ML	1/9	1	1/4	1/6
H	1/5	4	1	1/4
MW	1/2	6	4	1

Table A.5: Power; $CR = 0.045$

	CW	ML	H	MW
CW	1	3	1/2	1
ML	1/3	1	1/5	1/3
H	2	5	1	2
MW	1	3	1/2	1

Table A.6: Mass; $CR = 0.001$

	CW	ML	H	MW
CW	1	5	3	2
ML	1/5	1	1/3	1/4.5
H	1/3	3	1	1/3
MW	1/2	4.5	3	1

Table A.7: Reliability; $CR = 0.039$

	CW	ML	H	MW
CW	1	7	2	3
ML	1/7	1	1/5	1/4
H	1/2	5	1	2
MW	1/3	4	1/2	1

Table A.8: Complexity; $CR = 0.017$

	CW	ML	H	MW
CW	1	3	1/3	1
ML	1/3	1	1/5	1/3
H	3	5	1	3
MW	1	3	1/3	1

Table A.9: Volume; $CR = 0.016$

B | Appendix B

In this appendix, the pairwise comparison matrices for the Analytical Hierarchy Process procedure for the wheel and suspension technologies' trade-off, and explained in subsection 3.2.1 are presented with their consistency ratio.

Wheel trade-off

Parameters comparison

In Table B.1, the comparison matrix for the parameters explained in subsection 4.1.4 is presented. For a [2x2] matrix the consistency ratio is automatically CR = 0.

Parameters	Mass	Surface characteristics
Mass	1	2
Surface characteristics	1/2	1

Table B.1: Pairwise comparison matrix for the wheel trade-off parameters

Technologies comparison

In the following tables, the comparison matrices of the wheel technologies with respect to each parameter are presented. For [2x2] matrices the consistency ratio is automatically CR = 0.

	MMX	ExoMars
MMX	1	7
ExoMars	1/7	1

Table B.2: Mass

	MMX	ExoMars
MMX	1	1/5
exoMars	5	1

Table B.3: Surface characteristics

Suspension trade-off

Parameters comparison

In Table B.4, the comparison matrix for the parameters explained in subsection 4.2.5 is presented. For a matrix with 4 elements, the random index is RI = 0.89. The consistency ratio is CR = 0.0116.

Parameters	Mass	Power	Surface characteristics	Complexity
Mass	1	2	3	4
power	1/2	1	2	3
Surface characteristics	1/3	1/2	1	2
Complexity	1/4	1/3	1/2	1

Table B.4: Pairwise comparison matrix for the suspension trade-off parameters

Technologies comparison

In the following tables, the comparison matrices of the suspension technologies with respect to each parameter are presented. For a matrix with 4 elements, the random index is RI = 0.89.

	MMX	ExoMars	TS	RB
MMX	1	1.5	5	2
ExoMars	1/1.5	1	4	1.5
TS	1/5	1/4	1	1/4
RB	1/2	1/1.5	4	1

Table B.5: Mass; $CR = 0.0102$

	MMX	ExoMars	Ts	RB
MMX	1	1/2	1/3	1/2
ExoMars	2	1	1/2	1
TS	3	2	1	2
RB	2	1	1/2	1

Table B.6: Power; $CR = 0.0039$

	MMX	ExoMars	TS	RB
MMX	1	1/3	4	1/2
ExoMars	3	1	5	2
TS	1/4	1/5	1	1/4
RB	2	1/2	4	1

Table B.7: Surface characteristics; $CR = 0.0367$

	MMX	ExoMars	Ts	RB
MMX	1	1/3	1/4	1/2
ExoMars	2	1	1/2	2
TS	4	2	1	3
RB	2	1/2	1/3	1

Table B.8: Complexity; $CR = 0.0116$

List of Figures

List of Tables

List of Symbols

Symbol	Description
a	semi major axis
D	diameter
q	perihelion

List of Acronyms

Acronym	Description
AB	Asteroid Belt
ADS	Active descent System
AHP	Analytical Hierarchy Process
ATHLETE	All-Terrain Hex-Limbed Extra-Terrestrial Explorer
AU	Astronomical Unit
CEN	Centaur
CR	Consistency Ratio
DC	Direct Current
DOF	Degree Of Freedom
E-box	Electronic box
EMDD	Electro Mechanical Damping Device
ESA	Eupean Space Agency
FEM	Finite Element Method
HAMO	High Altitude Mapping Orbit
HED	howardite–eucrite–diogenite meteorites
HDRM	hold down and release mechanism
JAXA	Japan Aerospace Exploration Agency
JPL	Jet Propulsion Laboratory
JT	Jupiter Trojan
IEO	Inner Erth Object
IMB	Inner Main Belt
LAMO	Low Altitude Mapping Orbit
LSS	locomotion subsystem
MASCOT	Mobile Asteroid Surface Scout

Acronym	Description
MC	Mars Crossers
MINERVA	MIcro-Nano Experimental Robot Vehicle for Asteroid
MMB	Middle Main Belt
MMX	Martian Moon eXploration
NASA	National Aeronautics and Space Administration
NEA	Near Earth asteroid
NEO	Near Earth Object
OMB	Outer Main Belt
OSIRIS-REx	Origins, Spectral Interpretation, Resource Identification, Security, Regolith Explorer
PHA	Potentially Hazardous Asteroid
RI	Random Index
SSSB	Small Solar System Body
TAG	Touch And Go
TNO	Trans Neptunian Objects
YORP	Yrkovsky–O'Keefe–Radzievskii–Paddack

Acknowledgements

In primo luogo vorrei rivolgere un sentito ringraziamento al Professor Fabio Ferrari, al dottorando Samuele Vaghi e al ricercatore Iosto Fodde per avermi assistito e guidato, con grande professionalità e costanza durante tutto lo svolgimento di questa tesi.

Gli anni passati qui al Politecnico sono stati sicuramente duri e faticosi, dove ho pensato di non farcela e mollare tutto più di una volta. Ma con molta calma, poco sangue freddo, notti insonni al computer a star dietro ai vari progetti, esame dopo esame sono riuscita ad attraversare questo traguardo. Quindi un piccolo grazie direi che me lo dico anche da sola. Ma il merito non è solo mio, anzi, perchè ad ogni "non ce la faccio più" ho sempre trovato qualcuno pronto ad aiutarmi.

Grazie a mami e papo per il costante supporto e incoraggiamento. Grazie a papo perchè senza di lui decisamente non mi laureavo, l'aiuto in analisi 1, scienza delle costruzioni e in questa tesi sono stati indispensabili. Grazie a mami, senza la quale col cavolo che effettivamente facevo la tesi per finire questo percorso. Grazie per l'esempio che ci avete dato, spero di diventare come voi almeno un pochino. Grazie per la comprensione e l'aiuto, specialmente nell'ultimo periodo, spero di trovare la mia strada come voi e di rendervi fieri pure io. Vi voglio tanto bene.

Grazie a Silvia per essere diventata ufficialmente la cuoca del piano di sopra. Grazie per venire al cinema con me anche se è a Rozzano e per le opinioni fin troppo sincere sui miei vestiti. Non metti mai a posto niente e ti arrabbi per qualsiasi cosa troppo velocemente, ma grazie per essere mia sorella, ti voglio bene.

Grazie a tutti i nonni che mi hanno insegnato che con impegno, pazienza e costanza si può arrivare lontano. Grazie per i mesi di vacanza spensierata in montagna e al mare, per tutte le bruciacchiature del risotto fatte apposta, per le croste del parmigiano tenute da parte, per tutte le ricette imparate dai biscotti con le gocce alla pasta al forno. Grazie per averci sempre voluto bene.

Grazie agli zii Lorenza e Davide per le vacanze, i consigli della zia e i piatti strani dello zio. Grazie a Mina per avermi disconosciuto solo una volta in piazza. Grazie per essere entrati a far parte di famiglia.

Grazie a Lucy per aver guardato insieme a me in salotto un numero infinito di film e serie tv. Grazie per le coccole e le leccatine di conforto. Ti voglio tanto bene.

Grazie a Ludo, perchè i libri mi sono sempre piaciuti ma ora grazie a te ne ho capito il potere e soprattutto quello delle librerie. Sei stata un capo fantastico, difficilmente mi andrà così bene in futuro. Grazie per tutti i consigli letterari, filmici, culinari e non.

Grazie a Virgi e Marti, le mie più vecchie amiche. Anche se non ci sentiamo spessissimo, tutte le volte che ci si rivede è come se non fosse passato neanche un giorno dalle partite a scala quaranta e i gelati a Ceriale.

Grazie alle mie amiche Babi, Ceci, Kiki, Klari, Ludo, Mati e Silvi. Grazie per i weekend di divertimento e per le serate di psicoterapia a casa mia o di Silvi. Grazie per accompagnarmi a prendere il gelato prima di andare al bar a bere un drink. Grazie per avermi accompagnata a vedere dei film horror, perchè da sola col cavolo che andavo. Grazie per mettermi la crema solare cinquanta volte al giorno al mare e per aspettarmi quando sono stanca in salita e rimango indietro perchè non faccio abbastanza movimento. Grazie per i gossip e per le pep talk. Grazie per tutti i momenti passati a parlare delle vostre relazioni/situazioni, quelli romantici, quelli tristi, quelli da incazzarsi e quelli decisamente da mettersi a ridere. Grazie per i lupus in fabula e gli impostore. Grazie per i quarantamila tik tok che non sapevo estissero. Grazie per avermi permesso di rompervi le scatole su Avatar. Grazie per le serate dove ci addormentiamo tutte sul mio divano. Grazie per farmi rimanere a casa quando andate in discoteca. Grazie per avermi accettata e non considerarmi strana anche se siamo diverse milioni di anni di luce. Grazie per gli infiniti ricordi fatti e che ancora ci rimangono da fare insieme. Grazie per gli abbracci. Grazie di essere dell fantastiche pazze persone, grazie di essere voi e di essere mie amiche. Grazie per gli anni di costante comprensione e vicinanza anche quando non ve lo rendo facile. Senza di voi la mia vita sarebbe molto diversa e decisamente molto più triste e brutta, spero davvero di non dover mai scoprire quanto. Vi vogliotanto bene.

Quindi alla fine anche questo capitolo della mia vita è giunto al termine. Adesso ci si butta. Logicamente dove non si sa, però intonto ci si butta. Speriamo sia morbido in fondo.

Chiara